Exposure Characterization and Prediction of Ambient Particulate Matter: From Boston to the Middle East

EXPOSURE CHARACTERIZATION AND PREDICTION OF AMBIENT PARTICULATE MATTER: FROM BOSTON TO THE MIDDLE EAST

SHAHIR MASRI

A Dissertation Submitted to the Faculty of

The Harvard T.H. Chan School of Public Health

in Partial Fulfillment of the Requirements

for the Degree of Doctor of Science

in the Department of Environmental Health

Harvard University

Boston, Massachusetts.

May 2016

Dissertation Advisor: Dr. Petros Koutrakis **Shahir Masri**

Exposure Characterization and Prediction of Ambient Particulate Matter: From Boston to the Middle East

Abstract

Chapter one of this manuscript identifies the sources, composition, and temporal variability of fine ($PM_{2.5}$) and coarse ($PM_{2.5-10}$) particles. A Harvard Impactor was used to collect daily particle samples from 2002-2010 at a single site in Boston, MA. Filters were analyzed for elements, black carbon (BC), and total PM mass. Positive Matrix Factorization (PMF) identified BC, S, Pb, V, and Ni to be associated mostly with the fine particle mode, and Ca, Mn (road dust), and Cl (sea salt) mostly with the coarse mode. PMF identified six source types for $PM_{2.5}$, including regional pollution (48%), motor vehicles (21%), wood burning (19%), oil combustion (8%), crustal/road dust (4%), and sea salt (<1%). Three source types were identified for $PM_{2.5-10}$, including crustal/road dust (62%), motor vehicles (22%), and sea salt (16%). A linear decrease in PM concentrations with time was observed for both fine (-5.2%/yr) and coarse (-3.6%/yr) particles. That $PM_{2.5}$ is decreasing more sharply than $PM_{2.5-10}$ over time suggests the increasing importance of $PM_{2.5-10}$ and traffic-related sources for PM exposure and future policies.

Chapters two and three use variables related to $PM_{2.5}$ concentrations to quantify $PM_{2.5}$ exposure where PM monitoring does not exist. In chapter two, validation of a model calibrating the $PM_{2.5}$-visibility relationship using data collected in Kuwait from 2004-2005 demonstrated the ability to predict $PM_{2.5}$ exposure at monitoring sites. In chapter three, validation of a model calibrating the visibility-AOD relationship using data collected from 2006-2007 in Iraq

demonstrated the ability to predict visibility between monitoring sites at a fine resolution (1x1 km), and in turn estimate $PM_{2.5}$ spatially. Applying these relationships to predict $PM_{2.5}$ at locations exterior to the calibration sites showed high temporal and spatial variability in $PM_{2.5}$ exposure (10-365 $\mu g/m^3$).

The ability to obtain precise estimates of $PM_{2.5}$ concentrations in Southwest Asia and Afghanistan is of high utility for epidemiologists seeking to understand the relationship between chronic $PM_{2.5}$ exposure and respiratory diseases among deployed military personnel stationed throughout the region. That predicted $PM_{2.5}$ varies widely over space and time supports the ability to successfully utilize our estimates to understand this relationship in the region.

Table of Contents

LIST OF FIGURES

LIST OF TABLES

AWKNOWLEDGMENTS

I would like to extend great thanks to my advisor Dr. Petros Koutrakis for his guidance throughout the process of completing this dissertation. His willingness to assign me a project that was in line with my personal research interests is something I deeply appreciate. Further, his inspirational research ideas and sharing of relevant knowledge and skills have strengthened my ability to move forward as an independent researcher.

I would also like to sincerely thank my doctoral research committee members Dr. Eric Garshick and Dr. Brent Coull. These individuals have provided me with invaluable insight as to the direction of my research papers. It is because of their constructive input that my dissertation has achieved its present form.

Further, I am grateful to Choong-Min Kang, Walid Bouhamra, and Alexandra Chudnovsky for their guidance and generosity with data. Also, I am profoundly grateful to Alice Smythe for her tenacity and help with data acquisition, as well as her consistent dependability and kindness relating to meetings and scheduling.

Lastly, I am indebted to my family and friends for their tireless support of me over the years. It is with their encouragement and presence around me that I have maintained my motivation and perseverance. I would especially like to thank my grandfather who set my sights high from childhood, directing me to aim for the stars in academia. I would also like to give special thanks to my mother who inspired my deep passion for science and the environment. She instilled in me not only a deep appreciation for the beauty and complexity of our natural world, but an appreciation for its fragility and the importance of pollution prevention. I sincerely thank you all.

Shahir Masri

INTRODUCTION

The undesirable effects of atmospheric pollution have been recognized for at least two thousand years. In the Middle East, laws in the first and second centuries A.D required tanneries to be located away and upwind of neighboring towns due to noxious odor emissions (Mamane, 1987). It was not until the mid-twentieth century, however, with large-scale industry and the increased use of coal for energy that the importance of air pollution to health became fully realized. In 1952 a severe air pollution episode in London caused the death of over 4,000 individuals, demonstrating the ability of air pollution at ambient concentrations to affect not only morbidity, but mortality. Less severe events occurring in New York and Pennsylvania pointed to the same conclusion.

In the U.S., mounting concern of the harmful effects of air pollution lead to the passage of the Clean Air Act of 1970 as well as numerous studies to better understand air pollution, its sources, and relative impact to health. Most notably was the Harvard Six Cities Study which demonstrated a negative dose-response relationship between life expectancy and air pollution concentration across six cities in the U.S. (Dockery et al. 1993) This study drew particular attention to the importance of air pollutants in the form of suspended particulate matter (PM), as opposed to gaseous pollutants. Specifically, measured PM mass concentration with an aerodynamic diameter of less than 2.5 μm ($PM_{2.5}$) was shown to be the most important predictor of mortality compared to several other key air pollutants assessed. From these and other finding birthed the rapid evolution of air pollution science that has been critical to our understanding of the effects of air pollution, and specifically PM exposure, today.

Since the 1970s, epidemiological studies have shown exposure to $PM_{2.5}$ and other PM size fractions to be associated with increased mortality as well as several adverse respiratory, cardiovascular, and neurological conditions (Pope and Dockery, 2006; Roberts et al. 2013). In

most studies, PM exposure is usually characterized based on measured mass concentration of particles within three specific size ranges. These include particles with an aerodynamic diameter of less than 10 μm (PM_{10}), less than 2.5 μm (as described above), and between 2.5 and 10 μm ($PM_{2.5-10}$), also known as inhalable, fine, and coarse particles, respectively. Though size is a valuable metric by which to characterize PM, this approach does not take into account the chemical compositions of particles and is therefore unlikely to tell the entire story as it relates to human health effects resulting from airborne particle exposure.

Recent literature suggests that chemical components such as metals, elemental carbon, organic carbon compounds, among others, may play an important role in particle toxicity (Fanning et al. 2009; Lippmann, 2010). Epidemiological studies have provided some evidence about the importance of particle composition, as is the case in a recent study showing an association between autism spectrum disorder and exposure to airborne metals and diesel particles (Roberts et al. 2013). Other studies have linked components such as sulfur, copper, nickel, zinc, organic carbon (OC), and black carbon (BC), either alone or in mixtures, to increased cardiovascular disease and mortality (Vedal et al. 2013; Flemming et al. 2013; Valdes et al. 2012; Lippmann & Chen, 2009). Clinical and toxicological studies have also shown associations between specific PM components and physiological outcomes (Araujo et al. 2010). To date, a consensus has not surfaced as to precisely which constituents elicit specific outcomes.

Due to its chemical and biological composition, residence time, and ability to penetrate deep into the lung, $PM_{2.5}$ exposure has continued to receive deserved attention in the media and within political and scientific arenas as it relates to health. This is reflected by the 2012 revision of the U.S. National Ambient Air Quality Standards (NAAQS) for PM, in which the primary annual $PM_{2.5}$ standard was lowered from 15.0 to 12.0 $\mu g/m^3$. Importantly, however, clinical and

toxicological studies have reported that coarse particles resulting from road dust (mixed debris from brake wear, tire wear, road abrasion, and biological and geological matter) can be as toxic as fine particles on a mass basis (Thorpe and Harrison, 2008; Flemming, 2012). As the role of particle composition in producing toxicity is uncovered, it is increasingly important to investigate the compositional differences between $PM_{2.5}$ and $PM_{2.5-10}$ as well as identify their sources. This is of particular importance in urban settings, where traffic-related PM is higher and coarse particles are largely made up of re-suspended road dust (Manoli et al. 2002).

Studies aimed at understanding the origin of ambient PM have been conducted in various cities around the world. In some studies, source apportionment was conducted without considering coarse particles (Kim et al. 2005; Gugamsetty et al. 2012). While in other studies, fine and coarse particles are not collected concurrently, or are not collected in areas that reflect large-scale urban air (Khodeir et al. 2012; Davy et al. 2012). When fine and coarse PM is measured concurrently, source apportionment studies are still often limited in terms of their sample size and study length (Gietl et al. 2009; Dordevic et al. 2012; Clements et al. 2014; Contini et al. 2014); analyzing fewer than 200 samples and spanning a few years or less.

In chapter one of this manuscript, nearly 2,000 daily integrated particle samples are analyzed over a nine year period in order to investigate the composition of $PM_{2.5}$ and $PM_{2.5-10}$ at a single urban monitoring site (Boston, MA). Additionally, this chapter identifies and quantifies the source contributions of $PM_{2.5}$ and $PM_{2.5-10}$ as well as explores their temporal trends. With greater knowledge of the source and compositional differences between these two PM fractions, and with better insight as to the annual trends and seasonal variability of such concentrations, epidemiologists will be better equipped to understand the ensuing health implications of PM exposure. Finally, this chapter evaluates the seasonal and temporal tends in the fine- and coarse-

mode during the sampling period and investigates their relation to changes in sources contributions. This information is valuable in enabling better decision making concerning PM regulations.

An additional area of importance relating to PM exposure is the ability to quantify exposure where PM monitoring is not readily available. In the United States, $PM_{2.5}$ exposure characterization is made possible by an extensive network of PM monitoring stations maintained by the U.S. Environmental Protection Agency (EPA) and other bodies throughout the country. In other developed nations, similar networks are readily available. However, in under-developed nations and nations with nascent environmental protection programs, regular monitoring of PM, especially $PM_{2.5}$, is most often not conducted.

The lack of regular PM monitoring in other nations is of concern to the United States, particularly in regions of reportedly high PM concentrations where U.S. military personnel are deployed, usually for months at a time. This is the case in Southwest Asia and Afghanistan. Although wealthier countries in this region such as Kuwait, Qatar, and the United Arab Emirates have established networks for monitoring PM_{10} and gaseous criteria pollutants since the early 2000s, in general there are few integrated networks to provide comprehensive air pollution data throughout the region. For countries with networks, $PM_{2.5}$ measurements began only over the last five years and employ sampling methods that are inadequate to collect particles during dust storms, which are common occurrences each year (NRC, 2010).

In Southwest Asia and Afghanistan, military personnel have complaints of respiratory symptoms during and following deployment to the region (Sanders et al. 2005). However, causal inference is limited due to lack of objective exposure information (Morris et al. 2014). In response, the Department of Defense (DoD) conducted the Enhanced Particulate Matter Surveillance

Program (EPMSP) at military sites during 2006-2007. Results showed mean concentrations of $PM_{2.5}$ ranging from 33 to 144 $\mu g/m^3$ (NRC, 2010). This is considerably higher than the annual national average encountered in the U.S. during the same period (~12 $\mu g/m^3$) and exceeds the 1-year Military Exposure Guideline value (15 $\mu g/m^3$) set by the U.S. Army Center for Health Promotion and Preventive Medicine (USEPA, 2016).

According to the Institute of Medicine, sources of PM in Southwest Asia and Afghanistan include windblown dust and dust storms, as well as local combustion sources such as open-pit refuse burning, compression ignition vehicles, aircraft engines, diesel electric generators, households, and local industry (IOM, 2011). This mix of sources differs from those encountered in the U.S. and Europe, where most previous health studies have been conducted. This underscores the need for adequate exposure assessment and epidemiological research in the region, particularly relating to personnel stationed near military bases where anthropogenic pollution sources are more abundant.

Visibility has demonstrated particular promise for use as a $PM_{2.5}$ predictor, especially when $PM_{2.5}$ levels are above 10-20 $\mu g/m^3$. The relationship between particles and visibility is due to the light extinction (scattering and absorption) effects of particles with sizes similar to the wavelengths of visible light. In the U.S., the effect of PM on visibility has been shown empirically in studies since the 1960s (Burt, 1961; Noll et al. 1968; Charlson, 1969; Waggoner and Weiss, 1980). In numerous epidemiological studies, the relationship between visibility and particulate concentrations has been used to estimate PM exposure (Ozkaynak et al. 1985; Abby et al. 1995; Schwartz, 1991; Ostro, 1995; Yanosky et. al 2009; Laden et. al, 2006). Additionally, studies have reported visibility to be associated with hospital admissions (Thach, 2010; WenZhen, 2011).

An alternate measurement of light extinction by particles in the atmosphere is aerosol optical depth (AOD), collected by satellite. AOD is a vertical integration measure of the total abundance of particles in the entire atmospheric column, in contrast to visibility which is a measure of the particle abundance near the ground. Satellite imagery of the earth's surface and atmosphere represents an important tool for air quality and pollution monitoring due to its extensive spatial coverage and repeated observations. Like visibility, AOD can be used to estimate ground level PM exposure. Our research team has pioneered this area, developing methods for the application of high-resolution satellite data for exposure assessment and health effects studies (Kloog et al. 2011; Lee et al. 2012; Chudnovsky 2013b; Kloog et al. 2014).

In chapters two and three of this manuscript, we utilize the $PM_{2.5}$-visibility and $PM_{2.5}$-AOD relationships to demonstrate the ability to predict $PM_{2.5}$ concentrations spatially over the region. In chapter two, we utilize paired daily airport visibility and $PM_{2.5}$ measurements collected in Kuwait to develop a calibration model that can be used to convert visibility to $PM_{2.5}$ estimates in the Southwest Asia and Afghanistan region. In chapter three we utilize paired daily airport visibility and AOD measurements (1x1 km resolution) collected in Iraq to develop a calibration model that we then used to convert AOD to ground visibility estimates in the region.

Coupling chapters two and three enables the use of visibility and AOD measurements to predict $PM_{2.5}$ concentrations throughout Southwest Asia and Afghanistan, where $PM_{2.5}$ exposure data is otherwise lacking. In contrast to the limited monitoring of $PM_{2.5}$ concentrations, daily visibility data is readily collected at numerous airport visibility stations throughout the region. Similarly, daily AOD data is regularly collected by the U.S. National Aeronautic and Space Administration (NASA) and therefore widely available. The ability to estimate $PM_{2.5}$ concentrations spatially throughout Southwest Asia and Afghanistan enables epidemiologists to

take advantage of the large database of historical visibility and AOD readings to understand and estimate past and present $PM_{2.5}$ exposure among U.S. military personnel. What is more, these works build on top of existing methodological approaches to understanding and estimating air pollution exposure, which enables a better understanding of consequent health impacts.

Bibliography

Abbey, D., B. E. Ostro, G. Fraser, T. Vancuren, and R. J. Burchette. 1995. Estimating fine particulate less than 2.5 microns in aerodynamic diameter (PM2.5) from airport visibility data in California. *J. Exposure Analysis & Enviro Epi.* 5:161-180.

Burt, E. W. 1961. A Study of the Relation of Visibility to Air Pollution. *American Industrial Hygiene Ass. J.* 2: 102-108. doi:10.1080/00028896109343378.

Charlson, R. J. 1969. Atmospheric visibility related to aerosol mass concentration: review. *Environ. Sci. Technol.* 3:913–918. doi:10.1021/es60033a002.

Chudnovsky, A. et al., 2013b. A Critical Assessment of High-Resolution Aerosol Optical Depth Retrievals for Fine Particulate Matter Predictions. Atmospheric Chemistry and Physics, 13(doi:10.5194/acp-13-10907-2013): 10907 - 12013.

IOM (Institute of Medicine). 2011. Long-term health consequences of exposure to burn pits in Iraq and Afghanistan. Washington, DC: *The National Academic Press.*

Kloog, I., Koutrakis, P., Coull, B.A., Lee, H.-J. and Schwartz, J., 2011. Assessing Temporally and Spatially Resolved PM2.5 Exposures for Epidemiological Studies Using Satellite Aerosol Optical Depth Measurements. Atmospheric Environment, 45(35): 6267-6275.

Laden, F., J. Schwartz, F. Speizer, and D. Dockery. 2006. Reduction in Fine Particulate Air Pollution and Mortality Extended Follow-up of the Harvard Six Cities Study. *American J. Resp. & Critical Care Med.* 173:667-672. doi:10.1164/rccm.200503-443OC.

Lee, H.-J., Liu, Y., Coull, B., Schwartz, J. and Koutrakis, P., 2011. A Novel Calibration Approach of MODIS AOD Date to Preduct PM2.5 Concentrations. Atmospheric Chemistry and Physics, 11: 7991 - 8002.

Liu, Y.; Paciorek, C. J.; Koutrakis, P. Estimating regional spatial and temporal variability of PM2.5 concentrations using satellite data, meteorology, and land use information. Environ Health Perspect 2009, 117, 886−892.

Mamane, Y. 1987. Air pollution control in Israel during the first and second century. Atmospheric Environment. 21(8): 1861–1863.

Noll, K. E., P. K. Mueller, and M. Imada. 1967. Visibility and aerosol concentration in urban air. *Atmos. Enviro.* 2:465-475. doi:1016/0004-6981(68)90040-1.

NRC (National Research Council). 2010. Review of the department of defense enhanced particulate matter surveillance program report. Washington, DC: The National Academies Press.

Ostro, B. 1995. Fine Particulate Air Pollution and Mortality in Two Southern California Counties. *Enviro. Research.* 70:98-104. doi:10.1006/enrs.1995.1053.

Ozkaynak, H., A.D. Schatz, G.D. Thurston, R.G. Isaacs, and R.B. Husar. 1985. Relationships between Aerosol Extinction Coefficients Derived from Airport Visual Range Observations and Alternative Measures of Airborne Particle Mass. *J. Air Poll. Control Ass.* 35:1176-1185. doi:10.1080/00022470.1985.10466020.

Sanders, J.W., S.D. Putnam, C. Frankart, R. W. Frenck, M. R. Monteville, M.S. Riddle, D.M. Rockabrand, T.W. Sharp, and D. R. Tribble. 2005. Impact of illness and non-combat injury during operations Iraq Freedom and Enduring Freedom (Afghanistan). *Am. J. Trop. Med. Hyg.* 73:713–719.

Schwartz, J. 1991. Particulate air pollution and daily mortality in Detroit. *Enviro. Research.* 56:204-213.

Thach, T., C.M. Wong, K.P. Chan, Y.K. Chau, Y.N. Chung, C.Q. Ou, L. Yang, and A.J. Hedley. 2010. Daily visibility and mortality: assessment of health benefits from improved visibility in Hong Kong. *Environ. Res*. 110:617-23.

USEPA, 2016. Particulate matter. Online:http://www.epa.gov/airtrends/pm.html

Waggoner, A.P. and R. E. Weiss. 1980. Preliminary Communication: Comparison of fine particle mass concentration and light scattering extinction in ambient aerosol. Atmos. Enviro. 14:623-62.

WenZhen, G., C. RenJie, S.WeiMin, and K. Haidong. 2011. Daily visibility and hospital admission in Shanghai, China. *Biomed Environ Sci.* 24:117-121.

Yanosky, J. D.; Paciorek, C. J.; Schwartz, J.; Laden, F.; Puett, R.; Suh, H. H. Spatio-temporal modeling of chronic PM10 exposure for the Nurses' Health Study. Atmos. Environ. 2008, 42, 4047−4062.

Yanosky, J., C. Paciorek, and H. Suh. 2009. Predicting chronic fine and coarse particulate exposures using spatiotemporal models for the northeastern and Midwestern United States. *Environ. Health Perspectives.* 117:522-529. doi:10.1289/ehp.11692.

CHAPTER 1

Composition and Sources of Fine and Coarse Particles Collected during 2002-2010 in Boston, MA

Journal of the Air & Waste Management Association. 2015. 65(3): 287–297.

Abstract

Identifying the sources, composition, and temporal variability of fine ($PM_{2.5}$) and coarse ($PM_{2.5-10}$) particles is a crucial component in understanding PM toxicity and establishing proper PM regulations. In this study, a Harvard Impactor was used to collect daily integrated fine and coarse particle samples every third day for nine years at a single site in Boston, MA. A total of 1,960 filters were analyzed for elements, black carbon (BC), and total PM mass. Positive Matrix Factorization (PMF) was used to identify source types and quantify their contributions to ambient $PM_{2.5}$ and $PM_{2.5-10}$. BC and 17 elements were identified as the main constituents in our samples. Results showed that BC, S, and Pb were associated exclusively with the fine particle mode, while 84% of V and 79% of Ni were associated with this mode. Elements mostly found in the coarse mode, over 80%, included Ca, Mn (road dust), and Cl (sea salt). PMF identified six source types for $PM_{2.5}$ and three source types for $PM_{2.5-10}$. Source types for $PM_{2.5}$ included regional pollution, motor vehicles, sea salt, crustal/road dust, oil combustion, and wood burning. Regional pollution contributed the most, accounting for 48% of total $PM_{2.5}$ mass, followed by motor vehicles (21%) and wood burning (19%). Source types for $PM_{2.5-10}$ included crustal/road dust (62%), motor vehicles (22%), and sea salt (16%). A linear decrease in PM concentrations with time was observed for both fine (-5.2%/yr) and coarse (-3.6%/yr) particles. The fine-mode trend was mostly related to oil combustion and regional pollution contributions. Average $PM_{2.5}$ concentrations peaked in summer (10.4 μg/m3) while $PM_{2.5-10}$ concentrations were lower and demonstrated little seasonal variability. The findings of this study show that $PM_{2.5}$ is decreasing more sharply than $PM_{2.5-10}$ over time. This suggests the increasing importance of $PM_{2.5-10}$ and traffic-related sources for PM exposure and future policies.

Introduction

In numerous epidemiological studies, exposure to airborne particulate matter (PM) has been associated with increased mortality as well as several adverse respiratory, cardiovascular, and neurological conditions (Pope and Dockery, 2006; Roberts et al. 2013). In many such studies, exposure is usually characterized based on measured mass concentration of particles within specific size ranges. Typically, these include particles with an aerodynamic diameter of less than 10 μm (PM_{10}), less than 2.5 μm ($PM_{2.5}$), and between 2.5 and 10 μm ($PM_{2.5-10}$), also known as inhalable, fine, and coarse particles, respectively. Though valuable, this approach does not take into account the chemical compositions of particles and is therefore unlikely to tell the entire story as it relates to human health effects resulting from airborne particle exposure. Recent literature suggests that chemical components such as metals, elemental carbon, organic carbon compounds, among others, may play an important role in particle toxicity (Fanning et al. 2009; Lippmann, 2010). Epidemiological studies have provided some evidence about the importance of this particle composition, as is the case in a new study showing an association between autism spectrum disorder and exposure to airborne metals and diesel particles (Roberts et al. 2013). Other studies have linked components such as sulfur, copper, nickel, zinc, organic carbon (OC), and black carbon (BC), either alone or in mixtures, to increased cardiovascular disease and mortality (Vedal et al. 2013; Flemming et al. 2013; Valdes et al. 2012; Lippmann & Chen, 2009). Clinical and toxicological studies have also shown associations between specific PM components and physiological outcomes (Araujo et al. 2010). To date, a consensus has not surfaced as to precisely which constituents elicit specific outcomes.

Due to its chemical and biological composition, residence time, and ability to penetrate deep into the lung, $PM_{2.5}$ has received deserved attention in the media as well as within the political

and scientific arenas. This is reflected by the 2012 revision of the U.S. National Ambient Air Quality Standards (NAAQS) for PM, in which the primary annual $PM_{2.5}$ standard was lowered from 15.0 to 12.0 $\mu g/m^3$. Also, clinical and toxicological studies have reported that coarse particles resulting from road dust (mixed debris from brake wear, tire wear, road abrasion, and biological and geological matter) can be as toxic as fine particles on a mass basis (Thorpe and Harrison, 2008; Flemming, 2012). As the role of particle composition in producing toxicity is uncovered, it is increasingly important to investigate the compositional differences between $PM_{2.5}$ and $PM_{2.5-10}$ as well as identify their sources. This is of particular importance in urban settings, where traffic-related PM is higher and coarse particles are largely made up of re-suspended road dust (Manoli et al. 2002).

Studies aimed at understanding the origin of ambient PM have been conducted in various cities around the world. In some studies, source apportionment was conducted without considering coarse particles (Kim et al. 2005; Gugamsetty et al. 2012). While in other studies, fine and coarse particles are not collected concurrently, or are not collected in areas that reflect large-scale urban air (Khodeir et al. 2012; Davy et al. 2012). When fine and coarse PM is measured concurrently, source apportionment studies are still often limited in terms of their sample size and study length (Gietl et al. 2009; Dordevic et al. 2012; Clements et al. 2014; Contini et al. 2014); analyzing fewer than 200 samples and spanning a few years or less. The objective of this study is to analyze nearly 2,000 daily integrated particle samples collected every third day for a nine year period in order to investigate the composition of $PM_{2.5}$ and $PM_{2.5-10}$ at a single urban monitoring site (Boston, MA). Additionally, we aim to identify and quantify the source contributions of $PM_{2.5}$ and $PM_{2.5-10}$ as well as explore their temporal trends. With greater knowledge of the source and compositional differences between these two PM fractions, and with better insight as to the annual trends and

seasonal variability of such concentrations, epidemiologists will be better equipped to understand the ensuing health implications of PM exposure. Finally, we will evaluate the seasonal and temporal tends in the fine- and coarse-mode during the sampling period and investigate their relation to changes in sources contributions. This information is valuable in enabling better decision making concerning PM regulations.

Methods

Particle sampling and chemical analysis

Daily PM samples were collected from 2002-2010 at the Harvard supersite in Boston, Massachusetts, with the exception of a six-month period from 06/2009 – 01/2010 when monitoring equipment became unavailable. The Boston supersite is located atop the six-story Countway Library building of the Harvard Medical School, and sits within one block from a four-lane roadway as well as near two major highways; namely, Interstate 90 (I-90) which is approximately 1.5 km to the north and Interstate 93 (I-93) which is approximately 3 km to the south.

A total of 980 $PM_{2.5}$ and 980 PM_{10} daily integrated samples were collected concurrently every third day on 37 mm Teflon filters using Harvard Impactors (Marple, 1987). Filters, including blanks, were weighed on an electronic microbalance (MT-5 Mettler Toledo, Columbus, OH) prior to and after field measurements, after being equilibrated for a period of 48 hours in particle-free room of controlled temperature (22±5^{o}C) and relative humidity (40±5%). To eliminate the effects of static charge, the filters were passed over alpha ray sources prior to each weighing. Following gravimetric analysis, Teflon filters were analyzed using X-Ray fluorescence (XRF) spectroscopy (XRF, Model Epsilon 5, PANalytical, The Netherlands) to determine the elemental composition of the PM (USEPA, 1999). A total of 48 elements were measured. The elements measured were

those which are standard for XRF analysis due to their detectability using this measurement technique. Quality Assurance/Quality Control of XRF analyses is available in Kang et al., 2014. Black carbon (BC) concentrations were measured using a single (λ=880 nm) channel aethalometer (Model AE-16, Magee Scientific, Berkeley, CA). For days when aethalometer data were not available we measured BC using a Smokestain Reflectometer (Model M43D, Diffusion Systems Ltd., United Kingdom). $PM_{2.5}$ organic carbon (OC) measurements were collected from 2007 to 2010 using a semi-continuous carbon aerosol analyzer (Model 3, Sunset Laboratory, Tigard, OR), which uses a carbon-impregnated parallel plate organic denuder designed to remove gaseous organic compounds upstream of the collection filter (Kang et al. 2010). The OC measurements consisted of 357 samples. Blank medians and limits of detection (LOD) for each component used in this work are available in the supplementary materials. All analyses were conducted at the Harvard School of Public Health.

Mass closure analysis and annual trends

To perform mass closure analyses, we converted the molar masses of each element into the molar masses of their common oxides, since they rarely exist as pure elements in the environment. The oxides we accounted for included Al_2O_3, SiO_2, K_2O, CaO, TiO_2, FeO, Fe_2O_3, and ZnO. The iron oxides FeO and Fe_2O_3 were considered to be present in roughly equal amounts (Taylor, 1964). Additionally, S was assumed to be $(NH_4)_2SO_4$ (ammonium sulfate) while Na and Cl were assumed to be bound as NaCl (sea salt). For $PM_{2.5}$, we also accounted for BC and OC mass. Since OC measurements were available for only three years, we used the $OC/PM_{2.5}$ mass fraction calculated during this time period to conduct mass closure for this specie over the entire study duration. We also conducted mass closure when restricting all samples to the three year time period during which

OC samples were collected, however there was little impact to our results. With the exception of OC in the case of $PM_{2.5}$, mass closure analyses only accounted for the species that were included in our PMF models.

Annual trends for coarse and fine particles were assessed by fitting a trend line to average annual coarse- and fine-mode PM concentrations. To assess relative percentage annual change in PM concentrations, annual PM averages were first natural log transformed and then regressed over time. The slope of this trend line represented the relative percent annual change. To estimate the impacts of individual sources to annual fine and coarse particle trends, we performed univariate regression analyses comparing these trends with and without the inclusion of the mass contributions of each source type separately, using two regression models shown by the following equations:

$$\mathrm{Log}(PM_{ij}) = \alpha_{io} + \beta_{tio} * t + \mathrm{month}_a + \mathrm{weekday}_b \quad (1)$$

$$\mathrm{Log}(PM_{ij}) = \alpha_{ik} + \beta_{tik} * t + \beta_{fik} * f_{ikj} + \mathrm{month}_a + \mathrm{weekday}_b \quad (2)$$

where, $\mathrm{Log}(PM_{ij})$ is the natural logarithm of the mass concentration of particle size i, collected on sampling day j; β_{tio} is the time trend of PM_i concentrations before adjusting for the different source contributions; α_{io} is the intercept of the unadjusted model for size i; t is the time (in years) during which sample j was collected (e.g. t = 0 for year 2002, t = 1 for year 2003, etc.); α_{ik} is the intercept for the source contribution-adjusted model corresponding to particle size i and source k; β_{tik} is the time trend of PM_i concentrations after adjusting for the contribution of source k; f_{ikj} is the contribution of source k to the PM_i mass i on day j; and β_{fik} is the slope of f_{ikj}. In both

models we controlled for month and weekday since concentrations depend on these two variables. $Month_a$ and $Weekday_b$ are the month and weekday during which $sample_j$ was collected. The time slope, β_{tio}, equals the relative percent change of either fine or coarse particle mass per year. β_{tio} is positive when concentrations are increasing and negative when concentrations are decreasing. Furthermore, β_{tik} equals the relative percent trend in either fine or coarse mass concentrations, should the contributions of source k remain constant. Therefore, the impact of source k on the PM_i mass concentration trend can be estimated using the following equation:

$$\Delta t_{ik} = \beta_{tio} - \beta_{tik} \quad (3)$$

where, Δt_{ik} is the percent annual change in PM_i that is associated with the annual change in contributions of source k. If Δt_{ik} is positive, then changes in contributions of source k resulted in an increase in PM_i mass concentrations. Whereas, negative values indicate that source k was responsible for a decrease. If $\Delta t_{ik} = 0$, then source k had no effect.

Positive matrix factorization

To identify $PM_{2.5}$ and $PM_{2.5-10}$ sources and quantify their contributions, we used Positive Matrix Factorization (PMF) 3.0 software developed by the U.S. Environmental Protection Agency (Norris et al., 2008). PMF is a multivariate factor analysis tool that produces factor contributions and factor profiles based on inputted mass concentration files and estimated uncertainty files. In PMF, a speciated dataset is interpreted as a data matrix X with dimensions j by l, where j and l represent the number of samples and chemical species measured, respectively. The model defines X_{jl} as follows (Gugamsetty et al., 2012):

$$X_{jl} = \sum_{k=1}^{p} f_{kl} g_{jk} + e_{jl} \quad (4)$$

where, p is the number of factors, f is the species profile, g is the mass contribution, and e_{jl} is the error estimate for each sample. PMF enables for individual sample weighting which can account for missing or below detection limit data that is common in environmental sampling (Song et al. 2001). This constitutes a major advantage of this model. Additionally, PMF output is constrained so as to allow no negative source contribution. The goal of PMF is to minimize the object function Q, which is defined as follows (USEPA, 2008):

$$Q = \sum_{j=1}^{n} \sum_{l=1}^{m} \left[\frac{X_{jl} - \sum_{k=1}^{p} f_{kl} g_{jk}}{u_{jl}} \right]^2 \quad (5)$$

where, x_{jl} denotes measured concentrations, u_{jl} denotes estimated uncertainty, n denotes the number of samples, m denotes the number of species, and p denotes the number of factors included in the model. PMF has been described in greater detail elsewhere (Paatero, 1997; Paatero and Tapper, 1994).

In our analysis, mass and elemental concentrations and their uncertainty values for $PM_{2.5}$ and PM_{10} samples were obtained from our analytical environmental chemistry laboratory. $PM_{2.5-10}$ mass and elemental concentrations were estimated as the difference between their corresponding concentrations measured in PM_{10} and $PM_{2.5}$ samples. Since $PM_{2.5-10}$ mass and elemental concentrations were not measured directly, uncertainties for $PM_{2.5-10}$ components were assumed to be 10% of their respective concentration values. Elements with more than 50% of their concentration values below the limit of detection (LOD) were excluded from further analysis.

Concentration values below the LOD were kept as is for elements that were further analyzed. Exceptions to this exclusion criterion were Cu and Ba which we kept in our analysis because they are key tracer elements of vehicular wear debris (Lough et al. 2005; Garg et al. 2000; Hjortenkrans et al. 2007). For the remaining elements, negative concentration values were assumed to be zero, while zero uncertainty values were assumed to be 0.001 ng/m^3 (the most conservative uncertainty based on XRF data that looked at multiple elements). Of 48 elements analyzed, 17 were included for further analysis while 31 elements were excluded.

Since aethalometer measurements for PM_{10} BC were not available in this study, PM_{10} BC was predicted. To this end, we investigated the relationship between a subset of our PM_{10} and $PM_{2.5}$ BC samples, as measured by a reflectometer. This subset included 120 PM_{10} and 120 $PM_{2.5}$ samples, and was analyzed in our environmental chemical laboratory. The mass relationship between PM_{10} BC and $PM_{2.5}$ BC was slightly negative, suggesting that masking of dark BC particles by lighter particles had occurred. Masking may be more pronounced in PM_{10} since it contains more light-reflective aerosols such as crustal minerals and salt particles. Given that a negative relationship with concurrently measured PM_{10} and $PM_{2.5}$ BC is not possible, we assumed that BC instead accounted for a negligible mass fraction of coarse particles and therefore did not include $PM_{2.5\text{-}10}$ BC as a variable in our PMF analysis.

When running PMF, we distinguished between elements whose analysis was 'bad' (signal-to-noise ratio < 0.2), 'weak' (0.2 ≤ signal-to-noise ratio < 2), and 'strong' (signal-to-noise ratio ≥ 2) (Paatero and Hopke, 2003). Species categorized as 'bad' were eliminated from our analysis, while those considered 'weak' were down-weighted by tripling their uncertainty values. 'Strong' species were included in our analysis unchanged. Extreme concentrations that could be explained by episodic events such as firework celebrations were excluded from our analysis. Additional

outliers were identified and excluded based on analysis of each species' respective concentration time-series plot. Extreme values can be very influential since they may yield false factors/sources and/or distort source profiles.

PMF was run multiple times using 4 to 8 factors for $PM_{2.5}$. For coarse particles, PMF was run using 3 to 5 factors, since fewer sources were expected for these particles. For a given model run, the converged solution with the lowest Q value in the robust mode was assessed in relation to its corresponding Q value in the non-robust mode to ensure that remaining extreme values did not overly influence the model (Paatero, 2002). The PMF solutions chosen to represent $PM_{2.5}$ and coarse species were those deemed most physically reasonable and interpretable among all assessed solutions. Factors were then named according to the consideration of their abundance of key tracer elements, seasonal variability, and day-of-the-week contributions. Rotational ambiguity in solutions was explored using the FPEAK parameter ranging from -2 to 2, with the standard values of zero being the final choice. Goodness of fit for the PMF solutions was also examined by comparing predicted and measured concentration profiles for each species and their associated Percent Mean Relative Errors (MRE). MRE is equal to the absolute value of [(Measured Concentration – Predicted Concentration) / Measured Concentration]. This produces an easily interpretable error that is in the form of a fraction of measured values. P-values reported in this study were produced from paired t-test when assessing weekday/weekend variability and from Scheffé's method for multiple comparisons when assessing seasonal variability of PMF source contributions.

Results and Discussion

Contribution of coarse particles to total PM_{10} mass and elemental concentrations

Figure 1.1 depicts the percent contribution of coarse particles to PM_{10} mass and elemental concentrations. This enables us to identify to what extent PM_{10} constituents are associated with the coarse versus fine particle mode. BC, S, and Pb were exclusively associated with $PM_{2.5}$ particles. Similarly, 84% of V and 79% of Ni were associated with fine particles.

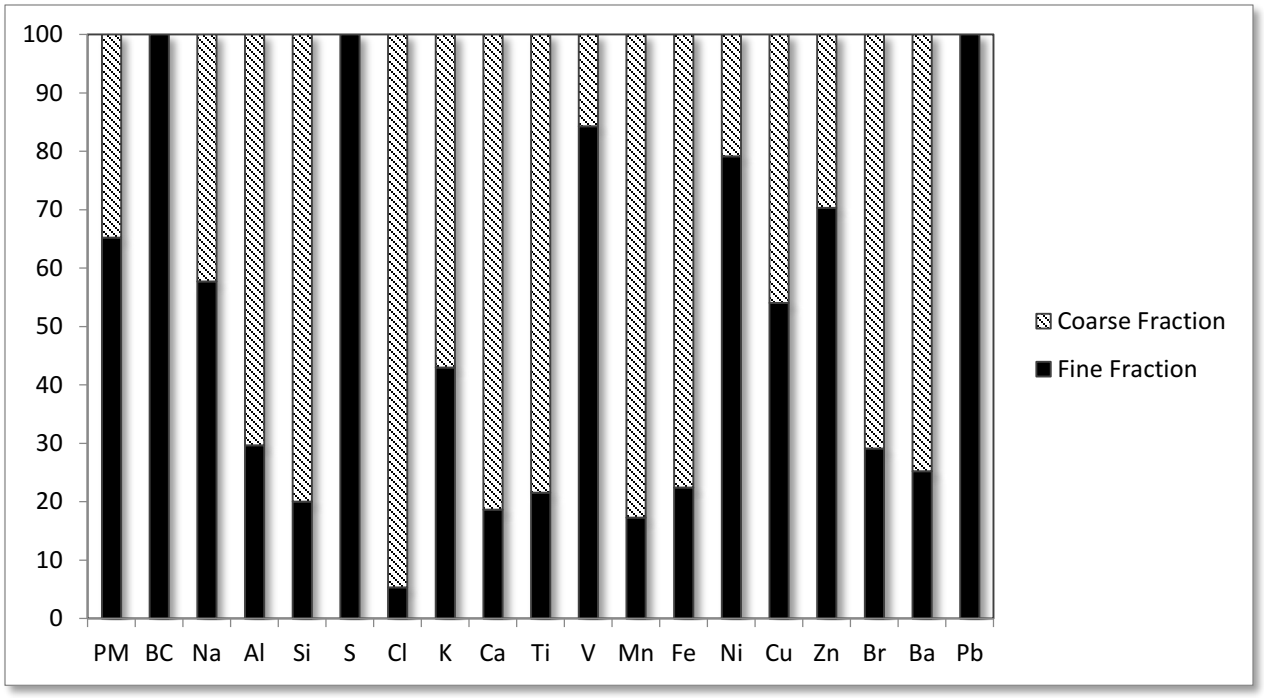

Figure 1.1. Relative contributions of coarse and fine particles to total PM_{10} mass.

Between 50 and 75% of Al, K, Br, and Ba measured in PM_{10} were contributed by the coarse mode. These elements are the major constituents of crustal and road dust. The elements that are mostly found in the coarse mode, over 75%, included the crustal and road dust elements Ca, Si, Ti, Fe, and Mn as well as Cl (sea salt). Hueglin et al. (2005) found similar results for coarse particles, except for K and Ti, which were reportedly mostly in the fine-mode. In terms of total

mass, the coarse-mode accounted for about one-third (5.0 μg/m^3) and the fine-mode accounted for two-thirds (9.5 μg/m^3) of PM_{10} (14.5 μg/m^3) mass.

Mass Closure Analysis

Figure 1.2 depicts mass closure results for coarse- and fine-mode particles. The elements selected for PMF analysis, together with OC and BC, accounted for 98% of total measured $PM_{2.5}$ mass. This percentage takes into account the elements Al, Si, K, Ca, Ti, Fe, and Zn in their common oxidized forms (labeled as metal oxides), as well as Na and Cl (labeled as sea salt). S as an oxidized sulfate was also considered (labeled as ammonium sulfate). The majority of fine-mode mass was made up of $(NH_4)_2SO_4$ and OC, accounting for 44 and 40% of total mass, respectively. BC, metal oxides, and sea salt accounted for 7, 5, and 2% of mass, respectively. While only 2% of mass was characterized as unknown, it is likely that our mass closure for $(NH_4)_2SO_4$ represents an overestimate of this fraction as not all sulfate particles exist as ammonium sulfate, but also as Na_2SO_4. If we assume all $(NH_4)_2SO_4$ instead exists as Na_2SO_4, our unknown fraction increases to 14%. The unknown mass of $PM_{2.5}$ is likely made up of unmeasured ammonium nitrate particles, trace metals, organic compounds, and crystalline water that we did not consider in this work.

For coarse particles, our study elements represented 41% of total coarse mass. As with the fine-mode, the same elements were considered in their compound forms. Metal oxides and sea salt were both enriched in the coarse mode relative to the fine mode, accounting for 28 and 8% of total coarse mass, respectively. This was expected as wind-blown soil, dust, and sea salt minerals tend to be larger particles. Other inorganics, which included Mn, Cu, Br, and Ba, accounted for 5% of total mass.

(a)

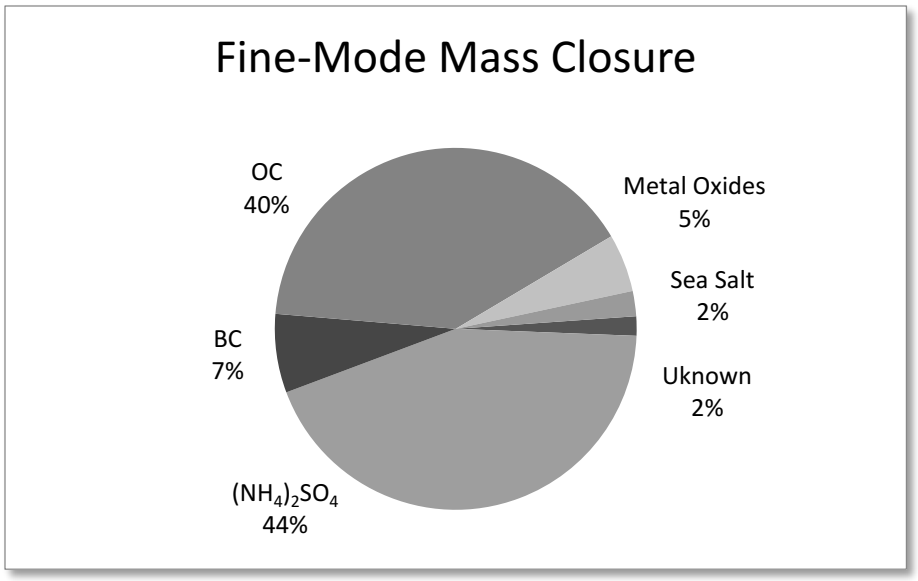

(b)

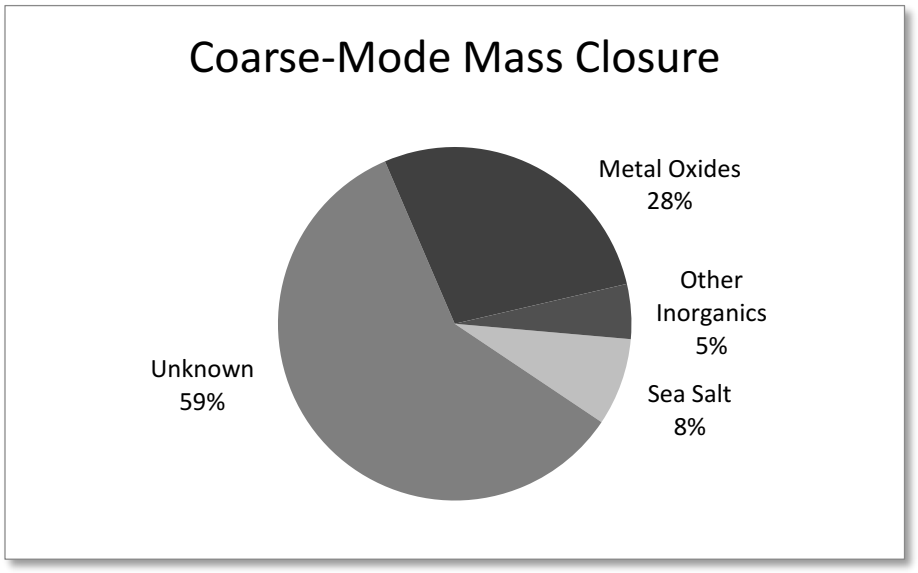

Figure 1.2. Mass closure results for (a) fine and (b) coarse particles.

As S was not present in the coarse mode, we expect that the remaining mass fraction of coarse particles can be explained by unaccounted for soil organics, nitrate compounds, trace elements, carbonates/bicarbonates, and biological aerosols. This is similar to other analyses, which

have shown trace elements, nitrates, elemental carbon, and organic matter to account for 24-40%, and unknown constituents 31-50%, of coarse mass, respectively (Hueglin, 2005). As described earlier, particle masking may have also led to an under prediction of BC in the coarse mode. Therefore, BC may comprise some of our unknown mass fraction.

Source contributions of fine-mode particles

PMF analysis identified six factors for fine-mode particles. These included regional pollution, motor vehicles, sea salt, crustal/road dust, oil combustion, and wood burning. The concentrations and source characterizations of the $PM_{2.5}$ constituents are presented in Table 1.1. Regional pollution was the major source contributor to $PM_{2.5}$ mass, accounting for 48%. This source type was characterized using sulfur as a tracer, since the atmospheric conversion of sulfur dioxide to sulfate particles is sufficiently slow that sulfate is not generated locally, but usually over long-range transport (Wojcik and Chang, 1997; Kang et. al 2010; Seinfeld and Pandis, 2006). Our analysis also shows sodium to be associated with regional pollution. This is likely a result of chloride depletion chemistry taking place in the atmosphere during transport and on sampling filter surfaces (Zhao and Gao, 2008; McInnes et al. 2012; Lee et al. 2011). That is, as acid sulfate particles H_2SO_4 and NH_4HSO_4 are transported (or collected on the Teflon filters) they react with neighboring NaCl molecules to form Na_2SO_4 and HCl. Since HCl is a gas it re-enters the air, leaving only Na_2SO_4 to be measured on the filter. Similar chloride depletion can occur through reactions involving nitrate and organic acids (Kerminen, 1998; Zhao and Gao, 2008; Kouyoumdjian et al. 2006). These phenomena, either alone or in combination, could be responsible for the association we observed between S and Na.

Regional pollution showed seasonal variability, ranging from 3.3 to 6.3 μg/m^3. Summer showed the highest source contribution, with a difference in contribution that was statistically significant from all other seasonal contributions ($p<0.05$). No other season had a significantly different contribution relative to other seasons. The summer peak of this source contribution was expected as atmospheric photochemical activity is at its peak during summer months, which translates to an increased conversion rate of emitted sulfur dioxide to sulfate particles. As expected, there was no difference in this source contribution between weekdays and weekends.

Table 1.1. Source contributions to fine particle mass and elemental concentrations (ng/m^3) at Harvard Supersite.

	Regional Pollution	Motor Vehicles	Sea Salt	Crustal/ Road Dust	Oil Combustion	Wood Burning	Estimate	Measured	%MRE
BC	105	350	1	3	81	43	583	658	12
Na	69	0	18	5	30	21	174	195	11
Al	9	7	0	29	1	1	47	47	1
Si	3	12	0	52	0	0	67	67	0
S	729	151	2	10	66	12	971	980	1
Cl	0	1	14	0	0	0	15	15	2
K	6	0	1	7	0	23	37	37	0
Ca	1	9	1	13	4	1	28	29	3
Ti	0	1	0	1	0	0	3	3	0
V	0	0	0	0	3	0	3	3	1
Fe	0	37	0	17	6	0	61	61	1
Ni	0	0	0	0	2	0	2	3	2
Cu	0	2	0	1	0	1	3	4	8
Zn	0	5	0	0	2	3	10	11	9
Pb	1	1	0	1	1	1	5	5	9
$PM_{2.5}$	4,220	1,836	48	383	663	1,648	8,798	9,353	6

The motor vehicles factor was the second highest contributor to $PM_{2.5}$ mass, accounting for 21%. This source accounted for 60% of BC mass and was also characterized by the elements Zn, Fe, Ti, and Cu. Seasonal variability was observed, ranging from 1.5 to 2.2 μg/m^3. The highest

source contribution was for fall season, followed by spring and then winter. Fall and summer were significantly different than spring, and fall was also significantly different than winter ($p<0.05$). Wind speed, boundary height, and precipitation partially accounted for these differences. Motor vehicles contributed greater during weekdays than weekends ($p<0.0001$) because vehicle emissions increase with weekday commuter traffic.

The source contribution of wood burning followed that of motor vehicles, accounting for 19% of $PM_{2.5}$ mass. This factor was characterized using K as a tracer, as this element is emitted during the combustion of wood and other forms of biomass (Fine et al. 2001; Khalil and Rasmussen, 2003). Wood burning is sometimes associated with quantities of Cl as well. That there is no Cl associated with this source type in our analysis may be due to the close proximity of the Atlantic Ocean, which serves as a much more dominant source of Cl. Alternatively, it could be due to chloride depletion chemistry, suggesting that wood burning sources could be originating from further away. The source contribution ranged from 1.4 to 2.4 $\mu g/m^3$, showing a statistically significant increase in contribution during winter relative to all other seasons ($p<0.05$). This increase is likely a result of greater firewood use for residential heating during the cold season. A statistically significant increase in wood burning source type was also observed during weekends relative to weekdays ($p<0.001$). As residential heating is an at-home activity, this increase is likely a reflection of the increase in hours spent at home during weekends in addition to outdoor activities such as barbeques.

Oil combustion factor represented 8% of $PM_{2.5}$ mass and was characterized by its large contribution to oil tracer elements Ni and V. Oil combustion varied by season and ranged from 0.5 to 0.9 $\mu g/m^3$, with a significantly higher contribution during winter months compared to all other seasons ($p<0.05$). Sources of oil combustion include oil-fired power plants, ships and ferries, as

well as homes and commercial buildings (for heating). The higher contribution of oil combustion during winter is likely due to wintertime heating of homes and buildings that burn oil, as opposed to natural gas or biomass, for fuel (Spengler, 1983). This is expected as a large proportion of Massachusetts residents (31%) tend to use oil for space heating (EIA, 2014). This factor showed no significant difference in contribution when comparing weekdays and weekends, even when looking only within winter months.

Crustal/road dust factor accounted for 4% of $PM_{2.5}$ mass and was mostly associated with Al, Si, Ca, and Ti. Often, Zn and Fe are more heavily associated with road dust, suggesting that this source type may be a mixture of crustal matter and road dust. The contribution of this source type varied by season and ranged from 0.3 in fall to 0.5 $\mu g/m^3$ in spring. Both spring and summer showed statistically high crustal/road dust contributions ($p<0.05$). The higher source contribution during spring can be explained by differences in seasonal wind speed. Mean wind speed was highest during the spring (5.3 m/sec), with significant differences ($p<0.05$) compared to fall (4.7 m/sec) and summer (4.3 m/sec). However, wind speed cannot explain the high source contribution during the summer as this season had the lowest mean wind speed. A likely factor influencing summertime contribution is temperature. During summer months, elevated temperatures lead to soil dryness, which contributes to particle re-suspension. This factor also demonstrated a statistically significant increase in contribution during weekdays relative to weekends ($p<0.001$). This increase is likely due to an increase in particle re-suspension from higher roadway traffic by commuters during the work week.

Sea salt factor contributed the least, accounting for less than 1% of total $PM_{2.5}$ mass. As sea salt is composed mainly of Na and Cl, these elements are used as tracers of this source. However, in our analysis, sea salt was characterized mostly by the presence of Cl, as Na was better

associated with regional sulfur as described earlier. Sea salt contribution ranged from zero to 0.1 $\mu g/m^3$. While the highest contributions occurred during fall and spring, followed by winter, these differences were mostly not significant. Except for the fall season, the sea salt contribution was higher during seasons of higher mean wind speed. Elevated salt contributions during winter and spring may also be due to the use of sea salt as a deicing agent along roadways and sidewalks. There was no significant difference in sea salt contribution between weekdays and weekends, as expected.

Source contributions of coarse-mode particles

PMF analysis identified three factors for coarse-mode particles. These included crustal/road dust, motor vehicles, and sea salt. The concentrations and source characterizations of $PM_{2.5-10}$ constituents are presented in Table 1.2. Crustal/road dust was by far the major contributor to coarse particle mass, accounting for 62%, and was characterized by Al, Si, K, Fe, Ba, Zn, Mn, and Ti. While K in the fine mode is mostly associated with wood burning, in the coarse fraction it is related to road dust and soil. Though Fe is a major crustal element, the Fe/Si ratio of this source type was considerably higher than that of earth's crust, suggesting a mixture of both soil and road dust (Taylor, 1964). The enrichment of Fe in road dust is related to traffic, since this element is typically present in brake-wear dust (Thorpe and Harrison, 2008; Pant and Harrison, 2013). The source contribution of this factor showed seasonal variability, ranging from 2.3 to 3.4 $\mu g/m^3$. Spring and summer had significantly high crustal/road dust contributions relative to fall and winter months ($p<0.05$). As with fine particles, the reason is likely due to high wind in the spring and elevated temperatures during summer. Also, partially thawed snow and wet road surfaces during winter months may reduce particle re-suspension. This factor demonstrated a significant increase

in contribution during weekdays relative to weekends ($p<0.0001$). Similar to PM_{25}, this can be explained by an increase in re-suspended particles from increased roadway traffic during the work week.

The motor vehicles factor contribution was much less than that of crustal/road dust, accounting for 22% of total coarse mass. This factor was characterized by the elements Cu, Ca, and Br, which are associated with gasoline and oil combustion as well as tire and brake wear (Lough et al. 2005; Garg et al. 2000; Hjortenkrans et al. 2007). In the context of vehicle emissions, Ca is related to combustion of motor oil additives and lubricant oil, although its presence could also suggest some overlap with the crustal/road dust factor (Lough et al. 2005; Garg et al. 2000; Cadle et al. 1997). Counter to $PM_{2.5}$, the motor vehicles source showed no seasonal variability for coarse particles, remaining at 0.7 $\mu g/m^3$ across all seasons. However, the contribution was significantly higher during weekdays than weekends ($p<0.001$), again reflecting decreased vehicle traffic during weekends.

In contrast to our $PM_{2.5}$ analysis, sea salt contributed substantially to coarse particle mass, accounting for 16% of total mass. This is expected since sea salt particles primarily exist in the coarse mode (Harrison, 1983; Herner, 2006). Sea salt contribution varied by season ($p<0.0001$) and ranged from 0.4 to 1.5 $\mu g/m^3$. The greatest contribution occurred during winter months, which was significantly different relative to all other seasons ($p<0.05$). Summer also showed a significantly lower contribution compared to fall ($p<0.05$). This could be due to higher wind speeds during other months (summer had the lowest average wind speed), leading to greater ocean turbulence and the increased aerosolization of salt particles (Contini et al. 2010). Additionally, the increased contribution during winter could be due to the wintertime application of sea salt as a

deicing agent to roadways and sidewalks. As expected, there was no significant difference in source contribution between weekdays and weekends.

Table 1.2. Source contributions to coarse particle mass and elemental concentrations (ng/m^3) at Harvard Supersite

	Crustal/ Road Dust	Motor Vehicles	Sea Salt	Estimated	Measured	%MRE
Na	21	17	99	137	155	12
Al	98	14	5	117	115	2
Si	235	40	0	275	273	1
Cl	3	9	245	258	263	2
K	38	8	5	51	52	1
Ca	24	101	0	125	125	0
Ti	9	3	0	12	12	0
Mn	2	1	0	4	4	12
Fe	143	56	4	203	211	4
Cu	2	2	0	3	3	6
Zn	2	2	0	4	5	10
Br	1	1	0	2	3	21
Ba	11	9	1	21	27	21
$PM_{2.5-10}$	2,782	981	732	4,495	5,049	11

Annual and Seasonal PM

Annual averages of coarse- and fine-mode particles as well as source contributions to annual trends were assessed using Equations 1-3. Depictions of annual average trends for both particle size fractions are presented in Figure 1.3. A significant linear decrease in PM concentrations with time was observed for both coarse ($p<0.0001$) and fine ($p<0.0001$) particles, though the decrease was more pronounced for fine particles. Average annual $PM_{2.5}$ concentrations were highest (11.1 μg/m^3) in 2002 and lowest (7.2 μg/m^3) in 2010, showing an annual average decrease of 5.2% per year over our study period. This was mostly due to decreases in oil

combustion and regional pollution source types, which accounted for a decrease equal to 59 and 47% of the annual decrease, respectively. The decrease in oil combustion sources could be reflecting the replacement of oil with natural gas for domestic heating. The motor vehicle source accounted for 30% of the annual decrease while crustal/road dust contributed to only a 4% decrease. Wood burning contributed positively, with an annual increase of 14%. That is, the contribution of this source increased over our study period, counteracting the decreases seen across other sources. Sea salt did not affect the annual trend. After controlling for our various source types, a 26% increase in annual PM concentrations is unexplained. This could be due to PM constituents not included in our PMF analysis, such as bioaerosols and ammonium nitrate, as well as uncertainties in our PMF model estimates.

Average annual $PM_{2.5\text{-}10}$ concentrations were at a maximum (5.8 $\mu g/m^3$) in 2003 and a minimum (4.3 $\mu g/m^3$) in 2009. The average annual decrease for this mode was 3.6% per year. The factor that contributed most to this trend was crustal/road dust, accounting for 17% of the annual decrease, while sea salt and motor vehicles contributed negligibly to the trend. This left 83% of the annual decrease unexplained by our source types. This is not surprising given our mass closure and PMF analyses, which showed a high fraction of unexplained mass and higher %MRE values for coarse particles, respectively.

In general, the temporal trends observed in this study can be explained by a number of factors such as the replacement of oil with natural gas for wintertime heating as well as the replacement of old with new vehicles in the city. Regarding traffic emissions, for example, in recent years the Massachusetts Bay Public Transportation system replaced many old buses with a new fleet. Just this year, Harvard University also replaced its entire M2 bus fleet with new

automobiles. Additionally, many taxi companies in Boston are now using hybrid vehicles, which produce fewer tailpipe emissions.

(a)

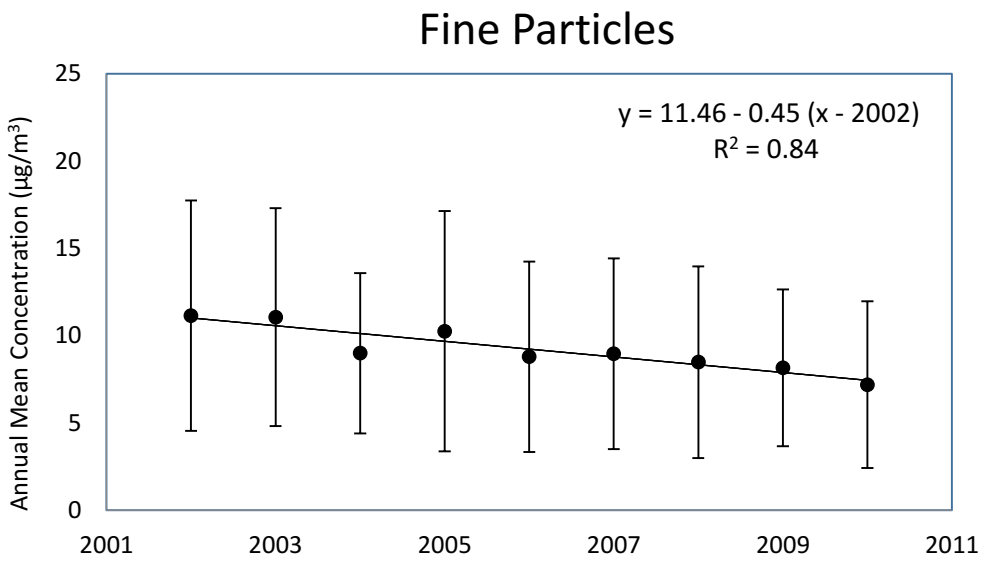

(b)

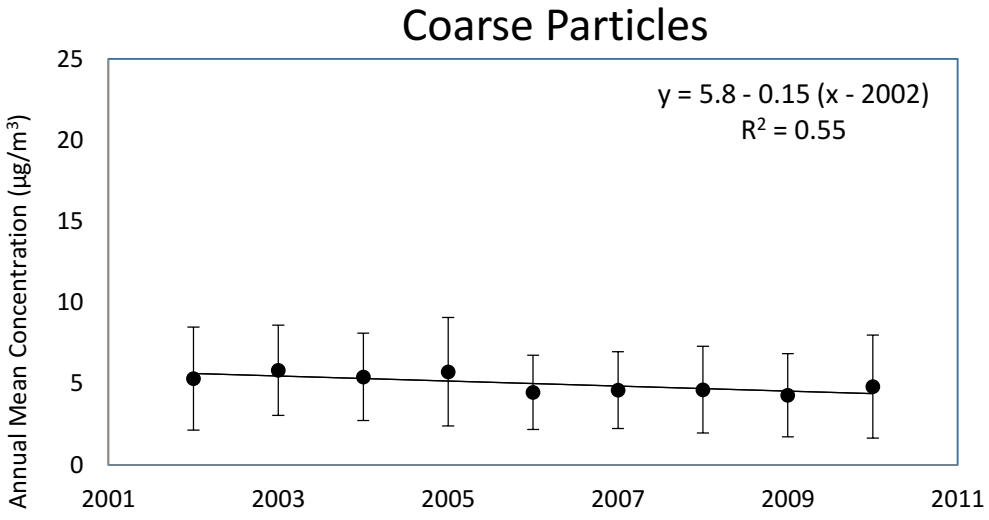

Figure 1.3. Annual average concentrations and standard deviations of (a) fine and (b) coarse particles.

With regard to long range transport, increased compliance with acid rain regulations has reduced sulfur emissions over time. The extent to which the source contribution trends in this study are generalizable to other locations depends on the specific source and size fraction of interest. Fine particles, particularly those originating from long range sources, are more likely to reflect concentrations observed elsewhere in the north east. Coarse particles concentrations, by contrast, are known to be more geographically heterogeneous given there rapid settling velocity, and are therefore difficult to extrapolate to other locations (USEPA, 2009).

For seasonal trends, the fine-mode demonstrated variability while the coarse-mode did not. Average fine particle concentrations were highest during summer (11.7 $\mu g/m^3$), followed by winter (9.6 $\mu g/m^3$). During summer, there was a statistically significant difference in concentrations relative to all other seasons, while wintertime concentrations were significantly different only when compared to spring ($p<0.05$). Spring and fall had average concentrations of 8.0 and 8.2 $\mu g/m^3$, respectively. This is consistent with our PMF results and is likely due to the increased atmospheric photochemistry that occurs during summer. Elevated wintertime levels are likely due to increased oil combustion and wood burning for heating. While coarse particle concentrations were highest in spring (5.2 $\mu g/m^3$) and lowest in winter (4.7 $\mu g/m^3$), seasonal differences for this size fraction were not significant. The slightly elevated concentration observed during spring may nonetheless be attributable to the increased re-suspension of particles by wind as this season corresponded to the highest average wind speed.

(a)

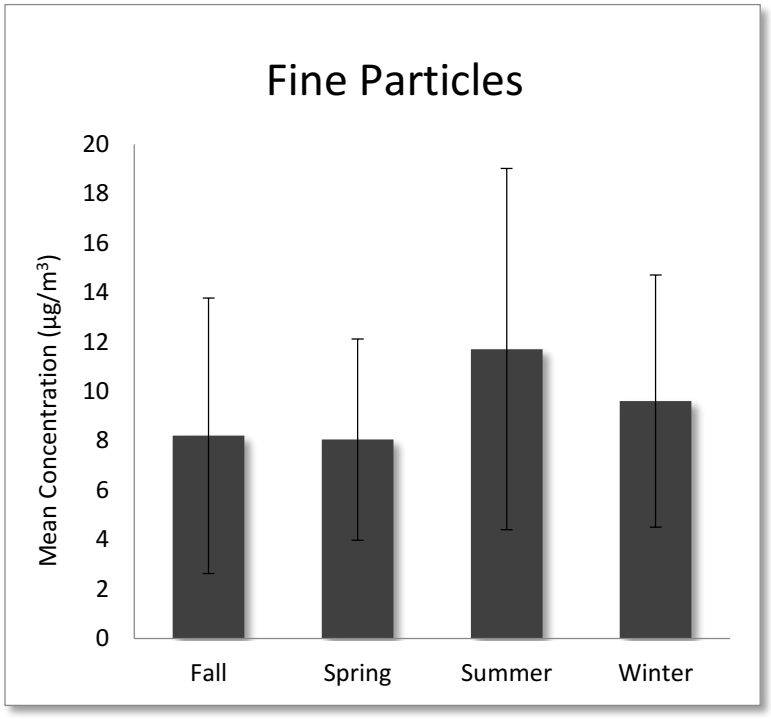

(b)

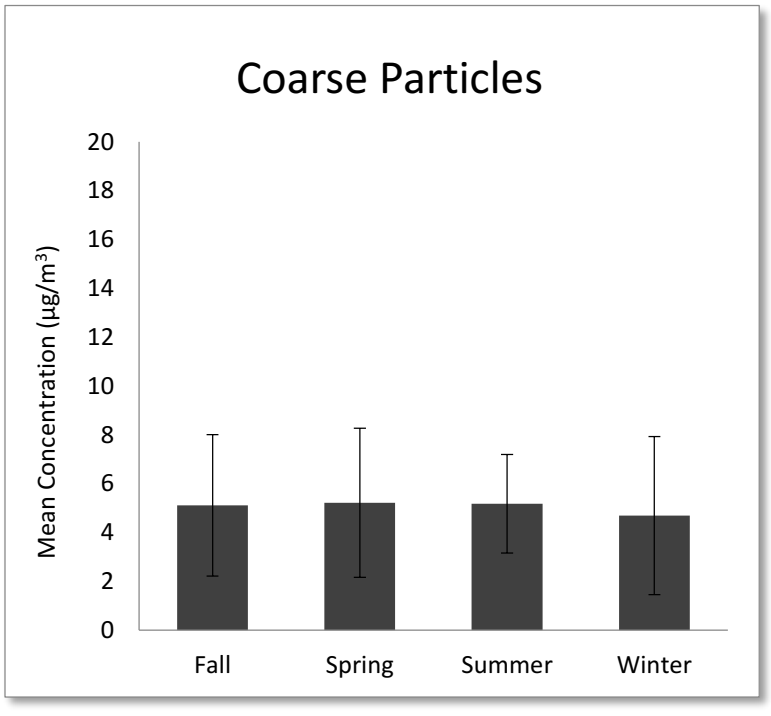

Figure 1.4. Seasonal average concentrations of (a) fine and (b) coarse particles.

Conclusions

The chemical compositions and sources of ambient fine- and coarse-mode particles were studied in Boston over a nine year period. The primary strengths of this study are the simultaneous collection of fine and coarse particles as well as the extended period over which samples were collected. Our results suggest that coarse and fine particles have very different elemental compositions, reflecting their different sources and mechanisms of formation, as well as different annual trends and seasonal variation.

Fine particles were associated mostly with regional pollution and accounted for two-thirds of PM_{10} mass, while coarse particles accounted for one-third of PM_{10} mass and consisted mostly of crustal/road dust elements. The coarse-mode contribution to PM_{10} reported in our study is similar to that reported in many urban environments (Marloes et al., 2012; Querol et al., 2004). Particularly noteworthy was the exclusive association between the combustion products S and BC in the fine particle mode. Pb was also associated exclusively with the fine mode, while V and Ni were highly associated with this mode. These findings are similar to those of Hueglin et al. (2005) who reported over 80% of both Pb and sulfate, and over 60% of V and N, to be present in the fine mode in the near-city environment. The elements that were mostly found in the coarse mode included the crustal and road dust elements Ca, Si, Ti, Fe, and Mn, as well as Cl (sea salt), similar to that reported by Hueglin et al. (2005). The assessment of coarse particle composition and concentration on a location-by-location basis is important in understanding the potential health implications to a given population, since coarse particles often originate from local sources and are known to be geographically heterogeneous, in contrast to fine particles which are more homogeneously dispersed over space (USEPA, 2009).

For mass closure, the species we analyzed accounted for 98% of total $PM_{2.5}$ mass and 41% of total $PM_{2.5-10}$ mass. The majority of fine-mode mass was made up of OC and sulfate. For the coarse mode, particles were more enriched with metal oxides and sea salt as compared to the fine mode, accounting for 28 and 8% of total coarse mass, respectively. This was expected as wind-blown soil, dust, and sea salt minerals tend to be larger particles. That coarse particles are enriched with metals has implications for coarse PM toxicity, as such metals have been implicated as key components responsible for the health effects associated with PM (Flemming et al. 2013; USEPA, 2009).

An annual decrease in PM concentrations was observed for both coarse and fine particles, though the decrease was more pronounced for fine particles. That $PM_{2.5}$ is decreasing more sharply over time than $PM_{2.5-10}$ suggests that $PM_{2.5-10}$ and traffic-related sources will be of increasing importance to PM exposure and environmental policies as we move into the future. The annual decline for $PM_{2.5}$ was mostly due to decreases in regional pollution and oil combustion source types. This decline in major source contributions of $PM_{2.5}$ appears to reflect the success of environmental acid rain policies to curb sulfur emissions as well as a gradual shift towards cleaner sources of fuel, such as natural gas, as the energy market changes. For $PM_{2.5-10}$, crustal/road dust contributed most to the annual decline. Fine-mode particles demonstrated seasonal variability, with the highest average concentrations occurring during summer and winter months. By contrast, coarse-mode particles did not exhibit seasonal variability.

PMF analysis identified six source types for $PM_{2.5}$ and three source types for coarse particles. Fine particle concentrations were predicted well by our factor analysis, as demonstrated by their low MREs. Regional pollution contributed the most to $PM_{2.5}$ concentrations, accounting for 48% by mass, followed by motor vehicles (21%), wood burning (19%), oil combustion (8%),

crustal/road dust (4%), and sea salt (<1%). These results are similar to those reported elsewhere in the U.S. (Lee et al. 2011; Kim et al. 2004; Kim et al. 2005). Regional pollution accounting for nearly half of fine particle mass lends merit to ongoing efforts to curb sulfur emissions, such as the U.S. Department of Energy's action in 2011 to convert the Northeast Home Heating Oil Reserve to ultra-low-sulfur diesel (ULSD) as well as the decisions by several northeastern states to begin requiring ULSD for heating (EIA, 2014). Overwhelmingly the greatest contributor to coarse mass was crustal/road dust (62%), followed by sea salt (16%) and motor vehicles (22%). These finding are similar to other studies which have found road dust and sea salt to contribute substantially to coarse-mode particles (Harrison, 1983; Herner, 2006).

Acknowledgements

This work was supported by the EPA Center for Particle Health Effects at the Harvard School of Public Health (grant RD-83479801-2), the National Institute of Environmental Health Sciences (NIEHS) Program Grant (P30-ES000002), and Ambient Particles and Cardiac Vulnerability in Humans Grant (P01-ES009825). However, any opinions, findings, conclusions, or recommendations expressed herein are those of the authors and do not necessarily reflect the views of the supporters. Further, our supporters do not endorse the purchase of any commercial products or services mentioned in this publication.

Bibliography

Araujo, J.A. 2010. Particulate air pollution, systemic oxidative stress, inflammation, and atherosclerosis. *Air Qual. Atmos. Health.* 4:79-93. 10.1007/s11869-010-0101-8.

Cadle, S. H., P. A. Mulawa, J. Ball, C. Donase, A. Weibel, J. C. Sagebiel, K. T. Knapp, and R. Snow. 1997. Particulate emission rates from in-use high-emitting vehicles recruited in Orange County, California. *Environ. Sci. Tech.* 31: 3405-3412. doi: 10.1021/es9700257.

Cassee, F.R., M.E. Heroux, M.E. Gerlofs-Nijland, and F.J. Kelly. 2013. Particulate matter beyond mass: recent health evidence on the role of fractions, chemical constituents and sources of emission. *Inhal. Toxicol*. 25: 802-812. doi:10.3109/08958378.2013.850127.

Clements, N., J. Eav, M. Xie, M. P. Hannigan, S. L. Miller, W. Navidi, J. L. Peel, J. J. Schauer, M. M. Shafer, and J. B. Milford. 2014. Concentrations and source insights for trace elements in fine and coarse particulate matter. *Atmos. Environ.* 89:373-381. doi:10.1016/j.atmosenv.2014.01.011.

Contini, D., D. Cesari, A. Genga, M. Siciliano, P. Ielpo, M.R. Guascito, M. Conte. 2014. Source apportionment of size-segregated atmospheric particles based on the major water-soluble components in Lecce (Italy). *Sci. Tot. Environ*. 472: 248-261. doi:10.1016/j.scitotenv.2013.10.127.

Contini, D., A. Genga, D. Cesari, M. Siciliano, A. Donateo, M. C. Bove, and M. R. Guascito. 2010. Characterisation and source apportionment of PM10 in an urban background site in Lecce. *Atmospheric Research*. 95:40-54. doi:10.1016/j.atmosres.2009.07.010.

Davy, P.K., T. Ancelet, W.J. Trompetter, A. Markwitz, and D.C. Weatherburn. 2012. Composition and source contributions of air particulate matter pollution in a New Zealand suburban town. *Atmos. Poll. Research*. 3:143-147. doi:10.5094/APR.2012.014.

Dordevic, D., A. Mihajlidi-Zelic, D. Relic, Lj. Ignjatovic, J. Huremovic, and A.M. Stortini. 2012. Size-segregated mass concentration and water soluble inorganic ions in an urban aerosol of the Central Balkans (Belgrade). *Atmos. Environ.* 46:309-17. doi:10.1016/j.atmosenv.2011.09.057.

Energy Information Administration (EIA). Massachusetts state profile and energy estimates. Available at: http://www.eia.gov/state/?sid=MA 2014 [Accessed 26 September 2014].

Fanning, E.W., J.R. Froines, M.J. Utell, M. Lippmann, G. Oberdorster, M. Frampton, J. Godleski, and T.V. Larson. 2009. Particulate matter (PM) centers (1999-2005) and the role of interdisciplinary center-based research. *Environ. Health Prospectives.* 117:167-174. doi:10.1289/ehp.11543.

Fine, P.M., G.R. Cass, and B.R.T. Simoneit. 2001. Chemical characteristics of fine particle emissions from the fireplace combustion of woods grown in the southern United States. *Environ. Sci. Tech.* 36: 1442-1451. doi:10.1021/es001466k.

Flemming, C.R., M. Heroux, M.E. Gerlofs-Nijland, and F.J. Kelly. 2013. Particulate matter beyond mass: recent health evidence on the role of fractions, chemical constituents and sources of emission. *Inhal. Toxicol*. 25:802-812. doi:10.3109/08958378.2013.850127.

Garg, B., S.H. Cadle, P.A. Mulawa, P.J. Groblicki, C. Laroo, and G.A. Parr. 2000. Brake wear particulate matter emissions. *Environ. Sci. & Tech.* 34: 4463-4469. doi: 10.1021/es001108h.

Gietl, J.K. and O. Klemm. 2009. Source identification of size-segregated aerosol in Munster, Germany, by factor analysis. *Aerosol Sci. Tech.* 43: 828-37.

Gugamsetty, B., H. Wei, C.N Liu, A. Awasthi, S.C. Hsu, C.J. Tsai, G.D. Roam, Y.C. Wu, and C.F. Chen. 2012. Source characterization and apportionment of PM10, PM2.5 and PM0.1 by using Positive Matrix Factorization. *Aerosol Air Qual. Research.* 12: 476–491. doi:10.4209/aaqr.2012.04.0084.

Harrison, R.M., and C.A. Pio. 1983. Size-differentiated composition of inorganic atmospheric aerosols of both marine and polluted continental origin. *Atmos. Environ.* 17:1733-1738. doi:10.1016/0004-6981(83)90180-4.

Herner, J.D, Q. Ying, J. Aw, O. Gao, and D.P.Y. Chang. 2006. Dominant mechanisms that shape the airborne particle size and composition distribution in Central California. *Aerosol Sci. Tech.* 40:827-844. doi:10.1080/02786820600728668.

Hjortenkrans, D.S.T., B.G. Bergback, and A.V. Haggerud. 2007. Metal emissions from brake linings and tires: care studies of Stockholm, Sweden 1995/1998 and 2005. *Environ. Sci. Tech.* 41:5224-5230. doi: 10.1021/es070198o.

Hueglin, C., R. Gehrig, U. Baltensperger, M. Gysel, C. Monn, and H. Vonmont. 2004. Chemical characterization of PM2.5, PM10 and coarse particles at urban, near-city, and rural sites in Switzerland. *Atmos. Environ*. 39:637-651. doi:10.1016/j.atmosenv.2004.10.027.

Kang, C.M., P. Koutrakis, and H.H. Suh. 2010. Hourly measurements of fine particulate sulfate and carbon aerosols at the Harvard-U.S. Environmental Protection Agency supersite in Boston. *J. Air Waste Manage. Assoc*. 60:1327-1334. doi:10.3155/1047-3289.60.11.1327.

Kang, C.M., S. Achilleos, J. Lawrence, J.M. Wolfson, P. Koutrakis. 2014. Interlab comparison of elemental analysis for low ambient urban PM2.5 levels. Environ. Sci. Technol. in press. doi: dx.doi.org/10.1021/es502989j. doi:10.1021/es502989j.

Khalil, M.A.K., and R.A. Rasmussen. 2003. Tracers of wood smoke. *Atmos. Environ.* 37:1211-1222. doi:10.1016/S1352-2310(02)01014-2.

Khodeir, M., M. Shamy, M. Alghamdi, M. Zhong, H. Sun, M. Costa, L.C. Chen, and P. Maciejczyk. 2012. Source apportionment and elemental composition of PM25 and PM10 in Jeddah City, Saudia Arabia. *Atmos. Poll. Research.* 3:221-240. doi:10.5094/APR.2012.037.

Kim, E., and P.K. Hope. 2004. Improving source identification of fine particles in a rural northeastern U.S. area utilizing temperature-resolved carbon fractions. *J. Geophys. Research.* 109:1984-2012. doi:10.1029/2003JD004199.

Kim, E., P.K. Hope, D.M. Kenski, and M. Koerber. 2005. Sources of fine particles in a rural Midwestern U.S. area. *Environ. Sci. Tech.* 39:4953-4960. doi:10.1021/es0490774.

Kouyoumdjian, H., and N.A. Saliba. 2006. Mass concentration and ion composition of coarse and fine particles in an urban area in Beirut: effect of calcium carbonate on the absorption of nitric and sulfuric acids and the depletion of chloride. *Atmos. Chem. and Phys.* 6:1865-1877. doi:10.5194/acp-6-1865-2006.

Lee, H.J., J.F. Gent, B.P. Leaderer, and P. Koutrakis. 2011. Spatial and temporal variability of fine particle composition and source types in five cities of Connecticut and Massachusetts. *Sci. Tot. Environ.* 409:2133-2142. doi:10.1016/j.scitotenv.2011.02.025.

Li, W.J., Z. B. Shi, C. Yan, L. X. Yang, C. Dong, and W. X. Wang. 2013. Individual metal-bearing particles in a regional haze caused by firecracker and firework emissions. Sci. Tot. Environ. 443: 464-469. DOI: 10.1016/j.scitotenv.2012.10.109.

Lippmann M., and L.C. Chen. 2009. Health effects of concentrated ambient air particulate matter (CAPs) and its components. *Crit. Rev. Toxicol.* 39:865-913. doi:10.3109/10408440903300080.

Lippmann, M. 2010. Targeting the components most responsible for airborne particulate matter health risks. J. *Exposure Science Environ. Epidemiology.* 20:117-118. doi:10.1038/jes.2010.1.

Lough, G.C., J.J. Schauer, J-S. Park, M.M. Shafer, J.T. Deminter, and J.P. Weinstein. 2005. Emissions of metals associated with motor vehicle roadways. *Environ. Sci. Tech.* 39:826-836. doi: 10.1021/es048715f.

Manoli, E., D. Voutsa, and C. Samara. 2002. Chemical characterization and source identification/apportionment of fine and coarse air particles in Thessaloniki, Greece. *Atmos. Environ.* 36:949–961. doi:10.1016/S1352-2310(01)00486-1.

Marloes, E., M.Y. Tsai, C. Ampe, B. Anwander, R. Beelen, T. Bellander, G. Cesaroni, M. Cirach, J. Cyrys, K. de Hoogh, A. de Nazelle, F. de Vocht, C. Declercq, A. Dėdelė, K. Eriksen, C. Galassi, R. Gražulevičienė, G. Grivas, J. Heinrich, B. Hoffmann, M. Iakovides, A. Ineichen, K. Katsouyanni, M. Korek, U. Krämer, T. Kuhlbusch, T. Lanki, C. Madsen, K. Meliefste, A. Mölter, G. Mosler, M. Nieuwenhuijsen, M. Oldenwening, A. Pennanen, N. Probst-Hensch, U. Quass, O. Raaschou-Nielsen, A. Ranzi, E. Stephanou, D. Sugiri, O. Udvardya, É. Vaskövia, G. Weinmayr, B. Brunekreef, and G. Hoek. 2012. Spatial variation of $PM_{2.5}$, PM_{10}, $PM_{2.5}$ absorbance and PM_{coarse} concentrations between and within 20 European study areas and the relationship with NO2 – Results of the ESCAPE project. *Atmos. Environ.* 63:303-317. doi:10.1016/j.atmosenv.2012.08.038.

Marple, V., K. Rubow, W. Turner, and J. Spengler. 1987. Low flow rate sharp cut impactors for indoor air sampling: design and calibration. *J. Air Poll. Control Assoc.* 37:1303-1307. doi:10.1080/08940630.1987.10466325.

McInnes, L.M., D.S. Covert, P.K. Quinn, and M.S. Germani. 2012. Measurements of chloride depletion and sulfur enrichment in individual sea-salt particles collected from the remote marine boundary layer. *J. Geophys. Research.* 99:8257-8268. doi:10.1029/93JD03453.

Norris, G., R. Vedantham, K. Wade, S. Brown, J. Prouty, and C. Foley. 2008. EPA positive matrix factorization (PMF) 3.0: Fundamentals & User Guide. U.S. Environmental Protection Agency.

Paatero, P. Least squares formulation of robust non-negative factor analysis. 1997. *Chemometrics Intelligent Lab. Syst.* 37:23-35. doi:10.1016/S0169-7439(96)00044-5.

Paatero, P., P. K. Hopke, X.H. Song, and Z. Ramadan. 2002. Understanding and controlling rotations in factor analytic models." *Chemom. Intell. Lab. Syst.* 60:253-264. doi:10.1016/S0169-7439(01)00200-3.

Paatero, P., and U. Tapper. 1994. Positive matrix factorization: a non-negative factor model with optimal utilization of error estimates of data values. *Environmetrics.* 5:111-126. doi:10.1002/env.3170050203.

Paatero, P., and P. K. Hopke. 2003. Discarding or downweighting high-noise variables in factor analytic models." *Anal. Chim. Acta.* (490): 277-289. doi:10.1016/S0003-2670(02)01643-4.

Pant, P., and R.M. Harrison. 2013. Estimation of the contribution of road traffic emissions to particulate matter concentrations from field measurements: A review. *Atmos. Environ.* 77:78-97. doi:10.1016/j.atmosenv.2013.04.028.

Pope, C.A., and D.W. Dockery. 2006. Health effects of fine particulate air pollution: lines that connect. *J. Air Waste Manage. Assoc.* 56:709-742. doi:10.1080/10473289.2006.10464485.

Roberts, A.L., K. Lyall, J.E. Hart, F. Laden, A.C. Just, J.F. Bobb, K.C. Koenen, A. Ascherio, and M.G. Weisskopf. 2013. Perinatal air pollutant exposures and autism spectrum disorder in the children of nurses' health study II participants. *Environ. Health Perspect.* 121:978-984. doi:10.1289/ehp.1206187.

Seinfeld, J.H., and S.N. Pandis. 2006. Atmospheric chemistry and physics: From air pollution to climate change. Wiley-Interscience. Second Edition.

Song, X.H., A.V. Polissar, and P.K. Hopke. 2001. Sources of fine particle composition in the northeastern US. *Atmos. Environ.* 35:5277-5286. doi:10.1016/S1352-2310(01)00338-7.

Spengler, J. D., and G. D. Thurston. 1983. Mass and elemental composition of fine and coarse particles in six U.S. cities. *J. Air Poll. Control Ass.* 33:1162-1171. doi:10.1080/00022470.1983.10465707.

Taylor, S.R. 1964. Abundance of chemical elements in the continental crust; a new table. *Geochimica et Cosmochimica Acta.* 28:1273-1285. doi:10.1016/0016-7037(64)90129-2.

Thorpe, A., and R. M. Harrison. 2008. Sources and properties of non-exhaust particulate matter from road traffic: a review. *Sci. Tot. Environ.* 400: 270-282. doi:10.1016/j.scitotenv.2008.06.007.

USEPA. 1999. Determination of metals in ambient particulate matter using X-Ray fluorescence (XRF) spectroscopy. Method IO-3.3. US EPA Office of Research and Development.

USEPA. 2008. EPA positive matrix factorization (PMF) 3.0 fundamentals and user guide. USEPA Office of Research and Development.

USEPA. 2009. Integrated science assessment for particulate matter. USEPA Office of Research and Development.

Valdés, A., A. Zanobetti, J.I. Halonen, L. Cifuentes, D. Morata, and J. Schwartz. 2012. Elemental concentrations of ambient particles and cause specific mortality in Santiago, Chile: a time series study. *Environ. Health.* 11:82. doi:10.1186/1476-069X-11-82.

Vedal, S., M.J. Campen, J.D. McDonald, T.V. Larson, P.D. Sampson, L. Sheppard, C.D. Simpson, and A.A. Szpiro. 2013. National particle component toxicity (NPACT) initiative report on cardiovascular effects. Health Effects Institute.

Wojcik, G.S., and J.S. Chang. 1997. A re-evaluation of sulfur budgets, lifetimes, and scavenging ratios for eastern North America. *J. Atmos. Chemistry*. 26:109-145. doi:10.1023/A:1005848828770.

X., Querol, A. Alastuey, M.M. Viana, S. Rodriguez, B. Artiñano, P. Salvador, S. Garcia do Santos, R. F. Patier, C.R. Ruiz, J. de la Rosa, A. Sanchez de la Campa, M. Menendez, and J.I. Gil. 2004. Speciation and origin of PM10 and PM2.5 in Spain. *J. Aerosol Sci.* 35:1151-1172. doi:10.1016/j.jaerosci.2004.04.002.

Yang, L., X. Gao, X. Wang, W. Nie, J. Wang, R. Gao, P. Xu, Y. Shou, Q. Zhang, and W. Wang. 2014. Impacts of firecracker burning on aerosol chemical characteristics and human health risk levels during the Chinese New Year Celebration in Jinan, China. Sci. Tot. Environ. 476:57-64. doi:10.1016/j.scitotenv.2013.12.110.

Zhao, Y., and Y. Gao. 2008. Acidic species and chloride depletion in coarse aerosol particles in the US east coast. *Sci. Tot. Environ.* 407:541-547. doi:10.1016/j.scitotenv.2008.09.002.

CHAPTER 2

Use of Visibility Measurements to Predict $PM_{2.5}$ Exposures in Southwest Asia and Afghanistan

Abstract

Military personnel deployed to Southwest Asia and Afghanistan were exposed to high levels of ambient particulate matter (PM) indicating the potential for exposure-related health effects. However, historical quantitative ambient PM exposure data for conducting epidemiological health studies are unavailable due to a lack of monitoring stations. Since visual range is proportional to particle light extinction (scattering and absorption), visibility can serve as a surrogate for $PM_{2.5}$ concentrations where ground measurements are not available. We used data on visibility, relative humidity (RH), and $PM_{2.5}$ ground measurements collected in Kuwait from years 2004 to 2005 to establish the relationship between $PM_{2.5}$ and visibility. Model validation obtained by regressing trimester average $PM_{2.5}$ predictions against $PM_{2.5}$ measurements in Kuwait produced an r^2 value of 0.84. Cross validation of urban and rural sites in Kuwait also revealed good model fit. We applied this relationship to location-specific visibility data at 104 regional sites between years 2000 and 2012 to estimate monthly average $PM_{2.5}$ concentrations. Monthly averages at sites in Iraq, Afghanistan, United Arab Emirates, Kuwait, Djibouti, and Qatar ranged from 10 to 365 $\mu g/m^3$ during this period, while site averages ranged from 22 to 80 $\mu g/m^3$, indicating considerable spatial and temporal heterogeneity in ambient $PM_{2.5}$ across these regions. These data support the use of historical visibility data to estimate location-specific $PM_{2.5}$ concentrations for use in future epidemiological studies.

Introduction

In response to concerns about particulate matter (PM) exposure in Southwest Asia and Afghanistan, the Department of Defense (DoD) conducted the Enhanced Particulate Matter Surveillance Program (EPMSP) to characterize airborne exposures at 15 military bases, mainly in Iraq and Afghanistan, for approximately 12 months during the period 2006-2007 (National Research Council, 2010). Although only a small number of samples were collected at each site, mean concentrations of particulate matter less than or equal to 2.5 microns in aerodynamic diameter ($PM_{2.5}$) ranged from 33 to 144 $\mu g/m^3$, which is much higher than ambient levels encountered in the U.S. (national average ~12 $\mu g/m^3$) during the same time period (USEPA, 2016). Sources of PM in this region include windblown dust and dust storms, as well as local combustion sources such as open-pit refuse burning, compression ignition vehicles, aircraft engines, diesel electric generators, households, and local industry (IOM, 2011). This mix of sources differs from those encountered in the U.S. and Europe, where most previous health studies have been conducted.

The potential for respiratory health effects occurring during deployment concerns PM exposures that are orders of magnitude higher than those commonly found in the U.S, and last several months to several years depending on the length and numbers of deployments. This is in contrast to studies conducted in the U.S. and Europe which assess the health effects attributable to relatively low exposures over both short (days, months) and long (years, decades) time scales. Results of studies in Europe and the U.S. assessing the impact of long-term PM exposures on pulmonary function, asthma, and COPD, suggest concern about the impact of deployment-related exposures on future respiratory health (Rice et al. 2015; Downs et al. 2007; Garshick, 2014; Young et al. 2014; Schikowski et al. 2014; Adam et al. 2015; Jacquemin et al. 2015).

Surveys of troops following deployment have reported high rates of respiratory illness and an increase in respiratory symptoms, including wheezing (Sanders et al. 2005; Roop et al. 2007). Reports have also documented asthma requiring treatment in returning deployers (Szema et al. 2011; Szema et al. 2010). Additionally, rates of encounters for asthma/COPD and allied conditions were significantly increased post deployment, as were rates for respiratory symptoms and asthma compared to those at U.S. bases (Abraham et al. 2012; Abraham et al. 2014). Similarly, in the Millennium Cohort Study, troops deployed to Iraq and Afghanistan had higher rates (14 vs. 10%) of newly reported respiratory symptoms compared to non-deployed troops (Smith et al. 2009). However, these reports, including the assessment of deployment-related changes in pulmonary function, are limited due to lack of objective exposure information (Morris et al. 2014).

In Iraq and Afghanistan, for instance, there is a general paucity of integrated air pollution monitoring networks, which makes it difficult to assess previous exposures to $PM_{2.5}$ using methods similar to those of U.S. and European studies. While wealthier countries such as Kuwait, Qatar, and U.A.E. have established networks for PM_{10} and gaseous criteria pollutants (since the early 2000s), $PM_{2.5}$ measurements did not start until three to five years ago. Additionally, the majority of particle sampling methods currently used in these regions are not adequate to collect particles during dust storms, which are common occurrences each year (National Research Council, 2010).

We assessed the use of airport visibility measurements to address the lack of $PM_{2.5}$ data. Visibility has demonstrated particular promise for use as a $PM_{2.5}$ predictor, especially when $PM_{2.5}$ levels are above 10-20 $\mu g/m^3$. The relationship between particles and visibility is due to the light extinction (scattering and absorption) effects of particles with sizes similar to the wavelengths of visible light. In the U.S., the effect of PM on visibility has been shown empirically in studies since the 1960s (Burt, 1961; Noll et al. 1968; Charlson, 1969; Waggoner and Weiss, 1980). In California,

the relationship between visibility and $PM_{2.5}$ estimated for multiple cities was strong, with r^2 values of up to 0.83 (Abbey et al. 1995). Cities in other nations have also shown visibility to be highly correlated with PM levels and hospital admissions (Thach, 2010; WenZhen, 2011). Additionally, previous U.S.-based epidemiological studies have used airport visibility as a surrogate for particulate exposure (Ozkaynak et al. 1985; Abby et al. 1995; Schwartz, 1991; Ostro, 1995; Yanosky et. al 2009; Laden et. al, 2006).

In this study, we used 648 paired daily airport visibility and $PM_{2.5}$ measurements collected in Kuwait to develop a calibration model that can be used to convert visibility to $PM_{2.5}$ estimates in this region. This enables us to take advantage of the large database of historical visibility readings collected by the military in Southwest Asia and Afghanistan.

Methods

The data used for the calibration model in this study were collected in Kuwait, a small desert country located at the northern end of the Persian Gulf, to the south of Iraq and northeast of Saudi Arabia, with weather conditions representative of Southwest Asia and Afghanistan. Kuwait is characterized by long summers of extreme heat and dryness, which extend for roughly five months, from May to September. Winters are short, lasting only three months from December to February, and are characterized by warm and sometimes rainy conditions. The general region is subject to intense dust storms that occur primarily during spring and summer (Idso, 1976).

Visibility and Relative Humidity Data

Measurements of visibility and relative humidity (RH) were obtained from the U.S. Air Force 14th Weather Squadron and included 104 sites in Iraq, Afghanistan, United Arab Emirates,

Kuwait, Djibouti, and Qatar between 2000 and 2012. Visibility and relative humidity were measured automatically using either an AN/FMQ-19 Automatic Meteorological Station or a TMQ-53 Tactical Meteorological Observing System, and reported approximately once per hour. Sensors generally evaluated visibility from less than 400 m to 9,999 m. In order to generate daily averages for use in the model calibration, we averaged hourly measurements over 24-hour periods that coincided with daily $PM_{2.5}$ measurements. Since visibility monitors are restricted to finite maximum readings, there inherently exists some truncation at the high end of visibility measurements, which can produce an underestimate of visibility. For RH, days with any hourly measurements showing near-saturated atmospheres (relative humidity $\geq$ 98%) were assumed to be rainy, and therefore not used for model calibration or $PM_{2.5}$ prediction.

$PM_{2.5}$ Data

$PM_{2.5}$ data were previously collected during an air pollution study in Kuwait during 2004-2005 (Brown et al. 2008). Integrated daily measurements were collected at three monitoring sites from 9:00 a.m. to 9:00 a.m. the following morning using a Harvard High-Capacity Impactor (HHI) operating at a flow rate of 10 L/min (Demokritou et al. 2004). In contrast to most particle sampling devices, which are prone to particle bounce and thus measurement error under conditions of extremely high PM, the HHI was specifically designed to function under conditions of high PM and extreme temperatures, making it ideal for sampling in Southwest Asia where dust storms and other extreme events are common. The system uses a slit acceleration jet with dual-stage polyurethane foam impaction surfaces in order to remove particles above 2.5 μm during sampling. The ability of the HII to minimize particle bounce-off onto the impaction substrate was successfully field-tested in Kuwait City by Brown (2008) et al. Using artificially generated

polydisperse aerosols, the device also demonstrated a high capacity (>35 mg of PM) for particle accumulation.

$PM_{2.5}$ samples were collected onto Teflon filters (Gelman Sciences 47-mm Teflo) and refrigerated immediately following collection in order to minimize losses of semi-volatiles. All gravimetric analyses were conducted at the Harvard School of Public Health using a Mettler MT-5 microbalance in a particle-free environment of controlled temperature (18-24 °C) and relative humidity (35-45%). Filters were equilibrated for a period of 24 hours prior to initial weighing and 48 hours prior to post-sampling weighing. For quality assurance, all $PM_{2.5}$ sample masses were blank-corrected using the mean mass (19.5 μg) of the field blanks (n = 114). The limit of detection (LOD) for $PM_{2.5}$ was calculated to be three times the standard deviation of the field blank values, and equated to 5 $\mu g/m^3$. Only a single sample was below the LOD. Further details on sampling, analysis, and quality assurance relating to the $PM_{2.5}$ data can be found elsewhere (Brown et al. 2008).

Model Development

We matched selected $PM_{2.5}$ and visibility sites based on proximity between sites, selecting those that were relatively close to one another (less than ~35 km between paired visibility and $PM_{2.5}$ collection locations). Matched PM sites included Kuwait University (central site), Um-Al-Aish (northern site), and Um-Al-Haiman (southern site), with elevations of 18, 80, and 26 m above sea level, respectively. These sites are visually depicted in Figure 2.1. The majority of $PM_{2.5}$ samples were collected at the central site (n=531); nearly every day from February 2004 to October 2005. This was an urban site impacted by traffic along with residential, commercial and other local sources. Samples were collected approximately once per week from February 2004 to February

2005 at the northern site (n=48) and once per week from February 2004 to July 2005 at the southern site (n=69). In contrast to the central site, the northern site was located in a remote desert area. This site was not near urban traffic or other such sources, and was generally upwind of urban centers. The southern site was located near both urban and industrial areas and was therefore more similar to the central site. This site was located downwind of multiple refineries and other large factories.

Although visibility monitoring in Kuwait was more available (16 stations) over time and geographic space than PM_{25} monitoring (3 stations), 13 visibility sites shared low temporal overlap (<18% in terms of daily observations) with the $PM_{2.5}$ sites. Of the remaining visibility sites, all had high (≥95%) temporal overlap with daily $PM_{2.5}$ measurements. These three sites were therefore the only visibility sites considered for matching with $PM_{2.5}$ stations. The selection criterion for matching a given visibility site (also containing RH data) with a $PM_{2.5}$ site was based on their proximity to one another. Since Kuwait International Airport was the closest visibility site to both our central and southern $PM_{2.5}$ monitoring sites, visibility at this station was matched with $PM_{2.5}$ observations at both of these $PM_{2.5}$ sites. That is, the visibility data were used twice. Kuwait International Airport is approximately 12 and 36 km from the central and southern $PM_{2.5}$ monitoring sites, respectively. The northern site was matched with visibility monitors at Camp Udairi, which is located approximately 33 km away. Since visibility measurements were collected multiple times per day, daily visibility represented the daily average of these measurements to enable matching of a single daily visibility observation with a single daily $PM_{2.5}$ observation. The selected visibility and $PM_{2.5}$ monitoring sites for this study are presented in Figure 2.1.

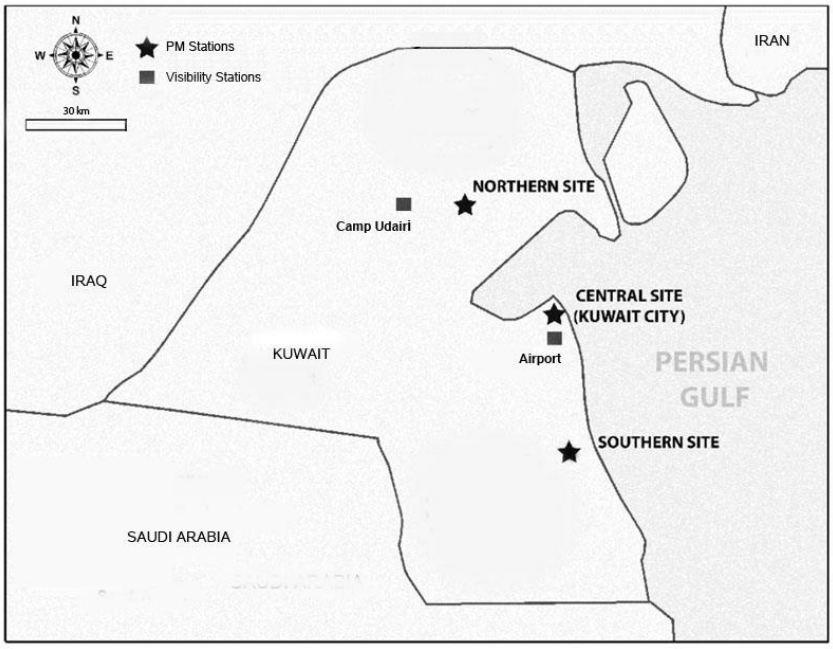

Figure 2.1. Map showing selected $PM_{2.5}$ and visibility sampling stations in Kuwait

Statistical Approach

To predict $PM_{2.5}$, we fit the following multiple linear regression model:

$$PM_{2.5} = \alpha + \beta_1 (1/\text{visibility}) + \beta_2 (\text{relative humidity})^2 \quad (1)$$

where, β_1 is the inverse of the effect of visibility on $PM_{2.5}$, β_2 is the effect of the squared relative humidity on $PM_{2.5}$, and α is the regression intercept. We conducted sensitivity analyses by excluding high values of $PM_{2.5}$ ($\geq$285 $\mu g/m^3$) to eliminate days with extreme events such as dust storms and other episodic phenomena, where the relationship between visibility and $PM_{2.5}$ may not be accurate, largely due to the difficulty of accurately measuring these variables at such high $PM_{2.5}$ concentrations.

In this model, inverse visibility was used since the functional relationship between $PM_{2.5}$ and visibility is known to be inverse. That is, as $PM_{2.5}$ increases, visibility decreases. Further, visibility is not driven by $PM_{2.5}$ concentrations alone, but also depends on meteorological variables. Specifically, since the extinction efficiency of a particle depends on its size, which for hygroscopic particles is a function of relative humidity, we also considered relative humidity as a covariate in the model (Malm and Day, 2001; Tang et al. 1981). We used the squared form of RH since the scattering efficiency of $PM_{2.5}$ has been shown to increase quadratically with increasing RH (Malm and Day, 2001; Tang et al., 1981). Other forms of this model were also tested, such as using the non-inversed and natural log forms of visibility as well as the non-squared form of RH. These alternative variable forms were tested by changing each variable separately as well as both together. Additional variables were also tested for inclusion into the model, such as temperature, wind speed, site, and season. Of note, while we applied an RH cutoff to exclude rainy days, no days exceeded this value. Therefore, all days were retained for model calibration.

After developing the model, predicted and measured daily $PM_{2.5}$ values were averaged over three month periods (trimesters) for each Kuwait site, since there were relatively few daily $PM_{2.5}$ measurements per month available for pairing with daily visibility. To assess the performance of the model, trimester averages of measured and predicted $PM_{2.5}$ were plotted for comparison. In order to verify that predictability was not affected by site-to-site variation of the $PM_{2.5}$-visibility relationship, we explored a mixed-effects model allowing for random slopes by site.

To validate the final model, we performed a 10-fold cross validation analysis. That is, our dataset was randomly sorted and divided into 10 splits. The model, fit to 90% (nine splits) of the data, was then used to predict the remaining 10% (one split). This process was repeated 10 times, holding out a new 10% split of data for each iteration. Goodness of fit for predictions was examined

by comparing predicted and measured trimester average concentrations and their associated Percent Mean Relative Errors (%MRE). Percent MRE was calculated as [(Measured Concentration – Predicted Concentration) / Measured Concentration] multiplied by a factor of 100. This produces an easily interpretable error that is in the form of a percent of measured values.

For further validation, we fit the model using only the central site data, and then predicted PM at the northern and southern sites. Since our dataset is heavily dominated by observations collected at the central site, this validation approach helps us determine whether the model can be used to predict $PM_{2.5}$ sites at a distance from the Kuwait International Airport.

Estimation of spatial and temporal variability

To examine the extent of spatiotemporal variability of predicted monthly $PM_{2.5}$ concentrations, we applied our final validated model using over a decade of weather data (2000-2012) to predict monthly average $PM_{2.5}$ mass at 104 different sites where visibility readings where available, including at military locations in Iraq, Afghanistan, United Arab Emirates, Kuwait, Djibouti, and Qatar. Only months with at least 90% of daily measurements available were used. As with model calibration, an exclusion criterion for rainy days was applied, resulting in the exclusion of approximately 5% of days. Note that while countries where $PM_{2.5}$ was predicted also include Kuwait, predictions for Kuwait were for a time period different than that used in model calibration.

For further quality assurance of predictions, we compared the predicted seasonal $PM_{2.5}$ averages of our Kuwait study region with combined seasonal averages of all other regional sites. To do this, predicted averages for a given season were averaged together over the group of three Kuwait study sites as well as the group of additional locations in Southwest Asian and Afghanistan.

This gave us a single set of seasonal averages for Kuwait (calibration sites) and a single set of averages representing all other sites. These values were then juxtaposed in a bar graph for comparison. Season was divided into fall (Sept-Nov), winter (Dec-Feb), spring (Mar-May), and summer (Jun-Aug) categories.

Results

In selecting the final calibration model (Equation 1), additional variables were also tested for inclusion such as temperature, wind speed, and site. However, these terms were not statistically significant (p-values ranging from 0.26-0.71), and were therefore left out of the model. To identify a $PM_{2.5}$ concentration cutoff for the regression analysis, cutoffs ranging from 100-320 $\mu g/m^3$ were explored. A cutoff of 285 $\mu g/m^3$ was selected because it resulted in the best model predictability when trimester averages of measured and predicted $PM_{2.5}$ were compared (r^2=0.84). Using this cutoff resulted in the exclusion of 9 $PM_{2.5}$ observations, or less than 2% of our data. When higher concentration days were left in our linear calibration model, however, results still had a high r^2 of 0.75. Due to the limited data, we chose not to fit a linear model using $PM_{2.5}$ exceeding 285 $\mu g/m^3$. However, above this value the $PM_{2.5}$/visibility relationship may deviate only slightly from linearity as $PM_{2.5}$ increases. Table 2.1 presents effect estimates for model covariates, along with standard errors, and p-values.

Table 2.1. Output for $PM_{2.5}$ predictive model.

Effect	Estimate	Standard Error	P-Value
Intercept	-39.3691	3.4377	<.0001
1/visibility	732372	26717	<.0001
RH^2	-0.00319	0.000550	<.0001

Figure 2.2 shows predicted *versus* measured $PM_{2.5}$ concentrations after calibrating the model using 639 matched $PM_{2.5}$ and visibility measurements from the three Kuwait study sites. To generate this graph, data at each site were averaged over three-month periods, producing a total of 20 data points. We chose to assess three-month averages due to limited site-specific $PM_{2.5}$ data and our objective to predict $PM_{2.5}$ exposures over longer periods. Regressing these trimester averages ($PM_{2.5}$ predictions *versus* $PM_{2.5}$ measurements) resulted in an r^2 value of 0.84, indicating a good predictive ability of the model. Additionally, the average %MRE of the predictions was -4.5%, indicating little bias.

To assess the extent to which the regression is driven by the highest data point in Figure 2.2, we also fit a line in the absence of this point. The regression equation, however, changed only negligibly when this point was removed ($y = 0.76*x + 10.44$). The r^2 value changed more noticeably after removing this point, but still showed a good relationship ($r^2=0.77$). Finally, we applied a mixed-effects model allowing for random slopes by site in order to assess the impact of site-to-site variation of the PM-visibility relationship. The mixed model, however, showed the random site terms to be non-statistically significant, and did not result in meaningful improvement to the prediction of $PM_{2.5}$ ($r^2=0.85$).

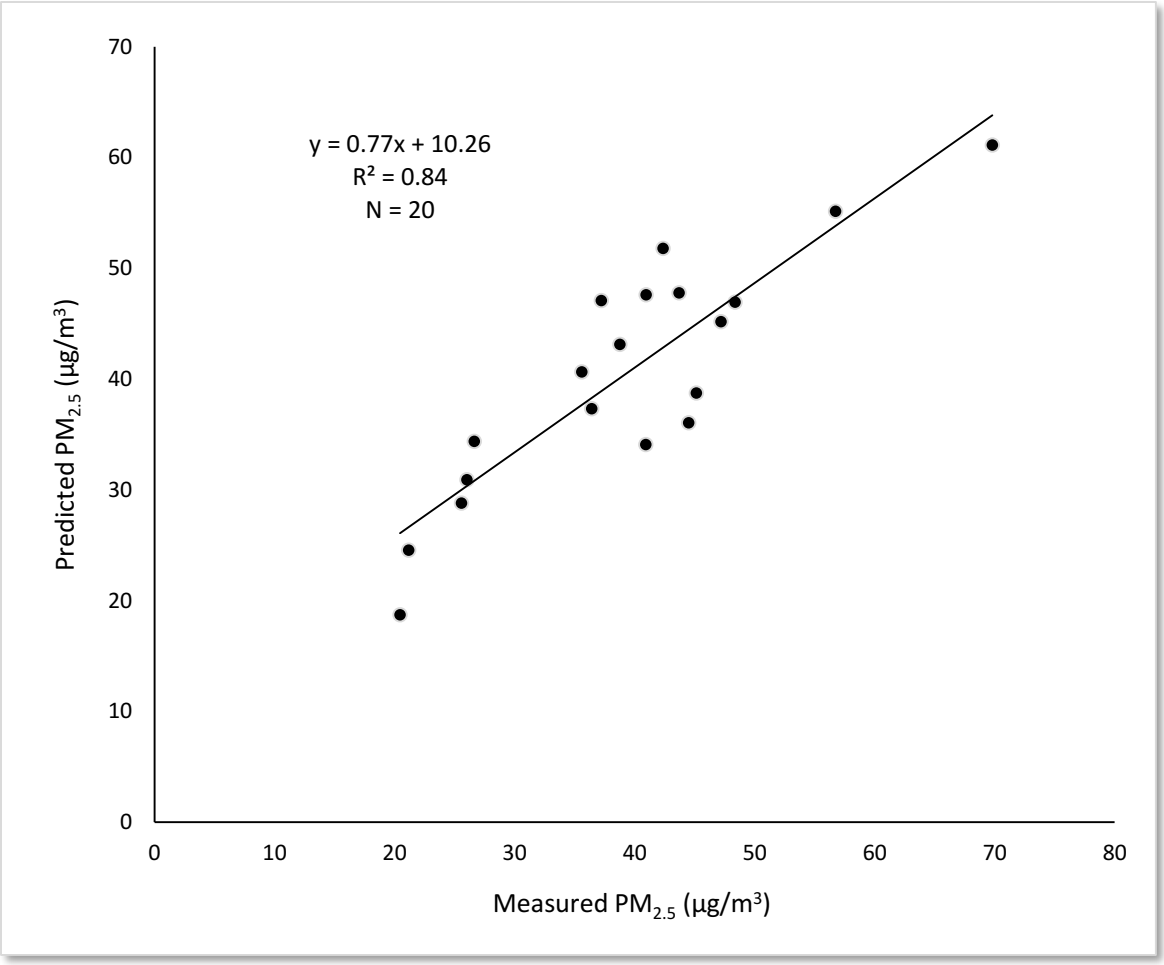

Figure 2.2. Relationship between trimester-averaged predictions and the corresponding $PM_{2.5}$ measurements in Kuwait

Table 2.2 presents 10-fold cross-validation results as well as predicted and measured $PM_{2.5}$ concentrations, and %MREs. Each trial represents the average of a non-overlapping 10% split of data. Trial averages (including %MREs) were calculated by first averaging within the various trimesters of a single trial. Subsequently, these trimester averages were averaged for that trial to get an overall trial average. This approach resembles the way in which a person's exposure would be predicted for an epidemiological study. That is, by averaging $PM_{2.5}$ over specified intervals

(trimesters or months), and then using these averages to calculate total exposure. In the table, %MREs are not presented in absolute value form in order to show the direction of potential model bias. Overall, $PM_{2.5}$ was predicted well as trial %MRE values were nearly all under 15%. That negative %MRE values occurred at a higher frequency than positive values suggests a tendency towards over prediction of $PM_{2.5}$. This tendency, however, was minimal overall (average %MRE = -5.3%) and therefore unlikely to be of consequence.

Table 2.2. 10-fold cross validation of mean trimester averaged $PM_{2.5}$ predictions and measurements.

Trial	**N**	**$PM_{2.5}$** ($\mu g/m^3$)	**Pred. $PM_{2.5}$** ($\mu g/m^3$)	**%MRE**
1	8	46.2	45.4	-7.5
2	6	55.3	50.5	5.1
3	9	55.9	45.1	6.3
4	8	47.1	46.5	-10.1
5	7	45.9	47.6	-5.2
6	10	43.2	46.8	-15.3
7	10	46.3	45.9	-3.2
8	8	39.7	43.8	-12.3
9	10	42.6	41.2	1.4
10	8	41.5	46.0	-12.1
Mean	8.4	46.5	45.9	-5.3

Figures 3 shows validation results from fitting the model to Kuwait data at only the central study site (~80% of total Kuwait calibration data), and then predicting $PM_{2.5}$ for two non-random divisions of the remaining data (northern and southern sites). Data collected at the northern and southern sites constituted 7% and 11% of our total data (after PM<285 $\mu g/m^3$ restriction), respectively. The Figure 2.3 plot of predicted *versus* measured $PM_{2.5}$ produced a high r^2 of 0.87. This suggests that the model also predicted well at the Northern (33 km) and Southern (36 km)

sites, away from the Central site. Since the r^2 value was high, it appears our use of mostly central site data (an urban location) for model calibration did not inhibit our ability to predict well at the other sites that included urban and rural locations. As the relationship shown in Figure 2.3 may be greatly influenced by the highest data point, we also fit a line in the absence of this point. Though reduced, the r^2 remained high at 0.75.

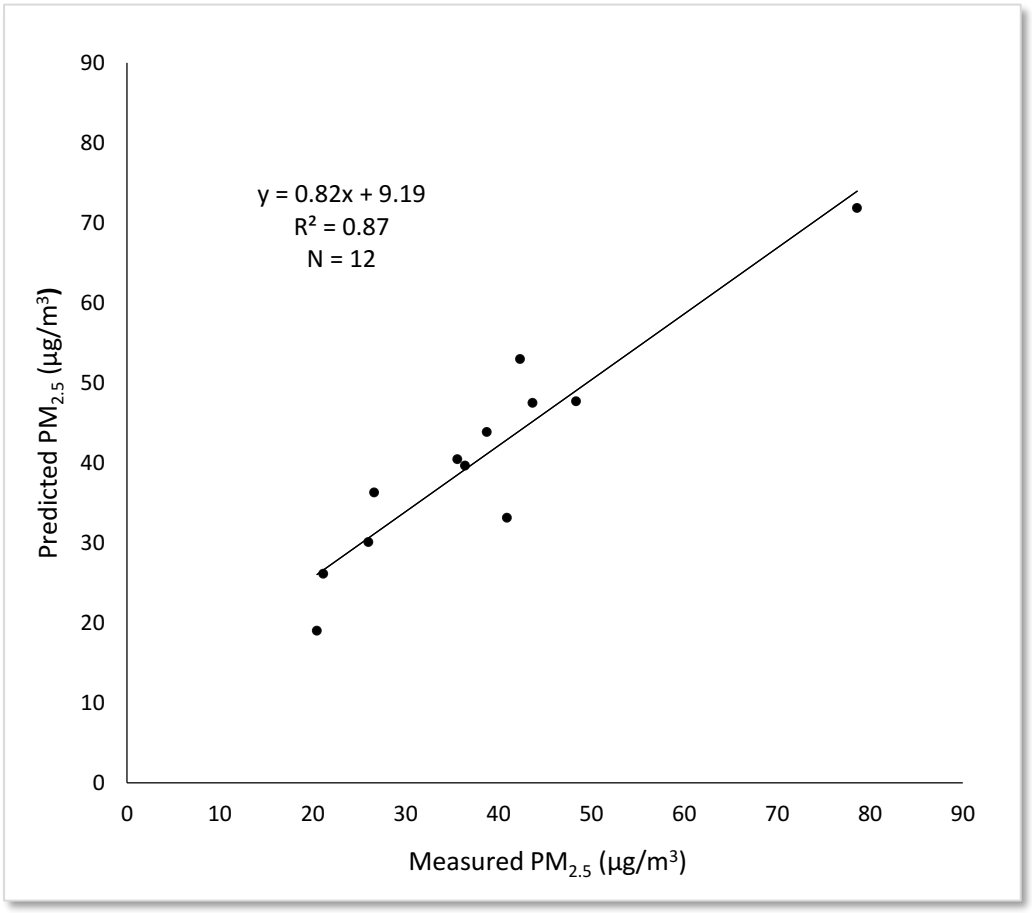

Figure 2.3. Internal cross validation using trimester averaged predicted *versus* measured $PM_{2.5}$ for the northern and southern sites in Kuwait

Figure 2.4 presents a histogram showing the frequency distribution of predicted monthly $PM_{2.5}$ exposure means for 104 locations including Iraq, Afghanistan, United Arab Emirates, Kuwait, Djibouti, and Qatar (spanning 2000-2012) to illustrate the extent of $PM_{2.5}$ exposure variability that could be expected for an epidemiological study of military personnel stationed at different locations. To enable better resolution, this plot restricts data to monthly averages below 200 $\mu g/m^3$. This resulted in the elimination of five predictions, with 3,964 predicted monthly averages remaining. Predicted averages ranged from approximately 10 to 365 $\mu g/m^3$ across these locations, with an overall mean and standard deviation of 42.8 and 22.7 $\mu g/m^3$, respectively. The median was 37.0 $\mu g/m^3$, suggesting a right-skewed distribution. When averaging predictions by site, predicted $PM_{2.5}$ ranged from 22.4 to 79.7 $\mu g/m^3$ over the 74 sites investigated (only sites with 12 or more months of data).

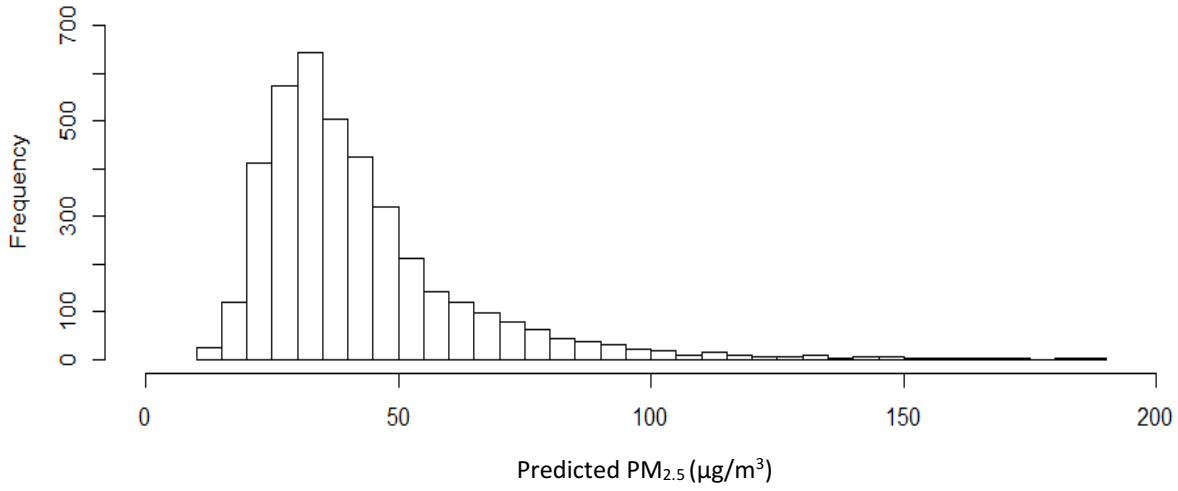

Figure 2.4. Frequency distribution of monthly $PM_{2.5}$ predictions for 104 military sites in Southwest Asia and Afghanistan from 2000-2012.

Figure 2.5 presents a scatter plot of predicted $PM_{2.5}$ concentrations averaged by month using the same data from Figure 2.4. In this case, individual monthly predictions are visible, as is the variability in predictions over time. As with Figure 2.4, this plot only shows predictions below 200 $\mu g/m^3$ to enable better resolution, therefore excluding the five highest predictions (max=365.0 $\mu g/m^3$). Within-site variability of monthly average predictions was similarly large, with predictions ranging by as much as 346 $\mu g/m^3$ (Max – Min concentration) for a single site. Over 50% of sites, and 20% of sites, had monthly predictions that differed by as much as 73 $\mu g/m^3$ and 120 $\mu g/m^3$, respectively, while nearly 10% of sites had monthly predictions that differed by more than 136 $\mu g/m^3$. On average, within-site monthly predictions varied by 83.2 $\mu g/m^3$, with a standard deviation of 54.4 $\mu g/m^3$.

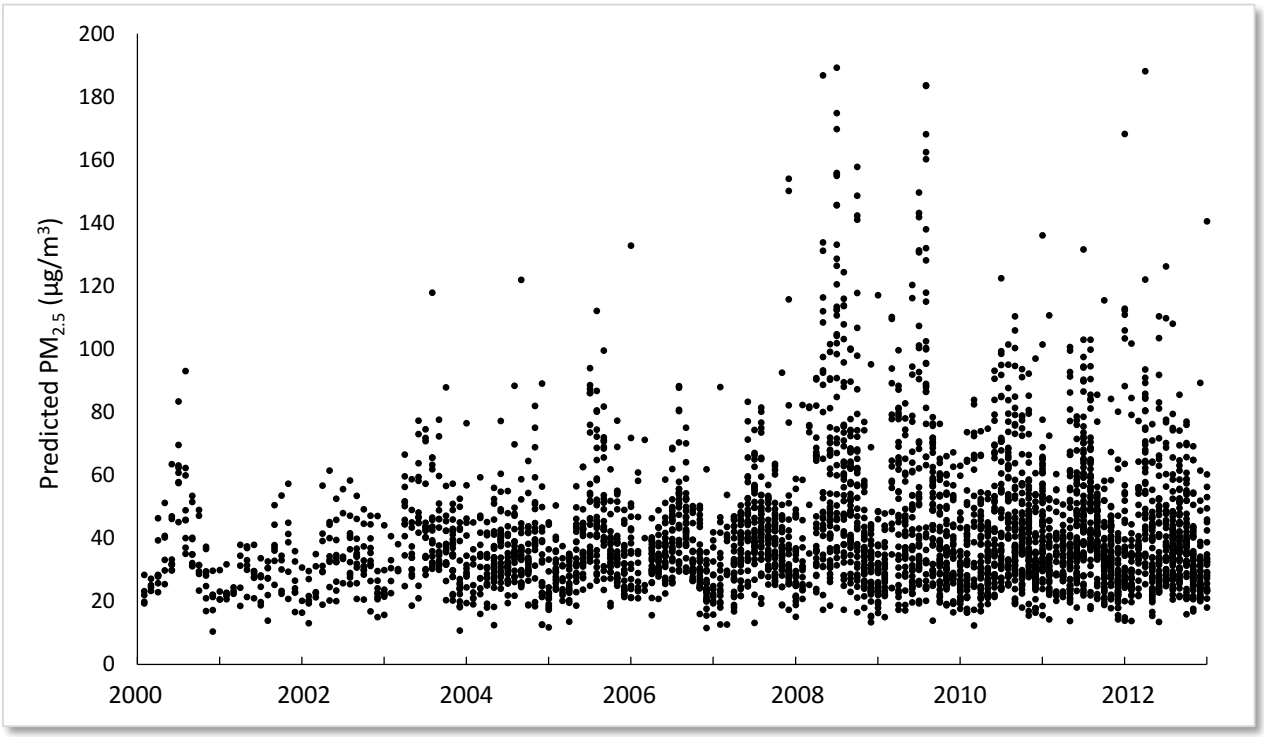

Figure 2.5. Monthly $PM_{2.5}$ predictions for 104 military sites in Southwest Asia and Afghanistan from 2000-2012.

A comparison of seasonal predictions for two groups of sites is provided in Figure 2.6. In the bar chart, "Kuwait Pred." refers to predictions at the Kuwait sites used for model calibration, while "SAA Pred." refers to predictions at additional sites across Southwest Asia and Afghanistan. It is important to note that seasonal $PM_{2.5}$ predictions for "Kuwait Pred." are nearly identical to their corresponding measured values since the model predicted on the same data used for calibration. Therefore, this chart is essentially a comparison of "SAA Pred." with field observations from Kuwait.

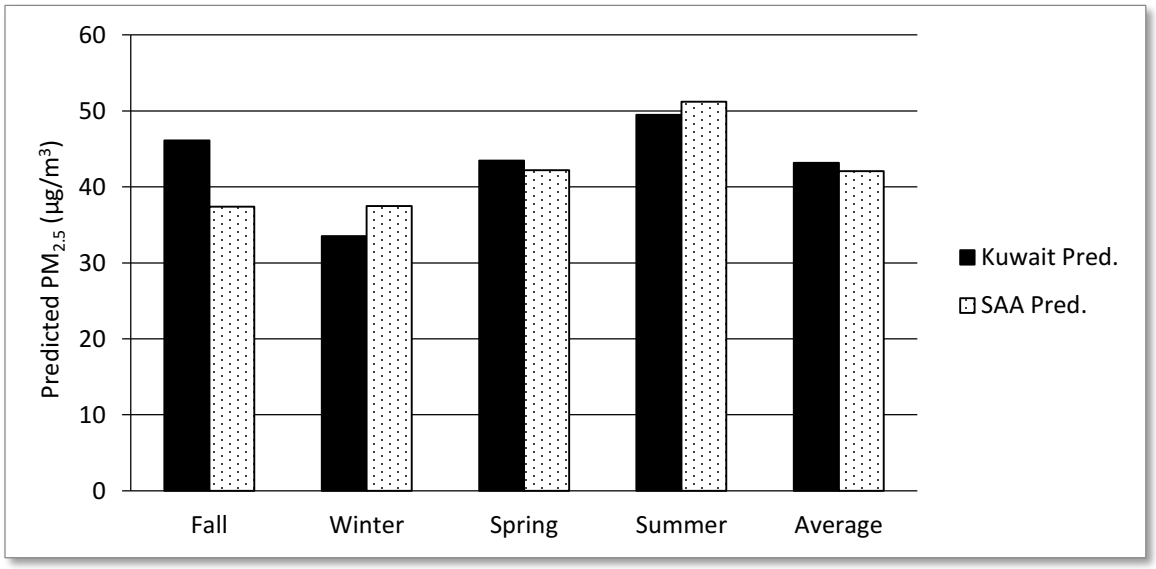

Figure 2.6. Comparison of mean $PM_{2.5}$ predictions for Kuwait study sites and sites in Southwest Asia and Afghanistan.

In general, after averaging across all site predictions for "SAA Pred.," fall and winter had the lowest average predicted concentrations (approximately 37 $\mu g/m^3$ for both), while summer had the highest predicted average (51.2 $\mu g/m^3$). Standard deviations for these seasons were 16.8, 20.5,

and 28.0 $\mu g/m^3$, respectively. The predicted average concentration for spring was 42.2 $\mu g/m^3$ with a standard deviation of 19.6 $\mu g/m^3$, respectively. As illustrated in Figure 2.6, averages do not differ markedly between Kuwait and other predicted sites except during fall. During this season, the seasonal average prediction for greater Southwest Asia and Afghanistan was approximately 10 $\mu g/m^3$ lower than that reported in Kuwait.

Discussion

This study demonstrates that visibility and relative humidity measurements are useful predictors of chronic $PM_{2.5}$ exposure in Southwest Asian and Afghanistan. Calibration of a model to predict $PM_{2.5}$ in Kuwait resulted in trimester average predictions that correlated well with observed averages (r^2=0.84). Further, results from mixed model regression demonstrated that predictability does not depend on site. These findings support the use of historical visibility data to estimate $PM_{2.5}$ concentrations in this region of the world. Additionally, this model has high utility for epidemiologists investigating the relationship between chronic exposure to $PM_{2.5}$ and respiratory diseases among deployed military personnel stationed at various military bases throughout the region. To date, such exposure data in this area is otherwise lacking.

For model performance, three-month averages were used since daily relationships can be noisy and since this model is designed to predict chronic and not daily or peak short-term exposures. That is, our goal was to predict $PM_{2.5}$ concentrations that are meaningful for assessing chronic exposure in a given individual. We used trimester rather than monthly averages because calibration requires $PM_{2.5}$ measurements, of which there were few available per month. For epidemiological studies, however, the availability of daily data will enable the estimation of average monthly exposure since daily visibility data are available, as demonstrated in this study.

This approach will reduce exposure error and is ideal since military personnel are often deployed for only a matter of months.

Several means of validating our model were conducted. 10-fold cross validation analysis showed our model to predict well across randomly divided splits of data as %MRE values were mostly under 15% for each validation trial. Further, given that prediction errors were low on average (~5%), bias appears to be minimal. Although our model calibration used data mostly collected at a single site, further internal validation showed predictability to remain high at sites exterior to this site, including at both urban and rural locations.

A limitation in using visibility measurements is that visibility monitors inherently predict $PM_{2.5}$ levels less accurately in cleaner atmospheres since they are restricted to finite maximum readings. In our study region, however, $PM_{2.5}$ levels are sufficiently high such that daily $PM_{2.5}$ can be predicted for the majority of days without this issue. This is demonstrated by our internal cross-validation, where the model predicted well for average trimester $PM_{2.5}$ concentrations as low as 20.5 $\mu g/m^3$. Monthly average predictions for 104 sites in Southwest Asian and Afghanistan were as low as 10 $\mu g/m^3$. Based on previous reporting, long-term $PM_{2.5}$ concentrations below these levels are not expected to occur in this region (National Research Council, 2010).

Notably, the model in this study was calibrated after excluding days of extremely high $PM_{2.5}$, where the relationship between visibility and $PM_{2.5}$ may not be accurate due to events such as dust storms and other episodic phenomena. To understand the potentially different $PM_{2.5}$/visibility relationship at higher $PM_{2.5}$ concentrations, a model that uses penalized splines can be considered. For this study, however, we did not have enough data to appropriately fit splines to assess the potential for non-linear relationships at higher concentrations.

In assessing seasonal $PM_{2.5}$, predicted seasonal averages for Southwest Asian and Afghanistan closely resembled that reported in Kuwait during most seasons, which lends support for the quality of our predictions. What is more, seasonal averages for sites in Kuwait as well as Southwest Asia and Afghanistan are consistent with previous PM studies of the area. Specifically, summer is known to be the peak season in terms of elevated PM concentrations. Similarly, winter levels are usually low throughout the region.

To examine the extent of spatiotemporal variability of predicted monthly $PM_{2.5}$ exposure in Southwest Asia and Afghanistan, we applied our calibrated model using over a decade (2000 - 2012) of weather data to predict $PM_{2.5}$ mass at 104 different military bases and airports in the region. Results showed predicted monthly averages to range from approximately 10 to 365 $\mu g/m^3$ between bases. Within-site variability was similarly high. Over 50% of sites, and 20% of sites, had monthly predictions that differed by as much as 73 $\mu g/m^3$ and 120 $\mu g/m^3$, respectively. On average, within-site monthly predictions varied by 83.2 $\mu g/m^3$. Importantly, while excluding days with precipitation could overestimate PM exposure, this is of negligible concern in this study due to the low frequency of rainy events in this region. Further, of the days we defined as rainy, 50% saw rain for less than three hours.

That $PM_{2.5}$ variability is large across time and geographic space in our study region suggests the ability to successfully use such data in epidemiological research. This is of high relevance to understanding the health implications of military deployment to Southwest Asia and Afghanistan. To date, very little $PM_{2.5}$ exposure data in this region exists partly due to the difficulties inherent to many military zones; namely, limited materials and available personnel to conduct the monitoring, variable temperatures and harsh weather conditions, lack of electricity, as well as low priority relative to the military mission at hand. Additional reasons for the paucity of

$PM_{2.5}$ data include the scarcity of regional $PM_{2.5}$ monitoring stations as well as the impracticality of outfitting soldiers with personal monitors in the field. As these conditions are unlikely to change, a means of assessing $PM_{2.5}$ exposure that does not rely on these factors is essential. This study aims to fill this gap.

Finally, the $PM_{2.5}$ predictions in this study are consistent with measured $PM_{2.5}$ reported in previous studies. The DOD Enhanced Particulate Matter Surveillance Program, for instance, reported average $PM_{2.5}$ concentrations ranging from 33-117 $\mu g/m^3$ across 15 sites in Southwest Asia and Afghanistan, with an average concentration of approximately 70 $\mu g/m^3$ across all sites (DRI, 2008). Other studies conducted in this region have reported similar findings, with average concentrations ranging from approximately 20 - 320 $\mu g/m^3$, depending on the site (Tsiouri et al. 2015; Brown et al. 2008; Goudarzi et al. 2014). Consistency with previously reported measurements reinforces the quality of our $PM_{2.5}$ predictions as well as suggests that PM exposure among U.S. military personnel is in excess of U.S. Environmental Protection Agency as well as World Health Organization PM standards. This underscores both the importance of future epidemiologic studies in this area and the importance of continued research in the area of predictive $PM_{2.5}$ exposure modeling in the Southwest Asia and Afghanistan region, particularly relating to the population of deployed military personnel.

Acknowledgements

This work was supported by the VA Cooperative Studies Program #595: Respiratory Health and Deployment to Iraq and Afghanistan, from the United States (U.S.) Department of Veterans Affairs, Office of Research and Development, Clinical Science Research and Development, Cooperative Studies Program. We appreciate the assistance of Mike Hunsucker and Jeff Zautner,

14th Weather Squadron (USAF), Asheville, NC. This publication was also made possible by USEPA grant RD-83479801. Its contents are solely the responsibility of the grantee and do not necessarily represent the official views of the USEPA, U.S. Department of Veterans Affairs, or U.S. Government.

Bibliography

Abbey, D. E., M. D. Lebowitz, P. K. Mills, F. F. Petersen, W. L. Beeson, and R. J. Burchette. 1995. Long-Term Ambient Concentrations of Particulates and Oxidants and Development of Chronic Disease in a Cohort of Nonsmoking California Residents. *Inhal. Tox.* 7:19-34. doi:10.3109/08958379509014268.

Abbey, D., B. E. Ostro, G. Fraser, T. Vancuren, and R. J. Burchette. 1995. Estimating fine particulate less than 2.5 microns in aerodynamic diameter (PM2.5) from airport visibility data in California. *J. Exposure Analysis & Enviro Epi.* 5:161-180.

Abraham, J. H., A. Eick-Cost, L. L. Clark, Z. Hu, C. P. Baird, R. DeFraites, S. K. Tobler, E. E. Riohards, J. M. Sharkey, R. J. Lipnick, and S. L. Ludwig. 2014. A retrospective cohort study of military deployment and post deployment medical encounters for respiratory condition. Military Medicine. 179:540-546. doi:10.7205/MILMED-D-13-00443.

Abraham, J. H., S.F. DeBakey, L. Reid, J. Zhou, and C. P. Baird. 2012. Does Deployment to Iraq and Afghanistan Affect Respiratory Health of US Military Personnel? *JOEM.* 54:740-745. doi: 10.1097/JOM.0b013e318252969a.

Adam, M, T. Schikowski, A. Carsin, Y. Cai, B. Jacquemin, M. Sanchez, A. Vierkötter, A. Marcon, D. Keidel, D. Sugiri, Z. Kanani, R. Nadif, V. Siroux, R. Hardy, D. Kuh, T. Rochat, P. Bridevaux, M. Eeftens, M. Tsai, S. Villani, H. Phuleria, M. Birk, J. Cyrys, M. Cirach, A. Nazelle, M. Nieuwenhuijsen, B. Forsberg, K. Hoogh, C. Declerq, R. Bono, P. Piccioni, U. Quass, J. Heinrich, D. Jarvis, I. Pin, R. Beelen, G. Hoek, B. Brunekreef, C. Schindler, J. Sunyer, U. Krämer, F. Kauffmann, A. Hansell, N. Künzli, and N. Probst-Hensch. Adult lung function and long-term air pollution exposure. ESCAPE: a multicenter cohort study and meta-analysis. 2015. *Eur. Respir. J.* 45:38-50. doi:10.1183/09031936.00130014.

Air Force Manual 15-111. 2003. Surface weather observations. http://ontology.ihmc.us/coi/Resources/Air%20Foce%20Surface%20Weather%20Observations%20Manual.pdf

Brown, K.W., W. Bouhamra, D. P. Lamoureux, J. S. Evans, and P. Koutrakis. 2008. Characterization of particulate matter for three sites in Kuwait. *J. Air & Waste Manage. Assoc.* 58:994-1003. doi:10.3155/1047-3289.58.8.994.

Burt, E. W. 1961. A Study of the Relation of Visibility to Air Pollution. *American Industrial Hygiene Ass. J.* 2: 102-108. doi:10.1080/00028896109343378.

Charlson, R. J. 1969. Atmospheric visibility related to aerosol mass concentration: review. *Environ. Sci. Technol.* 3:913–918. doi:10.1021/es60033a002.

Demokritou, P., S.J. Lee, and P. Koutrakis. 2004. Development and evaluation of a high loading PM2.5 speciation sampler. *Aerosol. Sci. Technol.* 38:111-119.

Downs, S. H., C. Schindler, S. Liu, D. Keidel, L. Bayer-Oglesby, M. H. Brutsche, M. W. Gerbase, R. Keller, N. Kunzli, P. Leuenberger, N. M. Probst-Hensch, J. Tschopp, J. Zellweger, T. Rochat, J. Schwartz, and U. Ackermann-Liebrich. 2007. Reduced Exposure to PM10 and Attenuated Age-Related Decline in Lung Function. N. Engl. J. Med. 357:2338-2347: doi:10.1056/NEJMoa073625.

DRI (Desert Research Institute). 2008. Department of Defense. Enhanced Particulate Matter Surveillance Program (EPMSP). 2215 Raggio Parkway. Reno, NV 89512-1095.

Garshick, Eric. 2014. Effects of short- and long-term exposures to ambient air pollution on COPD. *Eur. Rspir. J.* 44:558-561. doi:10.1183/09031936.00108814.

Goudarzi, G., M. Shirmardi, F. Khodarahmi, A. Hashemi-Shahraki, N. Alavi, K. Ahmadi Ankali, A. Babaei, Z. Soleimani, and M. Marzouni. 2014. Particulate matter and bacteria characteristics

of the Middle East Dust (MED) storms over Ahvaz, Iran. *Aerobiologia.* 30:345-356. 10.1007/s10453-014-9333-7.

Idso, SB. 1976. Dust storms. *Scientific American.* 235:108-114.

IOM (Institute of Medicine). 2011. Long-term health consequences of exposure to burn pits in Iraq and Afghanistan. Washington, DC: *The National Academic Press.*

Jacquemin, B., J., V. Siroux, M. Sanchez, A. Carsin, T. Schikowski, M. Adam, V. Bellisario, A. Buschka, R. Bono, B. Brunekreef, Y. Cai, M. Cirach, F. Clavel-Chapelon, C. Declercq, R. Marco, A. Nazelle, R. Ducret-Stich, V. Ferretti, M. Gerbase, R. Hardy, J. Heinrich, C. Janson, D. Jarvis, Z. Kanaani, D. Keidel, D. Kuh, N. Moual, M. Nieuwenhuijsen, A. Marcon, L. Modig, I. Pin, T. Rochat, C. Schindler, D. Sugiri, M. Stempfelet, S. Temam, M.Tsai, R. Varraso, D. Vienneau, A. Vierkötter, A. Hansell, U. Krämer, N. Probst-Hensch, J. Sunyer, N. Künzli, and F. Kauffmann. 2015. Ambient air pollution and adult asthma incidence in six European cohorts (ESCAPE). *Environ. Health Perspectives.* 123:613-621. doi:10.1289/ehp.1408206.

Kelsall, H.L., M.R. Sim, A.B. Forbes, D.P. McKenzie, D.C. Glass, J.F. Ikin, P. Ittak, and M.J. Abramson. 2004. Respiratory health status of Australian veterans of the 1991 Gulf War and the effects of exposure to oil fire smoke and dust storms. *Thorax.* 59:897-903.

Laden, F., J. Schwartz, F. Speizer, and D. Dockery. 2006. Reduction in Fine Particulate Air Pollution and Mortality Extended Follow-up of the Harvard Six Cities Study. *American J. Resp. & Critical Care Med.* 173:667-672. doi:10.1164/rccm.200503-443OC.

Malm, W.C. and Derek E. Day. 2001. Estimates of aerosol species scattering characteristics as a function of relative humidity. *Atmos Enviro.* 35:2845-2860.

Morris, M. J., D. W. Dodson, P. F. Lucero, G. D. Haislip, R. A. Gallup, K. L. Nicholson, and L. L. Zacher. 2014. Study of Active Duty Military for Pulmonary Disease Related to

Environmental Deployment Exposures (STAMPEDE). *American Thoracic Society.* 190:77-84. doi:10.1164/rccm.201402-0372OC.

National Research Council Board of Environmental Studies and Toxicology. Review of the department of defense enhanced particulate matter surveillance program report. *The National Academic Press.*

NRC (National Research Council). 2010. Review of the department of defense enhanced particulate matter surveillance program report. Washington, DC: The National Academies Press.

Noll, K. E., P. K. Mueller, and M. Imada. 1967. Visibility and aerosol concentration in urban air. *Atmos. Enviro.* 2:465-475. doi:1016/0004-6981(68)90040-1.

Ostro, B. 1995. Fine Particulate Air Pollution and Mortality in Two Southern California Counties. *Enviro. Research.* 70:98-104. doi:10.1006/enrs.1995.1053.

Ozkaynak, H., A.D. Schatz, G.D. Thurston, R.G. Isaacs, and R.B. Husar. 1985. Relationships between Aerosol Extinction Coefficients Derived from Airport Visual Range Observations and Alternative Measures of Airborne Particle Mass. *J. Air Poll. Control Ass.* 35:1176-1185. doi:10.1080/00022470.1985.10466020.

Polichetti, G., S. Cocco, A. Spinali, V. Trimarco, and A. Nunziata. 2009. Effects of particulate matter (PM10, PM2.5, and PM1) on the cardiovascular system. *Toxicology.* 261:1-8. doi:10.1016/j.tox.2009.04.035.

Rice, M. B., P. L. Ljungman, E. H. Wilker, K. S. Dorans, D. R. Gold, J. Schwartz, P. Koutrakis, G. R. Washko, G. T. O'Connor, and M. A. Mittleman. 2015. Long-Term Exposure to Traffic Emissions and Fine Particulate Matter and Lung Function Decline in the Framingham Heart

Study. *American J. Resp. & Critical Care Medicine.* 191:656-664. doi:10.1164/rccm.201410-1875OC.

Roop , S. A, A. S. Niven, B. E, Calvin, J. Bader, and L. L, Zacher. 2007. The Prevalence and Impact of Respiratory Symptoms in Asthmatics and Nonasthmatics during Deployment. Military Medicine. 172:1264-1269.

Sanders, J.W., S.D. Putnam, C. Frankart, R. W. Frenck, M. R. Monteville, M.S. Riddle, D.M. Rockabrand, T.W. Sharp, and D. R. Tribble. 2005. Impact of illness and non-combat injury during operations Iraq Freedom and Enduring Freedom (Afghanistan). *Am. J. Trop. Med. Hyg.* 73:713–719.

Schikowski, T., M. Adam, A. Marcon, Y. Cai, A. Vierko¨tter, A. Carsin, B. Jacquemin, Z. Kanani, R. Beelen, M. Birk, P. Bridevaux, B. Brunekeef, P. Burney, M. Cirach, J. Cyrys, K. Hoogh, R. Marco, A. Nazelle, C. Declercq, B. Forsberg, R. Hardy, J. Heinrich, G. Hoek, D. Jarvis, D. Keidel, D. Kuh, T. Kuhlbusch, E. Migliore, G. Mosler, M. Nieuwenhuijsen, H. Phuleria, T. Rochat, C. Schindler, S. Villani, M. Tsai, E. Zemp, A. Hansell, F. Kauffmann, J. Sunyer, N. Probst-Hensch, U. Kra¨mer, and N. Ku¨nzli. 2014. Association of ambient air pollution with the prevalence and incidence of COPD. *Eur. Respir. J.* 44: 614–626. doi:10.1183/09031936.00132213.

Schwartz, J. 1991. Particulate air pollution and daily mortality in Detroit. *Enviro. Research.* 56:204-213.

Smith, B., C. A. Wong, T. C. Smith, E. J. Boyko, G. D. Gackstetter, and M. A. K. Ryan. 2009. Newly reported respiratory symptoms and conditions among military personnel deployed to Iraq and Afghanistan: a prospective population-based study. *American J. Epidemiology.* 170:1433-1442. doi: 10.1093/aje/kwp287.

Szema, A. M., M. C. Peters, K. M. Weissinger, C. A Gagliano, and J. J. Chen. 2010. New-onset asthma among soldiers serving in Iraq and Afghanistan. Allergy & Asthma Proceedings. 31:67-71. doi: http://dx.doi.org/10.2500/aap.2010.31.3383.

Szema, A. M., W. Salihi, K. Savary, and J. J. Chen. 2011. Respiratory Symptoms Necessitating Spirometry Among Soldiers With Iraq/Afghanistan War Lung Injury. *JOEM.* 53:961-965. doi:10.1097/JOM.0b013e31822c9f05.

Tang, I.N., W.T. Wong, and H.R. Munkedwitz. 1981. The relative importance of atmospheric sulfates and nitrate in visibility reduction. *Atmos Enviro.* 15:2463-2471.

Thach, T., C.M. Wong, K.P. Chan, Y.K. Chau, Y.N. Chung, C.Q. Ou, L. Yang, and A.J. Hedley. 2010. Daily visibility and mortality: assessment of health benefits from improved visibility in Hong Kong. *Environ. Res*. 110:617-23.

Tsiouri, V., K. Kakosimos, and P. Kumar. 2015. Concentrations, sources and exposure risks associated with particulate matter in the Middle East Area—a review. *Air Qual. Atmos. Health.* 8:67–80. doi:10.1007/s11869-014-0277-4.

USEPA, 2016. Particulate matter. Online:http://www.epa.gov/airtrends/pm.html

Waggoner, A.P. and R. E. Weiss. 1980. Preliminary Communication: Comparison of fine particle mass concentration and light scattering extinction in ambient aerosol. Atmos. Enviro. 14:623-62.

WenZhen, G., C. RenJie, S.WeiMin, and K. Haidong. 2011. Daily visibility and hospital admission in Shanghai, China. *Biomed Environ Sci.* 24:117-121.

Yanosky, J., C. Paciorek, and H. Suh. 2009. Predicting chronic fine and coarse particulate exposures using spatiotemporal models for the northeastern and Midwestern United States. *Environ. Health Perspectives.* 117:522-529. doi:10.1289/ehp.11692.

Young, M. T., D. P. Sandler, L. A. DeRoo, S. Vedal, J. D. Kaufman, and S. J. London. 2014. Ambient air pollution exposure and incident adult asthma in a nationwide cohort of U.S. women. *American Thoracic Society*. 190: 914–921. doi:10.1164/rccm.201403-0525OC.

CHAPTER 3

A Novel Calibration Approach Using Satellite and Visibility Observations to Estimate $PM_{2.5}$ Exposures in Southwest Asia and Afghanistan

Abstract

Many epidemiological studies have shown exposure to airborne particulate matter (PM) to be associated with a number of adverse health outcomes. In most countries, however, PM monitoring does not exist to enable exposure characterization. This is of particular concern in regions where U.S. military personnel were deployed and often complain of respiratory symptoms. Satellite aerosol optical depth (AOD) and visibility are both highly related to atmospheric $PM_{2.5}$ concentrations. In this study, we employed a novel methodology using readily available airport visibility measurements to calibrate the AOD-visibility relationship and predict visibility over space and time (2006-2007) over an approximately 17,000 km^2 region of Iraq, resulting in daily visibility predictions that were highly associated with daily observations (r^2=0.87). We then converted spatial visibility predictions into $PM_{2.5}$ estimates. Since 1x1 km AOD measurements were used, we were able to predict $PM_{2.5}$ with a very high spatial resolution. Predicted $PM_{2.5}$ variability between sites was high, with daily concentrations differing by as much as ~30 $\mu g/m^3$ between all sites over all months. The ability to obtain precise estimates of $PM_{2.5}$ concentrations in Iraq supports the ability to characterize chronic $PM_{2.5}$ exposures in greater Southwest Asian and Afghanistan. This is of high utility for epidemiologists seeking to understand the relationship between chronic $PM_{2.5}$ exposure and respiratory diseases among deployed military personnel stationed at various military bases and over various periods throughout the region.

Introduction

Epidemiological studies have consistently shown exposure to airborne particulate matter (PM) to be associated with increased mortality as well as a number of adverse respiratory and cardiovascular conditions (Pope and Dockery, 2006). In the U.S. and much of Europe, the development of extensive PM monitoring networks has enabled the successful characterization of PM exposure. In most countries, however, monitoring does not exist. This lack of quantitative PM exposure information is of concern, particularly in regions of reportedly high PM where U.S. military personnel were deployed.. This is the case in Southwest Asia and Afghanistan.

Although wealthier countries in the region such as Kuwait, Qatar, and the United Arab Emirates have established networks for monitoring PM_{10} and gaseous criteria pollutants since the early 2000s, in general there are few integrated networks to provide comprehensive air pollution data throughout the region. For countries with networks, $PM_{2.5}$ measurements began only over the last five years and employ sampling methods that are inadequate to collect particles during dust storms, which are common occurrences each year (NRC, 2010).

The importance of adequate PM exposure information across Southwest Asia and Afghanistan is underscored by medical surveys and reports of returning military personnel. Following deployment to military bases in Southwest Asia and Afghanistan, U.S. military personnel have complained of persistent respiratory symptoms (Sanders et al. 2005). Specific reports have documented asthma requiring treatment in returning deployers as well as elevated rates of encounters for asthma/COPD and allied conditions relative to soldiers at U.S. bases (Szema et al. 2011; Szema et al. 2010; Abraham et al. 2012; Abraham et al. 2014). In response to early concerns, the Department of Defense (DoD) conducted the Enhanced Particulate Matter Surveillance Program (EPMSP) at military sites during 2006-2007 showing that mean

concentrations of particulate matter less than or equal to 2.5 micron in aerodynamic diameter ($PM_{2.5}$) ranged from 33 to 144 $\mu g/m^3$ (NRC, 2010). This is considerably higher than the annual national average encountered in the U.S. during the same period (~12 $\mu g/m^3$) and exceeds the 1-year Military Exposure Guideline value (15 $\mu g/m^3$) set by the U.S. Army Center for Health Promotion and Preventive Medicine (USEPA, 2016). Quantitative information of this kind is critical, albeit on a greater spatial and temporal scale, is critical to enabling causal inference.

Sources of PM near military bases in Southwest Asia and Afghanistan include windblown dust and dust storms, as well as local combustion sources such as open-pit refuse burning, compression ignition vehicles, aircraft engines, diesel electric generators, and local industry (IOM, 2011). This mix of pollution sources is different from that encountered in the U.S. and Europe, where most previous health studies have been conducted. Further, PM exposures in this region are orders of magnitude higher than those commonly found in the U.S., and last several months to several years depending on the length and numbers of deployments. This is in contrast to studies conducted in the U.S. and Europe, which assess the health effects attributable to relatively low exposures over both short (e.g. days) and long (e.g. years) time scales. Results of studies in Europe and the U.S. assessing the impact of long-term PM exposures on pulmonary function, asthma, and COPD, suggest concern about the impact of deployment-related exposures on future respiratory health (Rice et al. 2015; Downs et al. 2007; Garshick, 2014; Young et al. 2014; Schikowski et al. 2014; Adam et al. 2015; Jacquemin et al. 2015).

In recent work, we demonstrated the use of airport visibility and relative humidity (RH) to predict long-term $PM_{2.5}$ exposure in Southwest Asian and Afghanistan. This relationship between $PM_{2.5}$ and visibility is due to the light extinction (scattering and absorption) effects of particles with sizes similar to the wavelengths of visible light, which has been empirically shown in a

number of studies (Burt, 1961; Noll et al. 1968; Charlson, 1969; Waggoner and Weiss, 1980; Abbey et al. 1995). Though visibility is a useful surrogate of human exposures to ambient particles, measurements are spatially limited by the number of existing monitoring stations.

An alternate measurement of light extinction by particles in the atmosphere is aerosol optical depth (AOD), collected by satellite. AOD is a vertical integration measure of the total abundance of particles in the entire atmospheric column, in contrast to visibility which is a measure of the particle abundance near the ground. Satellite imagery of the earth's surface and atmosphere represents an important tool for air quality and pollution monitoring due to its extensive spatial coverage and repeated observations. Like visibility, AOD can be used to estimate ground level PM exposure. Our research team has pioneered this area, developing methods for the application of high-resolution satellite data for exposure assessment and health effects studies (Kloog et al. 2011; Lee et al. 2012; Chudnovsky 2013b; Kloog et al. 2014).

In the present study, we used 1,845 paired daily airport visibility and MODIS AOD measurements (1x1 km resolution) collected in Iraq to develop a calibration model that will be used to convert AOD to ground visibility estimates in the region. Using the relationship between visibility and $PM_{2.5}$ from our previous work in the region, we then estimated $PM_{2.5}$ over an area of approximately 17,000 km^2 in Iraq during a period of two years (2006 - 2007).

Methods

Data used for model calibration in this study were collected in Iraq, which is a large desert country located at the northern end of the Persian Gulf, to the west of Iran and east of Syria. In terms of climate, Iraq experiences summers that are hot and dry, extending for roughly four months, from June to September, and with temperatures often in excess of 38° (~100°F). Winters

are long but mild, lasting from December to March, and with nighttime temperatures typically above freezing. Precipitation and humidity are low, with annual precipitation averaging less than 25 cm across most of the country. The general region is subject to Shamal winds, which generate intense dust storms, usually during the summer months of June and July (NOAA, 2009).

For this study, we selected a region in Iraq of approximately 17,000 km^2 that includes Bagdad and Joint-Base-Balad (JBB), because of its high air pollution levels, spatial heterogeneity in $PM_{2.5}$, and high presence of U.S. military personnel (IOM, 2011). Additionally, the region is sufficiently large to encompass low population desert areas with fewer pollution sources, and in turn enable an understanding of the $PM_{2.5}$ in the region.

Aerosol Optical Depth

AOD measurements were collected by the Moderate Resolution Imaging Spectroradiometer (MODIS), which sits on two Earth Observing System (EOS) satellites launched by the National Aeronautic and Space Administration (NASA); namely Terra, launched in 1999, and Aqua, launched in 2002. The MODIS satellite provides daily AOD measurements for the entire Earth. Daily observations were retrieved for the years 2006 and 2007 for the entire area of Iraq. Recently, NASA developed a new algorithm, Multi-Angle Implementation of Atmospheric Correction (MAIAC), to process MODIS data. MAIAC retrieves aerosol parameters over land at a high resolution of 1x1 km, as compared to previously reported 10 km. Our research team has evaluated the first and second generation of MAIAC products and have applied them successfully to assess $PM_{2.5}$ exposures and health effects in New England (Fleisch et al. 2014). From our analyses, we have determined that MAIAC data can also be used for arid (desert) environments with high surface reflectance such as Iraq.

Visibility Data

Visibility data were obtained from the U.S. Air Force 14th Weather Squadron and included seven sites across the study region and period. Visibility was measured continuously using either an AN/FMQ-19 Automatic Meteorological Station or a TMQ-53 Tactical Meteorological Observing System, and was reported hourly. Most sensors measure visibility from approximately 400 to 9,999 m. Maximum measurements exceeding this typical upper limit become less accurate, which can introduce error and affect the relationship between visibility and atmospheric particle mass. Measurements greater than this cutoff were therefore truncated to 9,999 m in this analysis. In order to generate daily averages for use in model calibration, we averaged hourly measurements over 24-hour periods that coincided with daily AOD measurements. Rain and near-saturation periods, when relative humidity ≥98%, were not included in the analysis. However, since this region is arid with low rainfall, these conditions were observed for only a small fraction of days (~4%).

Statistical Approach

To calibrate the model, we matched each of seven visibility-monitoring stations with a corresponding 1x1 km AOD grid cell. Paired measurements were matched by selecting the AOD grid cell that contained the corresponding visibility station. In contrast to studies that use coarse resolution satellite data, our use of high resolution (1x1 km) AOD measurements enabled more precise pairing of AOD with visibility, and therefore more accurate calibration of the AOD-visibility relationship. In total, 1,845 paired AOD-visibility observations were used for model calibration, spanning a two-year period from January 2006 to Dec 2007. The locations of visibility monitoring stations are depicted in Figure 3.1. Visibility monitoring sites used in model calibration

were located in both rural and urban areas, and contributed variable amounts of data for model calibration (not all stations contained 365 daily observations). In terms of total data used in model calibration, however, an approximately equal amount of rural (45%) and urban (55%) observations were represented. This is important given the variable pollution sources from both land use types. Using our AOD-visibility matched measurements, we applied a mixed-effects model using AOD measurements as predictors to establish a relationship between visibility and AOD.

In order to estimate visibility and convert these estimates to $PM_{2.5}$ in each grid cell on each day, we conducted the prediction process in four stages. Before presenting each stage, we will first summarize the stages here. The Stage 1 model calibrates the AOD grid-level observations to the visibility monitoring data collected within 1 km of an AOD reading by regressing visibility monitoring data on AOD values. Since the relationship between AOD and visibility varies day to day (due to differences in mixing height, relative humidity, particle composition, vertical profiles, etc.) this calibration is performed on a daily basis. In Stage 2 we predict visibility concentrations in grid cells where no visibility monitoring exists but with available AOD measurements using the Stage 1 AOD-visibility relationship. This is achieved by applying the prediction equation obtained from the model fit in Stage 1 to these additional AOD values. In Stage 3, we fit a model using predicted visibility from Stage 2 and spatial associations among visibility values on a given day to estimate visibility in cells where both visibility and AOD data is missing. To convert visibility to $PM_{2.5}$ concentrations in each grid cell, Stage 4 then applies coefficients of the relationship between visibility and $PM_{2.5}$ demonstrated from previous work in the region. The four stages are applied to data at the 1×1 km grid cell level.

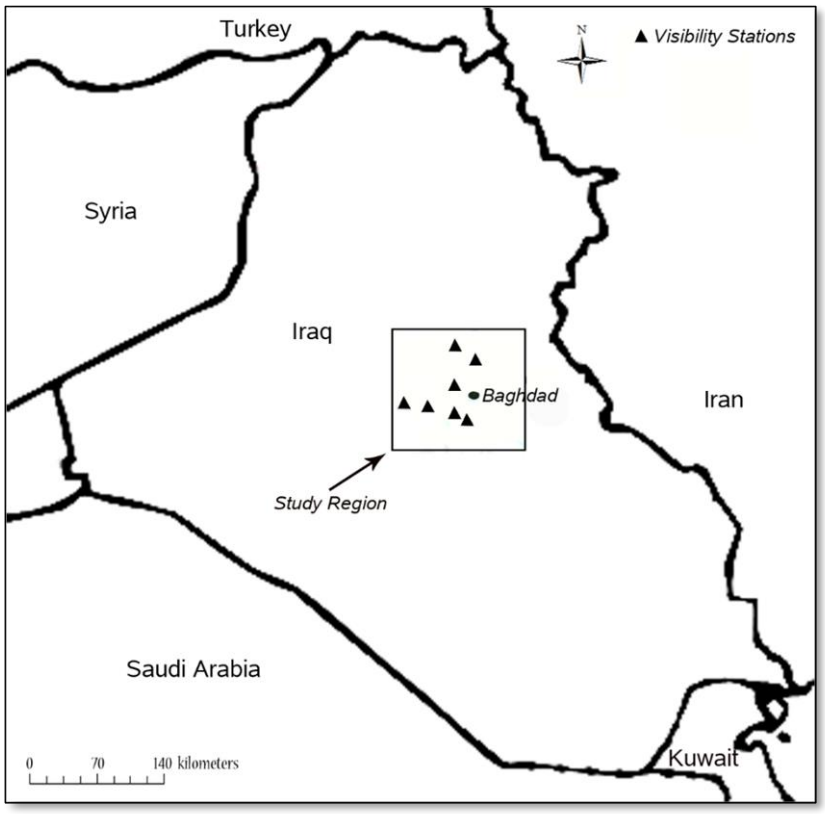

Figure 3.1. Map showing visibility monitoring stations in Iraq study region.

Stage 1

To predict visibility, we fit the following mixed-effects multiple linear regression model:

$$\mathrm{VIS_{ij}} = (\alpha + u_{\mathrm{j}}) + (\beta_{1\mathrm{AOD}} + v_{\mathrm{jAOD}})(1/\mathrm{AOD})_{\mathrm{ij}} + \varepsilon_{\mathrm{ij}} \quad (1)$$

$$(u_{\mathrm{j}}\ v_{\mathrm{jAOD}}) \sim \mathrm{N}[(0\ \ 0), \Sigma]$$

where, $\mathrm{VIS_{ij}}$ is the visibility measured at site i corresponding to grid cell i on day j; α and u_{j} are the fixed and day-specific random intercepts, respectively; $\mathrm{AOD_{ij}}$ is the AOD value in the grid cell i on day j; $\beta_{1\mathrm{AOD}}$ and v_{jAOD} are the fixed and day-specific random slopes for AOD; $\varepsilon_{\mathrm{ij}} \sim$

$N(0, \sigma^2)$ is the error term at site i on day j; and Σ is the variance-covariance matrix for the day-specific random effects.

In this model, inverse AOD was used since AOD is a measure of particles in the atmospheric column, and the functional relationship between atmospheric particulate and visibility is known to be inverse. That is, as particulate concentrations increase (increasing AOD), visibility decreases. Since the relationship of AOD and visibility (surrogate for $PM_{2.5}$) varies day to day, calibration was performed on a daily basis. Other covariates were tested such as season, weekday/weekend, elevation, wind direction, precipitation, and numerous land use variables (e.g. distance to oil fields, town centers, waterbodies, etc.). Such terms, however, were either not statistically significant or did not improve model performance. After developing the model, predicted and measured daily visibility values were then assessed on a scatter plot.

For validation, we performed a 10-fold cross validation analysis. This was accomplished by randomly sorting our dataset and dividing it into 10 splits. The model, fit to 90% (nine splits) of the visibility data, was then used to predict visibility in the remaining 10% (one split). This process was repeated 10 times, with each iteration holding out a new 10% split of data. Model performance was examined by comparing predicted and measured visibility for each of the 10 CV trials. Specifically, R^2 values were computed and tabulated for each trial along with the square root of the mean squared prediction errors (RMSPE). Further, we estimated the temporal R^2 by regressing the predicted $deltaVIS_{ij}$ against the measured$deltaVIS_{ij}$, where predicted $deltaVIS_{ij}$ is the difference between the predicted VIS_{ij} in a site corresponding to cell i on day j and its overall mean, and measured $deltaVIS_{ij}$ is defined similarly for the measured values. Lastly, we estimated the spatial R^2 by regressing the site-specific predicted VIS means on the measured one.

Stage 2

To predict visibility for grid cells containing AOD but no visibility measurements, we used the calibrated coefficients and parameters fitted in Stage 1. This resulted in two yearly sets of visibility predictions for all day-AOD cell available combinations yet still no predictions in day-cell combinations with missing AOD data.

Stage 3

To predict visibility for grid cells that contain neither visibility nor AOD measurements (often due to cloud cover), we used the output of Stage 1 (visibility predictions) to predict daily visibility for all grid cells in the study domain. Specifically, we fit a Generalized Additive Mixed Model (GAMM) with a smooth function of latitude and longitude (using the grid cell centroids) and a random intercept for each cell. This is similar to other established interpolation techniques, such as universal kriging, that use nearby grid cells to fill missing points. However, in our analysis we also regressed the daily visibility predictions on the average of those measured at the monitoring stations located within our study region. To allow for the visibility spatial patterns to vary with time, we fit a separate spatial surface for each two-month period of each year. This enabled our model to incorporate additional information about visibility values that classic interpolation techniques do not utilize. Specifically, we fit the following semiparametric regression model:

$$\mathrm{PredVIS}_{ij} = (\alpha + u_i) + (\beta_1 + v_i)\left(\mathrm{MVIS}_{ij}\right) + s(X_i, Y_i)_{k(j)} + \varepsilon_{ij} \qquad (2)$$

$$(u_i\ v_i) \sim \left[(0\ 0), \Omega_\beta\right]$$

where, $PredVIS_{ij}$ is the Stage 2 predicted visibility at grid cell i on a day j; $MVIS_{ij}$ is the mean of visibility values monitored at the sites in our study region for cell i on a day j; α and u_i are the fixed and grid-cell specific random intercepts, respectively; β_1 and v_i are the fixed and random slopes, respectively; X_i, Y_i are the latitude and longitude, respectively, of the centroid of grid cell i; and, $s(X_i, Y_i)_{k(j)}$ is a smooth function of location (modeled by thin plate splines) specific to the two-month period k(j) in which day j falls, thus a separate spatial smooth was fit for each two-month period.

As with model calibration, visibility predictions here were validated using 10-fold cross validation. In this case, we randomly selected 10% of the data across all visibility monitoring sites (seven grid cells) to leave out of the Stage 3 model predictions. The 90% remaining data from the seven sites was then combined with all data from all other grid cells. This combined data set was then used to predict the 10% left out data from the seven monitoring sites. This process was repeated 10 times, with each iteration holding out a new 10% split of monitoring data. Goodness of fit and model bias were then assessed by regressing predicted and measured visibility at the 10% left out data, and calculating the corresponding R^2 values for each of the 10 separate iterations. As with Stage 1, temporal and spatial cross validation was also applied.

Stage 4

In our previous work, daily-integrated $PM_{2.5}$ concentration data collected at several monitoring sites in Kuwait during the period 2004-2005 was used to calibrate a model for the relationship between $PM_{2.5}$ and visibility, with relative humidity as a covariate. This study produced $PM_{2.5}$ predictions that correlated well with observed averages (r2=0.84) and performed well through 10-fold internal cross validation. Further, results from mixed model regression in this

study demonstrated that predictability did not depend on location within the region. To convert visibility to spatially- and temporally-resolved $PM_{2.5}$ concentrations in the current study, we used the calibration equation coefficients generated from this previous work. The prediction equation is as follows:

$$\mathrm{PredPM_{2.5ij}} = \gamma_o + \gamma_v(\frac{1}{\mathrm{PredVIS_{ij}}}) + \gamma_m(\mathrm{RH^2})$$

where $\mathrm{PredPM_{2.5ij}}$ is the predicted $PM_{2.5}$ for cell i on a day j; $\mathrm{PredVIS_{ij}}$ is the visibility predicted for cell i on a day j; $\mathrm{RH^2}$ is the square of relative humidity for cell i on day j; γ_o, γ_v, and γ_m are the coefficients estimated from the previous analysis, which are equal to +39.3691, +732372, and -0.00319, respectively. Grid-specific $PM_{2.5}$ predictions over varying periods were then calculated and a map of grid-cell specific averaged $PM_{2.5}$ estimates over the entire study period was projected onto a map for visual representation.

Results

Figure 3.2 depicts the relationship between predicted and measured daily visibility. Each point represents a single day for a single station within one year. Importantly, there are only 1,845 observations presented in the plot because visibility observations were available for only short periods at some of the visibility stations (not 365 days of the year). Regressing daily visibility resulted in a high r^2 value of 0.87, indicating good model fit.

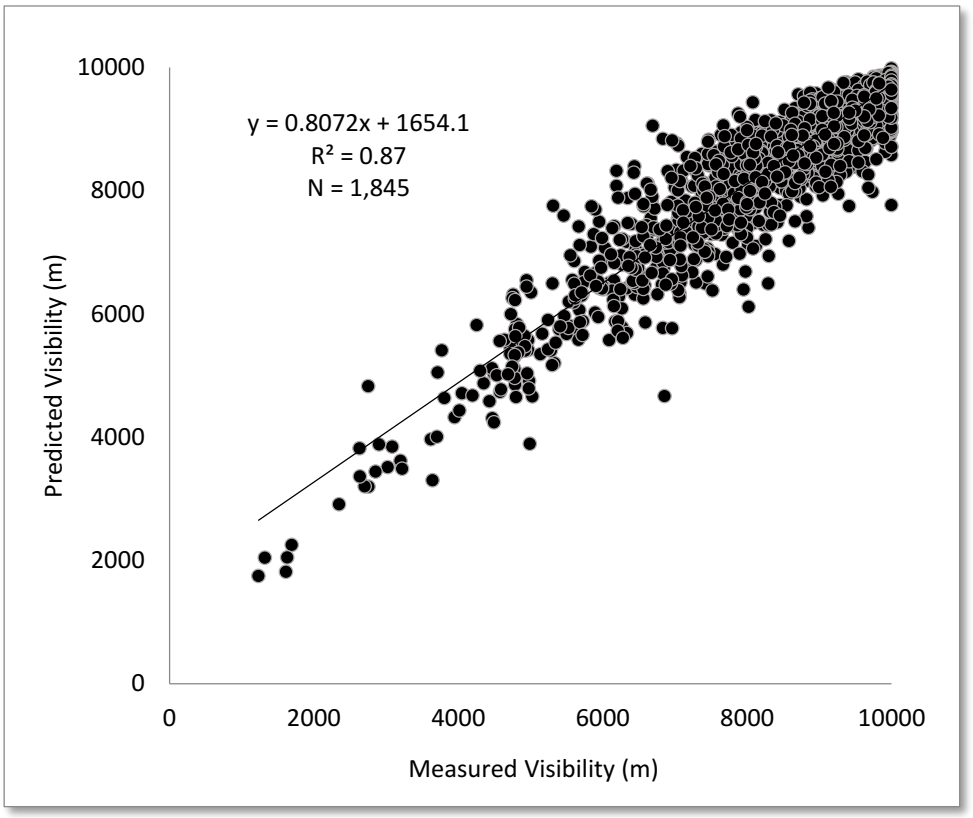

Figure 3.2. Relationship between predicted and measured monthly average visibility.

Table 3.1 presents results from the cross validation (CV) analysis. CV trials demonstrated good out-of-sample predictive ability, with a mean out-of-sample R^2 value of 0.71 and range from 0.63 to 0.83. Overall, a significant association is shown between visibility and AOD. Table 1 also presents results for spatial and temporal CV analyses. Results for the spatial analysis showed a high mean R^2 of 0.87 (range 0.60-0.98), while results for the temporal analysis showed an R^2 of 0.60 (range 0.51-0.73). In Figure 3.3, predicted and measured visibility for each of the 10 CV trials is plotted. The resulting plot shows a high R^2 of 0.85, further illustrating the high predictive power of the model.

Table 3.1. Prediction accuracy for 10-fold cross validation (CV) trials of Stage 1 calibration model.

Trial	CV R^2	CV R^2 $_{Spatial}$	CV R^2 $_{Temporal}$	RMSPE[a] (m)
1	0.83	0.96	0.73	580.5
2	0.67	0.89	0.56	831.8
3	0.71	0.86	0.67	795.6
4	0.76	0.60	0.63	679.4
5	0.74	0.77	0.60	703.6
6	0.67	0.84	0.51	886.5
7	0.76	0.98	0.64	816.2
8	0.63	0.94	0.51	909.3
9	0.64	0.95	0.55	913.3
10	0.71	0.63	0.51	798.2
Mean	0.71	0.87	0.60	790.7

[a]Root of the mean squared prediction errors.

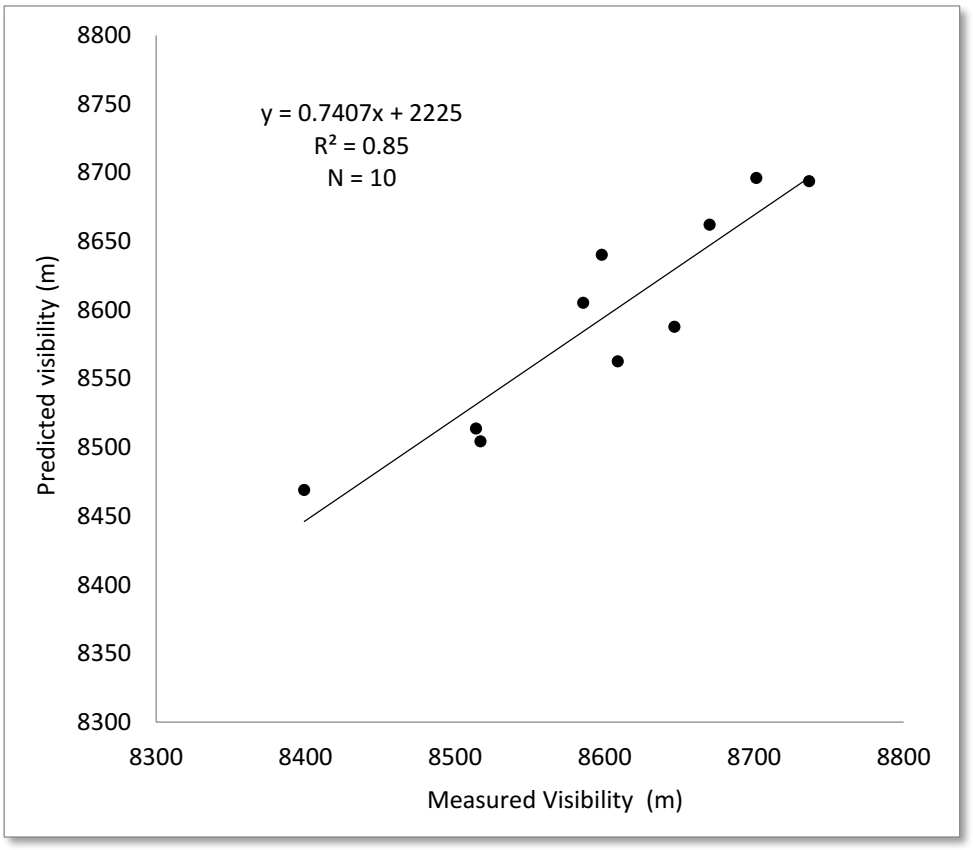

Figure 3.3. Plot of predicted *versus* measured visibility averages for each of 10 CV trials.

Table 3.2 presents results from cross validation (CV) analyses after predicting visibility where neither AOD nor visibility measurements are available, using Equation 2. CV trials suggested a very good model performance, with a mean out-of-sample R^2 value of 0.84 (range 0.78-0.91). This is a good performance, particularly considering the absence of both AOD and visibility measurements for the days and grid cells being predicted. Table 3.2 also presents results for spatial and temporal CV analyses. The spatial analysis produced a high mean out-of-sample R^2 of 0.91 (range 0.69-0.99). Results for the temporal analysis were lower, but still good, with a mean out-of-sample R^2 of 0.71 (range 0.56-0.84). In Figure 3.3, average predicted and measured visibility for each of the 10 CV trials is plotted.

Prediction errors (RMSPE, root mean squared prediction errors) for CV analyses of both models 1 and 2 were low on average (791 and 580 m, respectively), corresponding to an error of 9 and 7%, respectively, relative to the mean of visibility (~8,500 m) across CV trials. This indicates strong model performance.

Table 3.2. Prediction accuracy for 10-fold cross validation (CV) of Stage 3 calibration model.

Site	CV R^2	CV R^2 $_{Spatial}$	CV R^2 $_{Temporal}$	RMSPE[a] (m)
1	0.82	0.96	0.64	571.6
2	0.85	0.69	0.75	569.8
3	0.87	0.88	0.81	538.9
4	0.80	0.99	0.66	664.5
5	0.91	0.98	0.83	505.4
6	0.83	0.86	0.68	601.2
7	0.84	0.98	0.70	621.8
8	0.78	0.93	0.56	604.9
9	0.85	0.87	0.66	544.6
10	0.90	0.94	0.84	487.3
Mean	0.84	0.91	0.71	580.3

[a]Root of the mean squared prediction errors.

Figure 3.4 illustrates the spatial pattern of $PM_{2.5}$ predictions, with a high resolution of 1x1 km, averaged over the entire study period from 2006 to 2007. Major roadways as well as the city of Baghdad are labeled. The mean and median predicted $PM_{2.5}$ concentrations for this study area were 45.4 and 39.3 $\mu g/m^3$, respectively. The slightly skewed distribution of predicted concentrations may be due to episodic dust storms. In general, $PM_{2.5}$ concentrations ranged greatly between grid cells. The interquartile range of mean estimated $PM_{2.5}$ concentrations was 14.6 $\mu g/m^3$ (34.2 to 48.8 $\mu g/m^3$) with a 10^{th} and 90^{th} percentile of 28.8 and 66.7 $\mu g/m^3$, respectively.

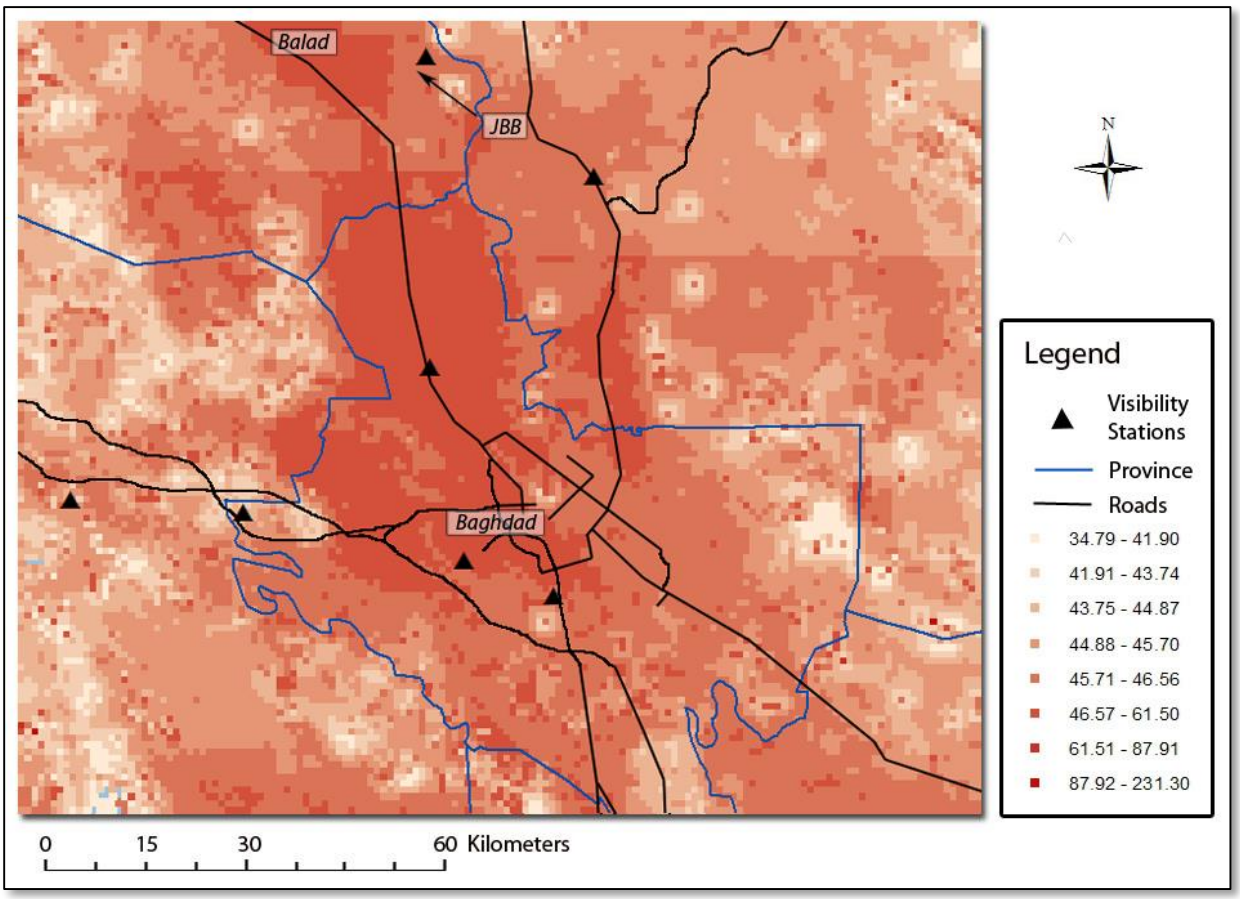

Figure 3.4. Spatial pattern of 1x1 km $PM_{2.5}$ predictions averaged over two years (2006-2007).

As seen in Figure 3.4, $PM_{2.5}$ predictions are highest in and around Baghdad and Balad as well as along certain roadways, with concentrations in the range of 46.6 to 61.5 $\mu g/m^3$. Joint Base Balad (JBB) military base had high $PM_{2.5}$ concentrations, although not as high as those of neighboring city centers.

When looking at seasonal $PM_{2.5}$ over the study period, summer had the highest predicted average, with a concentration of 51.8 $\mu g/m^3$. Averages across other seasons were markedly lower and comparable to one another, with averages of 41.5, 43.7, and 44.6 $\mu g/m^3$ for fall, spring, and winter, respectively. Mean predictions between the two study years were similar, with 2007 having a slightly higher average (47.6 $\mu g/m^3$) compared to 2006 (43.3 $\mu g/m^3$).

$PM_{2.5}$ monthly predictions for each of the seven military sites and their averages across sites during the 24-month study period are shown in Figure 3.

5. This figure demonstrates that predicted $PM_{2.5}$ varied substantially by month and site. Monthly average predictions ranged from 32.7 to 63.5 $\mu g/m^3$, with an overall mean of 45.4 $\mu g/m^3$. Consistent with seasonal patterns for this region, the model predictions were higher during summer due to seasonal Shamal winds during this season.

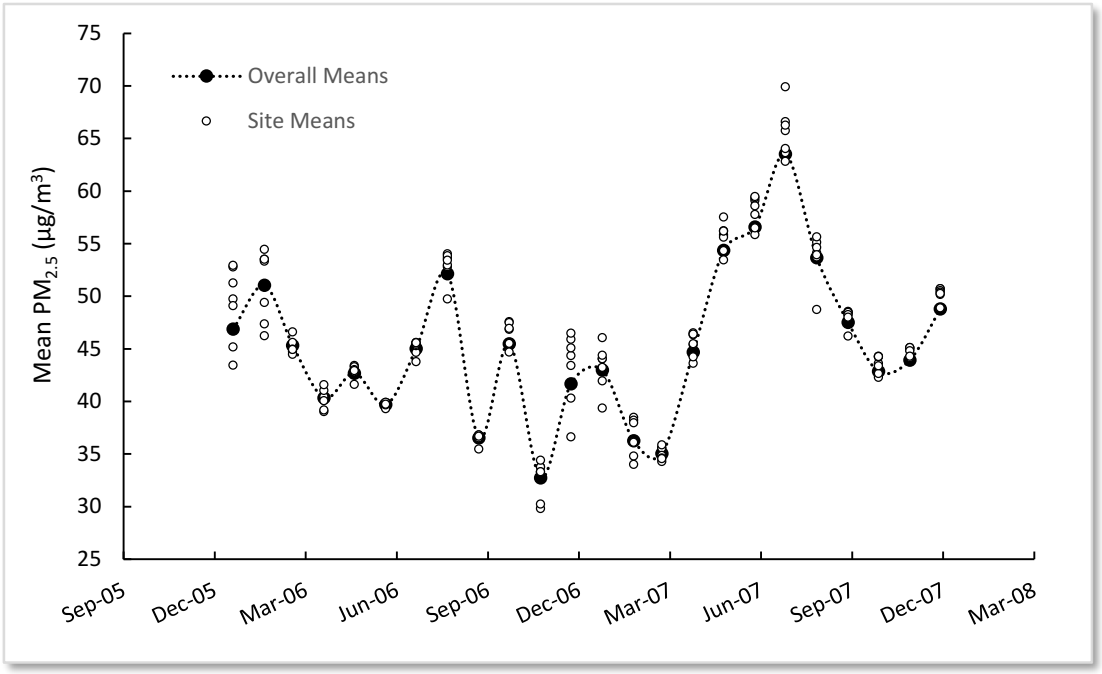

Figure 3.5. $PM_{2.5}$ monthly predictions by site and across sites during the study period.

While inter-site variability of estimated mean $PM_{2.5}$ concentration was low when averaging over the entire study period (range 44.5-47.3 µg/m^3), Figure 3.5 illustrates that much greater variability exists when assessing site averages on a monthly basis. Over the 24-month study period, monthly average predictions between sites ranged from 29.8 to 69.9 µg/m^3, with a mean and standard deviation of 46.0 and 7.8 µg/m^3, respectively. When assessing inter-site variability for individual months, monthly mean concentrations were less variable but still important. Inter-site variability for fixed months ranged from 0.60 to 9.9 µg/m^3. For specific months, sites did not deviate greatly from the mean, with a mean standard deviation of 1.4 µg/m^3 across all months. This suggests that location explains approximately 20% of the variability in monthly mean $PM_{2.5}$ estimates observed for the sites in this study. This is shown clearly in Figure 3.5, where inter-month variability of predicted $PM_{2.5}$ is high, while inter-site variability within months is relatively low.

Discussion

In previous studies, the AOD-$PM_{2.5}$ relationship has been calibrated in order to produce spatial $PM_{2.5}$ estimates (Kloog et al. 2012; Lee et al. 2011; Liu et al. 2009; Yanosky et al. 2008). In Southwest Asia and Afghanistan, however, such $PM_{2.5}$ measurements are mostly nonexistent. Therefore, in the current study we employed novel methodology using readily available airport visibility measurements to calibrate the AOD-visibility relationship and predict visibility over space and time, resulting in monthly average predictions that were highly associated with observed averages (r^2=0.94). In previous work, we established and cross-validated a relationship between visibility and $PM_{2.5}$ in Kuwait. Utilizing this work in the current study, we were able to convert spatial visibility predictions into $PM_{2.5}$ estimates.

Previous studies using satellite observations to predict $PM_{2.5}$ concentrations typically predict with a relatively coarse (10x10 km) spatial resolution and often present moderate predictive power (Lee et al. 2011; Kloog et al. 2012; Yanosky et al. 2008; Liu et al. 2009). A key advantage to our study is the fine 1x1 km resolution of predictions. This helps to reduce exposure error. Additionally, our models yielded high predictive power, in contrast to many other prediction models which assumed that the AOD-$PM_{2.5}$ relationship remains constants over time (Gryparis et al. 2009; Yanosky et al. 2008; Aguilera et al. 2007).

The ability to obtain precise monthly estimates of $PM_{2.5}$ concentrations in Iraq supports the ability to characterize chronic $PM_{2.5}$ exposures in greater Southwest Asian and Afghanistan. This is of high utility for epidemiologists seeking to understand the relationship between chronic $PM_{2.5}$ exposure and respiratory diseases among deployed military personnel stationed at various military bases and over various periods throughout the region. To date, exposure data of this kind is otherwise lacking at these locations.

Multiple means of validating the calibration model were employed in this analysis. Internal cross validation results demonstrated the ability of the model to predict visibility well across randomly divided splits of data, with low prediction errors (~6%) on average.

Given that visibility monitors are restricted to finite maximum readings, a limitation in using visibility measurements is that they are inherently less accurately in cleaner atmospheres. For this reason, it may not be feasible to use visibility as an intermediate to relate AOD with $PM_{2.5}$ mass in regions such as the U.S. where particulate levels are low. In the present study region, this is of little concern since the region is characterized by high concentrations of ambient $PM_{2.5}$ (NRC, 2010). Additionally, use of visibility is particularly advantageous here given the absence of $PM_{2.5}$ samplers in the study area and surrounding region. Through cross-validation, the model predicted well even towards the upper bound of visibility readings. Regarding precipitation, while excluding days with rain could overestimate PM exposure, this was of negligible concern in this study due to the low frequency of rain events in this region.

During the two-year period of this study, average predicted $PM_{2.5}$ was calculated to be 45.4 $\mu g/m^3$. This estimate places Iraq in roughly the midrange of ambient $PM_{2.5}$ relative to other countries in the region. For comparison, the World health Organization (WHO) reported $PM_{2.5}$ in Lebanon (2010) and Saudi Arabia (2011) at 20 and 28 $\mu g/m^3$, respectively, while Iran (2010) and Qatar (2012) had substantially higher reported $PM_{2.5}$ at 102 and 93 $\mu g/m^3$, respectively (WHO, 2014). Similarly, the DOD Enhanced Particulate Matter Surveillance Program reported average $PM_{2.5}$ concentrations ranging from 33 to 117 $\mu g/m^3$ across 15 sites in Southwest Asia and Afghanistan, with an average concentration of approximately 70 $\mu g/m^3$ across all sites (DRI, 2008). The average $PM_{2.5}$ prediction in the current study is similar to that reported in neighboring Jordan (48 $\mu g/m^3$), according to WHO.

Consistency with previously reported measurements reinforces the quality of PM2.5 predictions. Further, predictions from this analysis suggests that exposure among U.S. military personnel is in excess of U.S. EPA and WHO PM2.5 standards to protect health. Specifically, monthly predictions exceed the 24-hour mean standards set by EPA (25 μg/m3) and WHO (25 μg/m3). These are conservative comparisons still suggesting excess exposure. Annually averaged predictions in this study also exceeded EPA (12 μg/m3) and WHO (10 μg/m3) annual standards.

$PM_{2.5}$ predictions were the highest during the summer months mostly due to episodic Shamal winds that generate severe dust storms. . This pattern is consistent with previous PM studies in the area, including our previous work in Kuwait (NRC, 2010).

We examined the spatial patterns of the two-year average $PM_{2.5}$ estimates. Grid cells in and around Baghdad, Joint-Base-Ballad, and major roadways were characterized by the highest estimated $PM_{2.5}$ levels (45-60 $\mu g/m^3$). This is due to the presence of air pollution sources in these areas such as roadway traffic, industry, airports, and residential sources. Military bases often have additional sources from local diesel generators, heavy-duty vehicles, and open-pit waste incineration.

When assessing the variability in the predicted monthly $PM_{2.5}$ concentrations across seven sites used for model calibration, we saw that variability over both space and time was important. Variability between sites was high, with monthly averages differing by as much as ~30 $\mu g/m^3$ between all sites over all months. Approximately 20% of between-site variability over time was attributable to location, while 80% was attributable to month of year. Importantly, this study focused on a specific region in Iraq over a two-year period. It is likely that the variability in $PM_{2.5}$ estimates would be even greater when assessing a larger geographic area and over a longer period.

The large spatial and temporal variability in PM_{25} exposures is critical to efforts investigating the health implications of military deployment to Southwest Asia and Afghanistan. At present, very little $PM_{2.5}$ exposure data exists in this region. This is largely due to the difficulties inherent to many military zones; that is, limited materials and available personnel to conduct PM monitoring, variable and severe temperatures and weather conditions, lack of electricity, as well as low mission priority. Additional reasons for the paucity of $PM_{2.5}$ data include the lack of regional $PM_{2.5}$ monitoring stations and the impracticality of outfitting soldiers with personal monitors. As these conditions are unlikely to change, a means of assessing $PM_{2.5}$ exposure that does not rely on these factors is critical. This study aims to rectify this lack of exposure data.

Acknowledgements

This work was supported by the VA Cooperative Studies Program #595: Respiratory Health and Deployment to Iraq and Afghanistan, from the United States (U.S.) Department of Veterans Affairs, Office of Research and Development, Clinical Science Research and Development, Cooperative Studies Program. We appreciate the assistance of Mike Hunsucker and Jeff Zautner, 14th Weather Squadron (USAF), Asheville, NC. This publication was also made possible by USEPA grant RD-83479801. Its contents are solely the responsibility of the grantee and do not necessarily represent the official views of the USEPA, U.S. Department of Veterans Affairs, or U.S. Government.

Bibliography

Abbey D, Ostro BE, Fraser G, Vancuren T, Burchette RJ. Estimating fine particulate less than 2.5 microns in aerodynamic diameter (PM2.5) from airport visibility data in California. *J Expo Anal Environ Epidemiol.* 1995; 5:161-180.

Abraham JH, DeBakey SF, Reid L, Zhou J, Baird CP. Does Deployment to Iraq and Afghanistan Affect Respiratory Health of US Military Personnel? *JOEM.* 2012; 54:740-745. doi: 10.1097/JOM.0b013e318252969a.

Abraham JH, Eick-Cost A, Clark LL, Hu Z, Baird CP, DeFraites R, et al., editors. A retrospective cohort study of military deployment and post deployment medical encounters for respiratory condition. Mil Med. 2014; 179:540-546. doi:10.7205/MILMED-D-13-00443.

Adam M, Schikowski T, Carsin A, Cai Y, Jacquemin B, Sanchez M, et al., editors. Adult lung function and long-term air pollution exposure. ESCAPE: a multicenter cohort study and meta-analysis. Eur Respir J. 2015; 45:38-50. doi:10.1183/09031936.00130014.

Aguilera, I.; Sunyer, J.; Fernández-Patier, R.; Hoek, G.; AguirreAlfaro, A.; Meliefste, K.; Bomboi-Mingarro, M. T.; Nieuwenhuijsen, M. J.; Herce-Garraleta, D.; Brunekreef, B. Estimation of outdoor NOx, NO2, and BTEX exposure in a cohort of pregnant women using land use regression modeling. Environ. Sci. Technol. 2007, 42, 815−821.

Burt EW. A Study of the Relation of Visibility to Air Pollution. *Am Ind Hyg Assoc J.* 1961; 2: 102-108. doi:10.1080/00028896109343378.

Burt EW. A Study of the Relation of Visibility to Air Pollution. *Am Ind Hyg Assoc J.* 1961; 2: 102-108. doi:10.1080/00028896109343378.

Charlson RJ. Atmospheric visibility related to aerosol mass concentration: review. *Environ Sci Technol.* 1969; 3:913–918. doi:10.1021/es60033a002.

Chudnovsky, A. et al., 2013b. A Critical Assessment of High-Resolution Aerosol Optical Depth Retrievals for Fine Particulate Matter Predictions. Atmospheric Chemistry and Physics, 13(doi:10.5194/acp-13-10907-2013): 10907 - 12013.

Downs S H, Schindler C, Liu S, Keidel D, Bayer-Oglesby L, Brutsche MH, Gerbase MW, et al., editors. Reduced Exposure to PM10 and Attenuated Age-Related Decline in Lung Function. N Engl J Med. 2007; 357:2338-2347: doi:10.1056/NEJMoa073625.

Fleisch, A.F. et al., 2014. Air Pollution Exposure and Abnormal Glucose Tolerance during Pregnancy: The Project Viva Cohort. Environmental Health Perspectives, 122(4): 378 - 383.

Garshick E. Effects of short- and long-term exposures to ambient air pollution on COPD. Eur Respir J. 2014; 44:558-561. doi:10.1183/09031936.00108814.

Gryparis, A.; Paciorek, C. J.; Zeka, A.; Schwartz, J.; Coull, B. A. Measurement error caused by spatial misalignment in environmental epidemiology. Biostatistics 2009, 10, 258−74.

IOM (Institute of Medicine). 2011. Long-term health consequences of exposure to burn pits in Iraq and Afghanistan. Washington, DC: *The National Academies Press.*

Jacquemin B., Siroux V, Sanchez M, Carsin A, Schikowski T, Adam M, et al., editors. Ambient air pollution and adult asthma incidence in six European cohorts (ESCAPE). *Environ Health Perspect.* 2015; 123:613-621. doi:10.1289/ehp.1408206.

Kloog, I. et al., 2014. A New Hybrid Spatio-Temporal Model for Estimating Daily Multi-Year PM2.5 Concentrations Across Northeastern USA Using High Resolution Aerosol Optical Depth Data. Atmospheric Environment, 95(581 - 590).

Kloog, I., Koutrakis, P., Coull, B.A., Lee, H.-J. and Schwartz, J., 2011. Assessing Temporally and Spatially Resolved PM2.5 Exposures for Epidemiological Studies Using Satellite Aerosol Optical Depth Measurements. Atmospheric Environment, 45(35): 6267-6275.

Lee, H. J.; Liu, Y.; Coull, B. A.; Schwartz, J.; Koutrakis, P. A novel calibration approach of MODIS AOD data to predict PM2.5 concentrations. Atmos. Chem. Phys 2011, 11, 7991−8002.

Lee, H.-J., Liu, Y., Coull, B., Schwartz, J. and Koutrakis, P., 2011. A Novel Calibration Approach of MODIS AOD Date to Preduct PM2.5 Concentrations. Atmospheric Chemistry and Physics, 11: 7991 - 8002.

Liu, Y.; Paciorek, C. J.; Koutrakis, P. Estimating regional spatial and temporal variability of PM2.5 concentrations using satellite data, meteorology, and land use information. Environ Health Perspect 2009, 117, 886−892.

Morris MJ, Dodson DW, Lucero PF, Haislip GD, Gallup RA, Nicholson KL. Study of Active Duty Military for Pulmonary Disease Related to Environmental Deployment Exposures (STAMPEDE). *Ann Am Thorac Soc.* 2014; 190:77-84. doi:10.1164/rccm.201402-0372OC.

National Research Council. 2010. Review of the department of defense enhanced particulate matter surveillance program report. Washington, DC: The National Academies Press. *The National Academies Press.*

NOAA (National Oceanic and Atmospheric Administration). 2009. National Climatic Data Center: Climate of Iraq. Available at: http://www.ncdc.noaa.gov/oa/climate/afghan/iraq-narrative.html

Noll KE, Mueller PK, Imada M. Visibility and aerosol concentration in urban air. *Atmos Environ.* 1967; 2:465-475. doi:1016/0004-6981(68)90040-1.

Noll KE, Mueller PK, Imada M. Visibility and aerosol concentration in urban air. *Atmos Environ.* 1967; 2:465-475. doi:1016/0004-6981(68)90040-1.

Pope, C.A., and D.W. Dockery. 2006. Health effects of fine particulate air pollution: lines that connect. J. Air Waste Manage. Assoc. 56:709-742. doi:10.1080/10473289.2006.10464485.

Rice, MB, Ljungman PL, Wilker EH, Dorans KS, Gold DR, Schwartz J. Long-Term Exposure to Traffic Emissions and Fine Particulate Matter and Lung Function Decline in the Framingham Heart Study. *Am J* Respir Crit Care Med. 2015; 191:656-664. doi:10.1164/rccm.201410-1875OC.

Roberts, A.L., K. Lyall, J.E. Hart, F. Laden, A.C. Just, J.F. Bobb, K.C. Koenen, A. Ascherio, and M.G. Weisskopf. 2013. Perinatal air pollutant exposures and autism spectrum disorder in the children of nurses' health study II participants. Environ. Health Perspect. 121:978-984. doi:10.1289/ehp.1206187.

Roop SA, Niven AS, Calvin BE, Bader J, Zacher LL. The prevalence and impact of respiratory symptoms in asthmatics and nonasthmatics during deployment. Mil Med. 2007; 172:1264-1269.

Sanders JW, Putnam SD, Frankart C, Frenck RW, Monteville MR, Riddle MS, et al., editors. Impact of illness and non-combat injury during operations Iraq Freedom and Enduring Freedom (Afghanistan). *Am J Trop Med Hyg.* 2005; 73:713–719.

Schikowski T, Adam M, Marcon A, Cai Y, Vierko¨tter A, Carsin A, et al., editors. Association of ambient air pollution with the prevalence and incidence of COPD. *Eur Respir J.* 2014; 44: 614–626. doi:10.1183/09031936.00132213.

Smith B, Wong CA, Smith TC, Boyko EJ, Gackstetter GD, Ryan MAK. Newly reported respiratory symptoms and conditions among military personnel deployed to Iraq and Afghanistan: a prospective population-based study. *Am J Epidemiol.* 2009. 170:1433-1442. doi: 10.1093/aje/kwp287.

Szema AM, Peters MC, Weissinger KM, Gagliano CA, Chen JJ. New-onset asthma among soldiers serving in Iraq and Afghanistan. Allergy Asthma Proc. 2010; 31:67-71. doi: http://dx.doi.org/10.2500/aap.2010.31.3383.

Szema AM, Salihi W, Savary K, Chen JJ. Respiratory Symptoms Necessitating Spirometry Among Soldiers With Iraq/Afghanistan War Lung Injury. *JOEM.* 2011; 53:961-965. doi:10.1097/JOM.0b013e31822c9f05.

USEPA. Particulate matter. [Internet]. USEPA; 2015 [cited 2015 July 20]. Available from: http://www.epa.gov/airtrends/pm.html

Waggoner AP, Weiss RE. Preliminary Communication: Comparison of fine particle mass concentration and light scattering extinction in ambient aerosol. Atmos Environ 1980; 14:623-62.

WHO (World Health Organizatoin). 2014. Ambient (outdoor) air pollution in cities database 2014. Available at: http://www.who.int/phe/health_topics/outdoorair/databases/cities/en/

WHO Air quality guidelines for particulate matter, ozone, nitrogen dioxide and sulfur dioxide. 2005. Global update 2005. Available at: http://apps.who.int/iris/bitstream/10665/69477/1/WHO_SDE_PHE_OEH_06.02_eng.pdf

Yanosky, J. D.; Paciorek, C. J.; Schwartz, J.; Laden, F.; Puett, R.; Suh, H. H. Spatio-temporal modeling of chronic PM10 exposure for the Nurses' Health Study. Atmos. Environ. 2008, 42, 4047−4062.

Young MT, Sandler D.P, DeRoo LA, Vedal S, Kaufman JD, London SJ. Ambient air pollution exposure and incident adult asthma in a nationwide cohort of U.S. women. *Ann Am Thorac Soc*. 2014; 190: 914–921. doi:10.1164/rccm.201403-0525OC.

CONCLUSIONS

In chapter one of this manuscript, we analyzed the chemical compositions and sources of ambient fine- and coarse-mode particles in Boston over a nine year period. The primary strengths of this study are the simultaneous collection of fine and coarse particles as well as the extended period over which samples were collected. Our results suggest that coarse and fine particles have very different elemental compositions, reflecting their different sources and mechanisms of formation.

Fine particles were associated mostly with regional pollution and accounted for two-thirds of PM_{10} mass, while coarse particles accounted for one-third of PM_{10} mass and consisted mostly of crustal/road dust elements. The coarse-mode contribution to PM_{10} reported in this analysis is similar to that reported in many urban environments (Marloes et al., 2012; Querol et al., 2004). Particularly noteworthy was the exclusive association between the combustion products S and BC in the fine particle mode. Pb was also associated exclusively with the fine mode, while V and Ni were highly associated with this mode. These findings are similar to those of Hueglin et al. (2005) who reported over 80% of both Pb and sulfate, and over 60% of V and N, to be present in the fine mode in the near-city environment.

The elements that were mostly found in the coarse mode included the crustal and road dust elements Ca, Si, Ti, Fe, and Mn, as well as Cl (sea salt), similar to that reported by Hueglin et al. (2005). The assessment of coarse particle composition and concentration on a location-by-location basis is important in understanding the potential health implications to a given population, since coarse particles often originate from local sources and are known to be geographically heterogeneous, in contrast to fine particles which are more homogeneously dispersed over space (USEPA, 2009).

For mass closure, the species we analyzed accounted for 98% of total $PM_{2.5}$ mass and 41% of total $PM_{2.5-10}$ mass. The majority of fine-mode mass was made up of OC and sulfate. For the coarse mode, particles were more enriched with metal oxides and sea salt as compared to the fine mode, accounting for 28 and 8% of total coarse mass, respectively. This was expected as wind-blown soil, dust, and sea salt minerals tend to be larger particles. That coarse particles are enriched with metals has implications for coarse PM toxicity, as such metals have been implicated as key components responsible for the health effects associated with PM (Flemming et al. 2013; USEPA, 2009).

An annual decrease in PM concentrations was observed for both coarse and fine particles, though the decrease was more pronounced for fine particles. That $PM_{2.5}$ is decreasing more sharply over time than $PM_{2.5-10}$ suggests that $PM_{2.5-10}$ and traffic-related sources will be of increasing importance to PM exposure and environmental policies as we move into the future. The annual decline for $PM_{2.5}$ was mostly due to decreases in regional pollution and oil combustion source types. This decline in major source contributions of $PM_{2.5}$ appears to reflect the success of environmental acid rain policies to curb sulfur emissions as well as a gradual shift towards cleaner sources of fuel, such as natural gas, as the energy market changes. For $PM_{2.5-10}$, crustal/road dust contributed most to the annual decline. Fine-mode particles demonstrated seasonal variability, with the highest average concentrations occurring during summer and winter months. By contrast, coarse-mode particles did not exhibit seasonal variability.

PMF analysis identified six source types for $PM_{2.5}$ and three source types for coarse particles. Fine particle concentrations were predicted well by our factor analysis, as demonstrated by their low MREs. Regional pollution contributed the most to $PM_{2.5}$ concentrations, accounting for 48% by mass, followed by motor vehicles (21%), wood burning (19%), oil combustion (8%),

crustal/road dust (4%), and sea salt (<1%). These results are similar to those reported elsewhere in the U.S. (Lee et al. 2011; Kim et al. 2004; Kim et al. 2005). Regional pollution accounting for nearly half of fine particle mass lends merit to ongoing efforts to curb sulfur emissions, such as the U.S. Department of Energy's action in 2011 to convert the Northeast Home Heating Oil Reserve to ultra-low-sulfur diesel (ULSD) as well as the decisions by several northeastern states to begin requiring ULSD for heating (EIA, 2014). Overwhelmingly the greatest contributor to coarse mass was crustal/road dust (62%), followed by sea salt (16%) and motor vehicles (22%). These finding are similar to other studies which have found road dust and sea salt to contribute substantially to coarse-mode particles (Harrison, 1983; Herner, 2006).

Chapters two and three of this manuscript demonstrate the ability to utilize satellite AOD measurements to predict visibility and subsequently convert visibility into $PM_{2.5}$ concentrations spatially across Southwest Asia and Afghanistan. In chapter two, calibration of a model to predict $PM_{2.5}$ in Kuwait resulted in trimester average predictions that correlated well with observed averages. Further, results from mixed model regression demonstrated that predictability does not depend on site. Similarly, in chapter three, a novel methodology using airport visibility measurements to calibrate the AOD-visibility relationship and predict visibility over space and time in Iraq resulted in monthly average predictions that were highly associated with observed averages. Since 1x1 km AOD measurements were used, we were able to predict $PM_{2.5}$ with a very high spatial resolution, compared to other studies using relatively coarse (10x10 km) measurements (Kloog et al. 2012; Lee et al. 2011; Liu et al. 2009; Yanosky et al. 2008). The findings from these chapters support the use of historical visibility data to estimate $PM_{2.5}$ concentrations in this region of the world. Importantly, these models have high utility for epidemiologists investigating the relationship between chronic exposure to $PM_{2.5}$ and respiratory

diseases among deployed military personnel stationed at various military bases throughout the region. To date, such exposure data in this area is otherwise lacking.

For model performance in chapter two, three-month averages were used since daily relationships can be noisy and since this model is designed to predict chronic and not daily or peak short-term exposures. That is, the goal was to predict $PM_{2.5}$ concentrations that are meaningful for assessing chronic exposure in a given individual. Trimester rather than monthly averages were used because calibration requires $PM_{2.5}$ measurements, of which there were few available per month. In chapter three, however, the availability of daily data enabled the estimation of average monthly exposure, which reduces exposure error and is ideal since military personnel are often deployed for only a matter of months.

Several means of validating the models presented in chapters two and three were conducted. In chapter two, 10-fold cross validation analysis showed the model to predict well across randomly divided splits of data as %MRE values were mostly under 15% for each validation trial. Further, given that prediction errors were low on average (~5%), bias appeared to be minimal. Although our model calibration used data mostly collected at a single site, further internal validation showed predictability to remain high at sites exterior to this site, including at both urban and rural locations. In chapter three, additional means of validating the calibration model were employed. In general, internal cross validation results demonstrated the ability of the model to predict visibility well across randomly divided splits of data, with low prediction errors (~6%) on average.

Given that visibility monitors are restricted to finite maximum readings, a limitation in using visibility measurements is that they are inherently less accurately in cleaner atmospheres. For this reason, it may not be feasible to relate visibility to either AOD or $PM_{2.5}$ mass in regions

such as the U.S. where particulate levels are low. In the present study region, however, this is of little concern since the region is characterized by high concentrations of ambient $PM_{2.5}$ (NRC, 2010). Additionally, use of airport visibility measurements in the present analyses particularly advantageous given the absence of $PM_{2.5}$ samplers in the region. Further, in chapter two it was demonstrated by internal cross-validation that the model predicted well for average trimester $PM_{2.5}$ concentrations as low as 20.5 μg/m3. Monthly average predictions for 104 sites in Southwest Asian and Afghanistan were as low as 10 μg/m3. Based on previous reporting, long-term $PM_{2.5}$ concentrations below these levels are not expected to occur in this region (NRC, 2010). Similarly, in chapter three, cross-validation demonstrated the models to predict well even towards the upper bound of visibility readings. Regarding precipitation, while excluding days with rain could overestimate PM exposure, this was of negligible concern in this study due to the low frequency of rain events in this region.

In both chapters two and three, assessing seasonal $PM_{2.5}$ showed average concentrations and seasonality consistent previous reports for the area (NRC, 2010). Specifically, summer is known to be the peak season in terms of elevated PM concentrations, while winter levels are usually lower throughout the region. The increase in PM during summer is mostly due to episodic Shamal winds that generate severe dust storms. Consistency of PM predictions with regional weather patterns and previous reports lends support for the quality of predictions in the analyses.

Variability in $PM_{2.5}$ predictions was explored in both chapters two and three. In chapter two, to examine the extent of spatiotemporal variability of predicted monthly $PM_{2.5}$ exposure, we applied our calibrated model using over a decade of weather data to predict $PM_{2.5}$ mass at 104 different military bases and airports in the region. Results showed predicted monthly averages to

range from approximately 10 to 365 μg/m^3 between bases. Within-site variability was similarly high. Over 50% of sites, and 20% of sites, had monthly predictions that differed by as much as 73 μg/m^3 and 120 μg/m^3, respectively. On average, within-site monthly predictions varied by 83.2 μg/m^3. In chapter three, an assessment of the variability in predicted monthly $PM_{2.5}$ concentrations across seven sites used for model calibration demonstrated showed that variability over both space and time was important. Variability between sites was high, with monthly averages differing by as much as ~30 μg/m^3 between all sites over all months. Approximately 20% of between-site variability over time was attributable to location, while 80% was attributable to month of year. Importantly, this study focused on a specific region in Iraq over a two-year period. It is likely that the variability in $PM_{2.5}$ estimates would be even greater when assessing a larger geographic area and over a longer period.

That $PM_{2.5}$ variability is large across time and geographic space in both analyses reinforces the ability to successfully use our models and $PM_{2.5}$ estimates in epidemiological research. This is of high relevance to understanding the health implications of military deployment to Southwest Asia and Afghanistan. To date, very little $PM_{2.5}$ exposure data in this region exists partly due to the difficulties inherent to many military zones; namely, limited materials and available personnel to conduct the monitoring, variable temperatures and harsh weather conditions, lack of electricity, as well as low priority relative to the military mission at hand. Additional reasons for the paucity of $PM_{2.5}$ data include the scarcity of regional $PM_{2.5}$ monitoring stations as well as the impracticality of outfitting soldiers with personal monitors in the field. As these conditions are unlikely to change, a means of assessing $PM_{2.5}$ exposure that does not rely on these factors is essential. These chapters aim to fill these gaps.

Bibliography

Flemming, C.R., M. Heroux, M.E. Gerlofs-Nijland, and F.J. Kelly. 2013. Particulate matter beyond mass: recent health evidence on the role of fractions, chemical constituents and sources of emission. *Inhal. Toxicol*. 25:802-812. doi:10.3109/08958378.2013.850127.

Harrison, R.M., and C.A. Pio. 1983. Size-differentiated composition of inorganic atmospheric aerosols of both marine and polluted continental origin. *Atmos. Environ.* 17:1733-1738. doi:10.1016/0004-6981(83)90180-4.

Herner, J.D, Q. Ying, J. Aw, O. Gao, and D.P.Y. Chang. 2006. Dominant mechanisms that shape the airborne particle size and composition distribution in Central California. *Aerosol Sci. Tech.* 40:827-844. doi:10.1080/02786820600728668.

Hueglin, C., R. Gehrig, U. Baltensperger, M. Gysel, C. Monn, and H. Vonmont. 2004. Chemical characterization of PM2.5, PM10 and coarse particles at urban, near-city, and rural sites in Switzerland. *Atmos. Environ*. 39:637-651. doi:10.1016/j.atmosenv.2004.10.027.

Kim, E., and P.K. Hope. 2004. Improving source identification of fine particles in a rural northeastern U.S. area utilizing temperature-resolved carbon fractions. *J. Geophys. Research.* 109:1984-2012. doi:10.1029/2003JD004199.

Kim, E., P.K. Hope, D.M. Kenski, and M. Koerber. 2005. Sources of fine particles in a rural Midwestern U.S. area. *Environ. Sci. Tech.* 39:4953-4960. doi:10.1021/es0490774.

Kloog, I., Koutrakis, P., Coull, B.A., Lee, H.-J. and Schwartz, J., 2011. Assessing Temporally and Spatially Resolved PM2.5 Exposures for Epidemiological Studies Using Satellite Aerosol Optical Depth Measurements. Atmospheric Environment, 45(35): 6267-6275.

Lee, H.J., J.F. Gent, B.P. Leaderer, and P. Koutrakis. 2011. Spatial and temporal variability of fine particle composition and source types in five cities of Connecticut and Massachusetts. *Sci. Tot. Environ.* 409:2133-2142. doi:10.1016/j.scitotenv.2011.02.025.

Lee, H.-J., Liu, Y., Coull, B., Schwartz, J. and Koutrakis, P., 2011. A Novel Calibration Approach of MODIS AOD Date to Preduct PM2.5 Concentrations. Atmospheric Chemistry and Physics, 11: 7991 - 8002.

Liu, Y.; Paciorek, C. J.; Koutrakis, P. Estimating regional spatial and temporal variability of PM2.5 concentrations using satellite data, meteorology, and land use information. Environ Health Perspect 2009, 117, 886−892.

Marloes, E., M.Y. Tsai, C. Ampe, B. Anwander, R. Beelen, T. Bellander, G. Cesaroni, M. Cirach, J. Cyrys, K. de Hoogh, A. de Nazelle, F. de Vocht, C. Declercq, A. Dėdelė, K. Eriksen, C. Galassi, R. Gražulevičienė, G. Grivas, J. Heinrich, B. Hoffmann, M. Iakovides, A. Ineichen, K. Katsouyanni, M. Korek, U. Krämer, T. Kuhlbusch, T. Lanki, C. Madsen, K. Meliefste, A. Mölter, G. Mosler, M. Nieuwenhuijsen, M. Oldenwening, A. Pennanen, N. Probst-Hensch, U. Quass, O. Raaschou-Nielsen, A. Ranzi, E. Stephanou, D. Sugiri, O. Udvardya, É. Vaskövia, G. Weinmayr, B. Brunekreef, and G. Hoek. 2012. Spatial variation of $PM_{2.5}$, PM_{10}, $PM_{2.5}$ absorbance and PM_{coarse} concentrations between and within 20 European study areas and the relationship with NO2 – Results of the ESCAPE project. *Atmos. Environ.* 63:303-317. doi:10.1016/j.atmosenv.2012.08.038.

NRC (National Research Council). 2010. Review of the department of defense enhanced particulate matter surveillance program report. Washington, DC: The National Academies Press. The National Academies Press.

USEPA. 2009. Integrated science assessment for particulate matter. USEPA Office of Research and Development.

Yanosky, J. D.; Paciorek, C. J.; Schwartz, J.; Laden, F.; Puett, R.; Suh, H. H. Spatio-temporal modeling of chronic PM10 exposure for the Nurses' Health Study. Atmos. Environ. 2008, 42, 4047−4062.